Interface Dilation

The Overflowing Cylinder Technique

Promotor: dr. A. Prins
hoogleraar in de fysica en de fysische chemie van levensmiddelen met bijzondere aandacht voor de zuivel

Co-promotor: dr. ir. H.J. Bos
universitair docent in de theoretische aerodynamica

D.J.M. Bergink-Martens

Interface Dilation

The Overflowing Cylinder Technique

Proefschrift

ter verkrijging van de graad van doctor
in de landbouw- en milieuwetenschappen
op gezag van de rector magnificus,
dr. H.C. van der Plas,
in het openbaar te verdedigen
op dinsdag 15 juni 1993
des namiddags te vier uur in de Aula
van de Landbouwuniversiteit te Wageningen.

Abstract

Bergink-Martens, D.J.M., (1993). Interface Dilation. The Overflowing Cylinder Technique. Ph.D. thesis, Agricultural University, Wageningen.
(pp. 151, English, German and Dutch summaries).
CIP-gegevens Koninklijke Bibliotheek, Den Haag; ISBN 90-5485-128-7

Keywords:

interface dilation, surface dynamics, overflowing cylinder technique, falling liquid film, surface tension gradient, Marangoni-effect, dynamic interfacial tension, surface dilational viscosity.

Abstract:

A pure steady-state dilation of a liquid interface, either liquid-air or water-oil, can be accomplished far from equilibrium by means of the overflowing cylinder technique. The resulting dynamic surface tension data correlate well with characteristic parameters of processes like foaming, emulsification, and the spreading of droplets and thin liquid layers.

Fundamental knowledge of the physical mechanism of operation of the overflowing cylinder technique is obtained by analyzing the relation between interface dilation and underlying bulk flow. Upon the addition of a surfactant the interface velocity increases considerably, since the propulsion mechanism changes from driven by the bulk flow to surface tension gradient driven.

The surface rheological behaviour of the expanding interface is studied for various surfactant solutions. Generally practical systems give rise to a major increase in surface tension during interface dilation. The results are discussed in terms of the transport of surfactant components.

The present findings explain why the overflowing cylinder technique is such a useful tool for studying many practical processes which imply interface dilation far from equilibrium. Meanwhile, however, they urge a reconsideration of the meaning of the surface dilational viscosity.

Stellingen

1 De grootte van de oppervlaktedilatatieviscositeit zegt vaak meer over de zuiverheid van een oppervlakte-actieve oplossing dan over zijn oppervlakte gedrag in expansie ver van evenwicht.
Dit proefschrift.

2 De aanwezigheid van een oppervlaktespanningsgradiënt kan - beter dan door middel van een rechtstreekse bepaling - aangetoond worden via een meting van de oppervlakte snelheid.
Dit proefschrift.

3 Nu uitvoering geven aan de filosofie 'niet doen wat je vindt dat je moet doen, maar doen waar je goed in bent', kan straks in een spiraalwerking een verenging van 'de zaken waar je goed in bent' betekenen.

4 De universiteiten en de publieke omroepen verkeren binnen de Nederlandse samenleving in verschillende opzichten in dezelfde positie. Met het oog op de versterking van beider positie hebben zij elkaar over en weer meer te bieden dan nu zichtbaar en hoorbaar is.

5 Jonge ouderen (55 - 70 jaar) realiseren zich vaak niet of nauwelijks dat ook zij in de schijnwerpers staan in dit Europese jaar van de ouderen. Dit tekent de wijze waarop zij met het ouder worden omgaan.

6 De geplande reductie van het aantal verzorgingsplaatsen in de provincie Noord-Holland stelt niet alleen een verbetering van de kwaliteit van de zorg binnen het verzorgingstehuis in het vooruitzicht, maar stelt tevens deze kwaliteit zwaar op de proef.
Kaderplan: voorzieningen voor ouderen; periode 1993 - 1996; provincie N-Holland.

7 Voor een bruidspaar levert een huwelijk dat in de R.K.-kerk ten overstaan van een pastoraal medewerker 'gesloten' is, kerkjuridisch niet, maar feitelijk wel meer problemen op bij een scheiding dan men op grond van de formele status zou mogen verwachten.

8 De beeldcultuur wordt in onze samenleving steeds dominanter; dat veel intellectuelen dit niet (willen) onderkennen en de voorkeur blijven geven aan letters boven beeldlijnen, wordt ook geïllustreerd door de aanblik van wetenschappelijke posters.

9 Als pakkende variatie op de bestaande leus "Een béétje vent strijkt zijn eigen overhemd" zal "Een échte man kan er in de keuken óók wat van" meer aandacht van de doelgroep trekken.

10 Deze laatste stelling wordt veelal niet als laatste gelezen.

Stellingen bij het proefschrift "Interface Dilation. The Overflowing Cylinder Technique" door Diane J.M. Bergink-Martens. Wageningen, 15 juni 1993.

Voorwoord

Een proefschrift is een beschrijving van eigen proeven
en een beproeving van eigen schrijven

Juist hier bij aanvang van dit werk
wordt - in een jamben reeks verpakt -
bewust de bovenstaande leus
op 't woordje 'eigen' afgezwakt.

De eigen proeven werden noest
diep in de kelder uitgevoerd
naar een idee dat vaak door Prins
zeer enthousiast was aangeroerd.

Betrokken én nieuwsgierig, ook,
kwam Prins zeer dikwijls naar benee;
als echte 'veldambassadeur'
bracht hij dan soms bezoekers mee.

Ook Arne, Marjo, Stephanie
verkregen in hun doctoraal
na wat gestoei met nattigheid,
discussiestof voor dit verhaal.

Het eigen schrijven werd beproefd,
doch afstand neem je niet maar zo;
een welkom duwtje werd verleend
door de promotor en zijn 'co'.

Prins tastte heel zorgvuldig af
en trad ook vaak beschermend op;
dan had zijn 'co' een and're kijk,
uitdagend zelfs: Bos op en top.

De sectie bood een prima sfeer,
leuk met collega's onderling.
Grafieken poetste Bertram op,
terwijl zijn 'rust' onrust verving.

Elkeen gaf richting aan de weg
die ik in vier jaar ben gegaan.
Dit dichterlijke woord van dank
bied ik hen daarom heel graag aan.

Contents

Chapter 1

General introduction

It is considerably important to study the dynamic surface behaviour of surfactant solutions far from equilibrium, because this behaviour plays a crucial role in numerous technological processes. Surface dilational properties can be studied under steady-state conditions by means of the overflowing cylinder technique (§1.1). Although various researchers have already succesfully used the overflowing cylinder technique for their investigations, a more detailed description of the physical mechanism which underlies the operation of the technique, has not been given so far (§1.2). The aim of the present investigation directly follows from the experienced lack of knowlegde of the operation of the overflowing cylinder technique (§1.3).

1.1 Surface dynamics

The application of surfactant solutions in processes invariably implies the creation of non-equilibrium situations. Due to the fact that interfaces between two liquid phases are mobile, in processing applications deformation of interfaces occurs. Foaming and emulsification are examples of processes having such a dynamic character. These processes involve the break-up of large bubbles and drops of the disperse phase into smaller parts. Generally the resulting deformation of the interface will not be homogeneous. Moreover in foaming and emulsifying machines conditions of flow may be such that zones of different deformation rates exist side by side. Once foams and emulsions have been created, the dynamic character shows again, since the quiescent dispersions are principally unstable. Due to a lack of complete thermodynamic equilibrium, the dispersion properties may vary in time. So during preparation, storage, and usage of dispersions, liquid interfaces are continuously exposed to all kinds of disturbances and instabilities may arise. Dynamic behaviour not only comes to play when foams and emulsions are

considered. Many other processes in practice imply deformation of liquid interfaces. In many of these processing applications the time scale of the deformation does not allow for surfactant molecules to be in equilibrium at the liquid interface. Consequently such processes cannot be understood and controlled on the basis of equilibrium studies only. The study of dynamic surface phenomena is of paramount importance to the knowlegde of these non-equilibrium applications of surfactants.

The study of dynamic surface phenomena is covered by the field of surface rheology. This subject can be approached from a phenomenological point of view [1]. Within this approach the surface of the liquid system under investigation can experimentally be subjected to different types of mechanical disturbances: (i) a periodic change in surface area in a dynamic experiment, (ii) a transient disturbance in a so-called relaxation experiment, and (iii) a continuous deformation of the surface under steady-state conditions. Whereas dynamic experiments take place around the equilibrium situation, the continuous deformation under steady-state conditions generally concerns a mechanical disturbance far from equilibrium. Shear, curvature, and compression or expansion of the surface are distinquished as possible deformations.

The present investigation is carried out within the framework of this last category of experimental conditions in phenomenological surface rheology. The deformation considered is expansion. So this thesis confines itself to a study of continuous expansion of the surface in a steady-state situation far from equilibrium.

A continuous expansion of a liquid surface can be accomplished in different ways. The surface can be expanded by means of two barriers, moving apart at an appropriate velocity, like Van Voorst Vader et al [2] did in their steady-state experiments. Ronteltap [3] carried out similar experiments by using a

Langmuir trough equipped with a caterpillar belt with several barriers. More frequently the falling film apparatus is used [4,5,6]. This apparatus is designed to imitate the rapid drainage in the early stages of a freshly made foam. The maximum-bubble-pressure-method is also widely known. Although the method indeed implies a continuous expansion of a liquid surface, the process does not take place under steady-state conditions [7]. The present study is limited mainly to the overflowing cylinder technique, one of the techniques accomplishing a pure dilation (without any shear-components) of a liquid surface under steady-state conditions far from equilibrium.

Expanding liquid surfaces in practice

In practice especially the behaviour of expanding liquid surfaces far from equilibrium plays an important role in a lot of processes which take place in various branches of industry. A few examples will be given to illustrate this statement.

During foaming and emulsification of surfactant solutions new interfaces are formed. This implies an enormous expansion of the total interface area in a relatively short time. The newly formed bubbles and droplets will rapidly be exposed to the threat of coalescence with each other or with the surrounding atmosphere. The stability of the freshly made foams and emulsions against coalescence, however, is directly linked to the stability of the created thin liquid films in between respectively the air bubbles and the emulsion droplets. Since these thin liquid films can be made unstable especially when they are subjected to expansion, as happens during preparation of the dispersions, the study of the behaviour of expanding interfaces can result in a better understanding of the foaming and emulsifying properties of surfactant solutions.

Another example is the growth of bubbles in carbonated beverages like beer and champagne. Inhomogeneities in the wall of the glass into which the carbonated beverage is poured, may contain gas pockets giving rise to bubble growth. During this process the bubble surface expands very rapidly [3]. Surface dilational properties influence the process of bubble growth and the

moment of detachment from the glass wall.

Application of a thin liquid layer on a solid surface implies expansion of the layer surface. This example refers for instance to sticker productions where a carrier has to be covered with a thin layer of glue, or surfaces which have to be painted, printed or coated. During these processes undesirable holes may be formed in the thin film. In order to prevent this from happening the applied liquid substance has to have the right surface dilational properties.

In addition to these examples interface formation and surface expansion comes into play in numerous other processes like detergency [8], the spraying of plants [9] and the dyeing, finishing and impregnation of fibrous materials [10].

Knowledge of surface dilational properties counts for all of these examples, since a better understanding of the behaviour of expanding liquid surfaces may lead to improvement of products or production processes. Experimental studies in which the liquid surface is subjected to a continuous expansion under steady-state conditions far from equilibrium, may contribute substantially to the desired knowledge of surface dilational properties. Such experimental studies can be carried out by means of the overflowing cylinder technique.

1.2 The acquaintance with the overflowing cylinder technique

Already in the fifties researchers like Padday [11] and Piccardi and Ferroni [12,13] have used the overflowing cylinder technique for various fluids. They carried out dynamic surface tension measurements at its expanding surface. Since that time also variations on the concept of the overflowing cylinder have been introduced. Barber [14] and Joos and De Keyser [15] e.g. used an overflowing funnel and Schunk and Scriven [16] studied an overflow cell within the framework of their fundamental research of the process of coating.

More recently the overflowing cylinder appeared again in various publications. Ronteltap [3] used the apparatus as a tool to characterize different beers. De Ruiter et al [9] demonstrated that the retention of plant spray on plant species with reflective leave surfaces benefits from a low surface tension as measured during expansion of the surface of the spray liquid in the overflowing cylinder. Clark et al used among other techniques the overflowing cylinder to correlate the surface dynamics of mixtures of surface active food components with dispersion stability [17]. In one of the papers [18] preceeding this thesis it was qualitatively demonstrated that also the process of foaming benefits from a low surface tension as measured during expansion of the surface of a foamable surfactant solution in the overflowing cylinder.

Besides these published results obtained by means of the overflowing cylinder or one of its variations, there are even more unpublished results, as many Dutch companies in various branches of industry succesfully use the overflowing cylinder to study the surface dilational properties of their own products without spreading this abroad. For these companies knowledge of the properties may lead to improvement of products or production processes.

A lack of fundamental knowledge

In general the overflowing cylinder is experienced to be a very handy and useful tool in studying surface dilational properties of surfactant solutions. In addition the overflowing cylinder happens to create an expanding surface having an expansion rate (see also chapters 2 and 6) which shows to be practically relevant to many applications of surfactant solutions. This makes the overflowing cylinder technique extremely suitable for all kinds of fluids which are used in practice.

Despite its observed practical utility, there is a lack of fundamental knowledge of the operation of the overflowing cylinder. Some of the researchers mentioned above tried to relate the expansion rate of the surface to the flow rate of liquid through the cylinder or the funnel. This problem

appeared to be a difficult one, because it required insight in how the overflowing cylinder physically operates. None of these investigations, however, resulted in a more detailed description of the physical mechanism which explains the operation of the overflowing cylinder technique.

1.3 Outline of this study

It may be concluded from the previous paragraph that although the overflowing cylinder has already widely been used and highly valued for its practical utility, there is a lack of fundamental knowledge of the operation of the overflowing cylinder technique. The aim of the present investigation directly follows from this conclusion. In this thesis the relations existing between the physical parameters which determine the operation of the overflowing cylinder technique are studied. Attention will be paid to the forces responsible for the propulsion of the liquid surface. Simultaneously experimental results for various surfactant solutions obtained by means of the overflowing cylinder are presented and discussed. In this way the study may provide users background information giving insight in both the possibilities and the limitations of the overflowing cylinder technique.

In industry the overflowing cylinder is used to experiment on practical systems. Since these systems are far from being model solutions, the scope of this study has been to investigate so called 'dirty systems' rather than model systems. This implies that the behaviour of solutions of model surfactants has not been studied extensively.

This thesis continues with an introduction of the physical parameters (chapter 2) which play an important role in the operation of the overflowing cylinder technique. In chapter 3 some theoretical aspects are dealt with. Attention is paid to the fluid dynamics of the overflowing cylinder, the transport of

surfactant components to the expanding surface, as well as to theoretical relations between different parameters. Chapter 4 describes the materials and methods used. In chapter 5 the results of the experiments with the overflowing cylinder technique are presented and discussed in the perspective of the theoretical aspects dealt with in chapter 3. As for some of the researchers mentioned above [14,15] the key problem of the overflowing cylinder was to relate the surface expansion rate to other quantities like the flow rate through the cylinder, in chapter 6 special attention is paid to the factors which influence the magnitude of the expansion rate of the surface. This subject is also considered to be very important for all present-day users of the overflowing cylinder. A new dimension to the overflowing cylinder is formed by creating the possibility of expanding a water-oil interface. The opportunity of studying a continuous expanding water-oil interface is especially important when the preparation of emulsions is considered. This extension of the known overflowing cylinder technique will be elucidated in chapter 7. To conclude chapter 8 features a general view of the operation of the overflowing cylinder based on the results of the present study.

Acknowledgments. This research was supported by the Netherlands Technology Foundation (STW) and by Shell Amsterdam. The author wishes to thank the STW users committee for valuable discussions and suggestions.

References Chapter 1

[1] M. van den Tempel, J. Non-Newtonian Fluid Mech., 2 (1977) 205.

[2] F. van Voorst Vader, Th. F. Erkens and M. van den Tempel, Trans. Faraday Soc., 60 (1964) 1170.

[3] A.D. Ronteltap, Beer Foam Physics, Ph.D. thesis, Agricultural University Wageningen, (1989).

[4] D.R. Brown, J. Fluid Mech., 10 (1961) 297.

[5] M.G. Antoniades, J. Coll. Int. Sci., 77 (1980) 583.

[6] S.P. Lin and G. Roberts, J. Fluid Mech., 112 (1981) 443.

[7] K.J. Mysels, Coll. Surf., 43 (1990) 241.

[8] M. van den Tempel and E.H. Lucassen-Reynders, Adv. Coll. Int. Sci., 18 (1983) 281.

[9] H. de Ruiter, A.J.M. Uffing, E. Meinen and A. Prins, Weed Science, 38 (1990) 567.

[10] D.E. Hirt, R.K. Prud'Homme, B. Miller and L. Rebenfeld, Coll. Surf., 44 (1990) 101

[11] J.F. Padday, Proc. Int. Congr. Surf. Act. I, (1957).

[12] G. Piccardi and E. Ferroni, Ann. Chim. (Rome), 41 (1951) 3.

[13] G. Piccardi and E. Ferroni, Ann. Chim. (Rome), 43 (1953) 328.

[14] A.D. Barber, A Model for a Cellular Foam, Ph.D. Thesis, Nottingham, (1973).

[15] P. Joos and P. de Keyser, The Overflowing Funnel as a Method for Measuring Surface Dilational Properties, Levich Birthday Conference, Madrid, (1980).

[16] P.R. Schunk and L.E. Scriven, Dynamic Surface Tension by the Overflow Cell, Ann. Meeting of the American Institute of Chem. Eng., New Orleans, (1988).

[17] D.C. Clark, P.J. Wilde and D.R. Wilson, in E. Dickinson and P. Walstra (Eds.), Food Colloids and Polymers: Stability and Mechanical Properties, Royal Society of Chemistry, Cambridge, (1993), pp. 354-364.

[18] D.J.M. Bergink-Martens, C.G.J. Bisperink, H.J. Bos, A. Prins and A.F. Zuidberg, Coll. and Surf., 65 (1992) 191.

Chapter 2

Introduction of the physical parameters

In this thesis the relations between the physical parameters describing and determining the operation of the overflowing cylinder technique are studied. In this chapter schematic representations of the overflowing cylinder are given and the relevant parameters are introduced. Only the values of the flow rate and the length of the wetting film can be imposed on the overflowing liquid. The solution determines autonomously the values of all other parameters, the surface expansion rate included. The resulting combination of parameters is characteristic for a particular solution (§2.1). This behaviour is indicative of the nature of the surface flow (§2.2).

2.1 Schematic representations of the overflowing cylinder

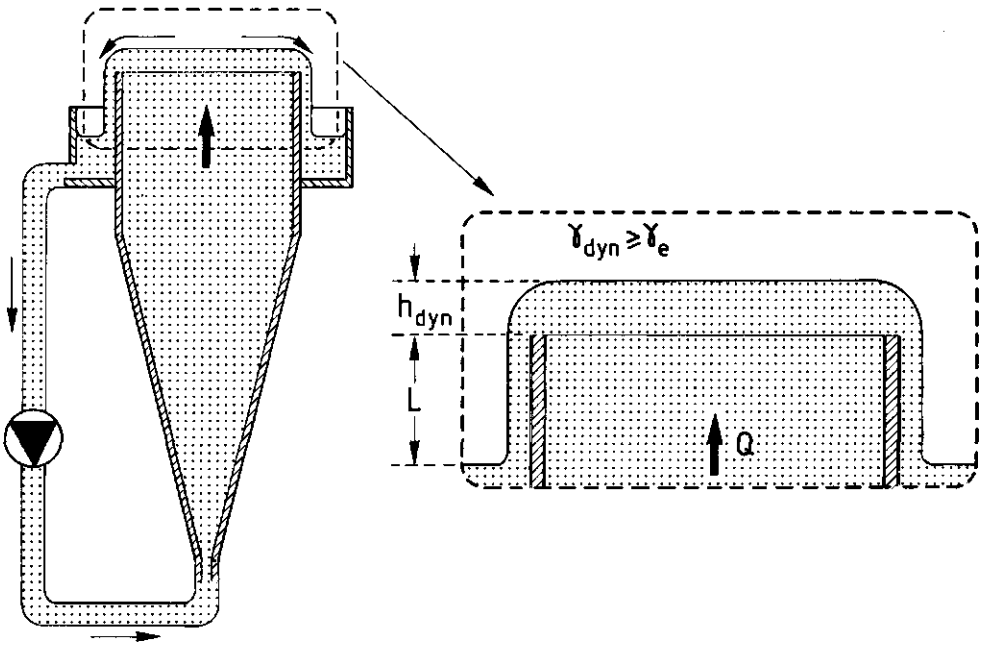

Fig. 2.1: Schematic representation of a cross-section of the overflowing cylinder.

In Fig. 2.1 a part of the cross-section of the overflowing cylinder has been enlarged. The parameters are indicated by their respective symbols. **Q** is the flow rate of liquid through the closed system of the overflowing cylinder. The liquid is allowed to flow over the top rim of a cylinder of radius **R**, causing the circular liquid surface to be expanded continuously in a radial direction. The surface tension under these dynamic conditions, γ_{dyn}, is generally higher than the equilibrium surface tension, γ_e, due to the surfactant depletion which occurs in the expanding area. So the excess surface tension which is represented by $\Delta\gamma$ ($= \gamma_{dyn} - \gamma_e$), generally deviates from the zero value. The height of the centre of the meniscus above the rim of the cylinder is symbolized by h_{dyn}. On the outside of the cylinder a wetting film of length **L** is formed.

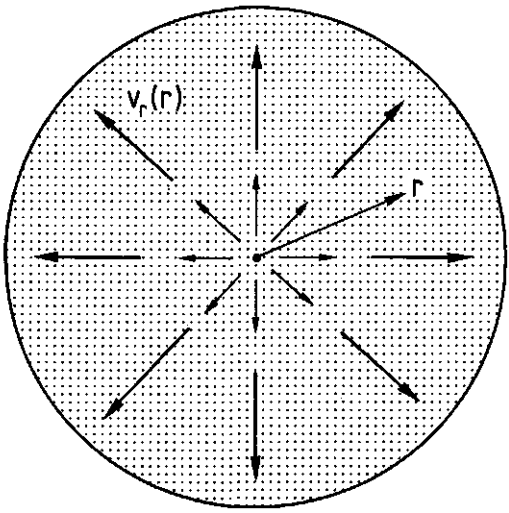

Fig. 2.2: *Topview of the expanding surface of the overflowing cylinder.*

Fig. 2.2 shows the velocity profile of the expanding surface. Since we are dealing with a steady state situation, this surface dilation pattern is a constant in time. Hence for a given experimental set-up, keeping all other parameters constant, the radial velocity of the surface, v_r, is only a function of the radial coordinate **r**.

Fig. 2.3 shows the liquid flow over the top rim of the vertical cylinder in detail. The horizontal free surface is in fact slightly convex, but may be considered to be almost flat in the vicinity of the axis of symmetry of the cylinder. When the liquid flows over the top rim the surface is curved with a radius of curvature R_2 in the plane of drawing. Next the liquid forms a wetting film on the outside of the cylinder. The thickness of this film near the rim of the cylinder is indicated by δ_0, whereas the surface velocity of the wetting film at the same position is symbolized by v_s^0.

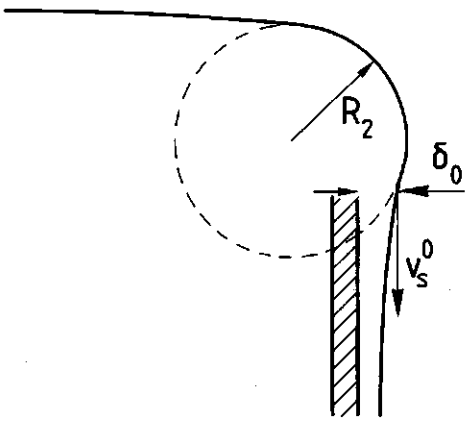

Fig. 2.3: Part of the cross-section of the overflowing cylinder.

Adjustable parameters

From all the parameters which have been introduced in this paragraph, for a given experimental set-up only the values of the flow rate Q and the length of the wetting film L can be imposed on the liquid system in the overflowing cylinder. Q can be adjusted by means of a needle valve and L can be varied by changing the total amount of fluid present in the system. All other parameters, included the surface velocity, can not be adjusted. The solution itself determines autonomously what the values will be. When L and Q are given quantities having fixed values, for each solution studied in the overflowing cylinder a unique combination of all other parameters is found.

By means of the overflowing cylinder the surface dilational viscosity of a liquid surface, η_s^d [N·s/m], can be determined. This well known physical quantity is defined by the equation

$$\gamma_{dyn} - \gamma_e = \Delta\gamma = \eta_s^d \cdot d\ln A/dt, \tag{2.1}$$

where dlnA/dt represents the relative expansion rate of the surface area A. This relation is based on a suggestion of Boussinesq [1] and generally specifies η_s^d being a constant of proportionality between the excess surface tension of the expanding (or compressed) surface and the relative rate of expansion (or compression).

Under the condition that the horizontal surface is almost flat in the region near the geometrical centre of the surface, it follows from the symmetry of the cylinder that the relative expansion rate of the overflowing cylinder depends on the radial velocity of the surface $v_r(r)$ according to

$$d\ln A/dt = \frac{v_r}{r} + \frac{\partial v_r}{\partial r}. \tag{2.2}$$

This equation has already been derived in one of the papers preceeding this thesis [2]. As v_r is one of the parameters which can not be adjusted, but is generated by the solution itself, also the value of the relative surface expansion rate is considered to be created autonomously by the liquid system in the overflowing cylinder.

In practice during the preparation, storage and usage of dispersions the value of the surface expansion rate is not imposed on the liquid system either. Only process conditions like the mixing rate, the pressure difference or the flow rate, are imposed on the system. Under these process conditions the system 'chooses' its own value of the surface expansion rate. As the same happens in the overflowing cylinder, it is not surprising that the overflowing cylinder creates an expanding surface having an expansion rate which shows to be practically relevant to many applications of surfactant solutions.

2.2 Nature of the surface flow

It was concluded in the previous paragraph that the liquid system itself determines what the value of the relative surface expansion rate of the overflowing liquid will be. This is in contrast with the way in which most of the other surface dilational apparatuses mentioned in Chapter 1, operate.
From a physical point of view Prins [3] distinguishes between three kinds of dilational deformations of a flat liquid surface:

a) an area-driven surface deformation. In practice this deformation for instance occurs, when bubbles grow in carbonated beverages. The area-driven surface deformation can experimentally be accomplished by the maximum-bubble-pressure method. Another method to change the area under investigation in an area-driven experiment is by applying moving barriers in a Langmuir trough. Among others Van Voorst Vader et al [4] and Ronteltap [5] used varieties of this trough. It counts for all of these techniques that, of course within the experimental limits, the desired surface expansion rate can be imposed on the liquid system under investigation.

b) a hydrodynamically driven surface deformation. This deformation is caused by the motion of the liquid in the close neighbourhood of the surface and takes for instance place during homogenizing, when bubbles are elongated and disrupted. When a surfactant solution is studied in the falling film apparatus, the surface of the vertical film is hydrodynamically driven. Due to the downward liquid flow the film surface at the top is expanded, whereas the surface at the bottom where the liquid falls into a vessel, is compressed.

c) a surface tension gradient driven surface deformation. An example of this kind of deformation is the spreading of an oil droplet over the surface of an aqueous solution.

It may be clear that the deformation of the horizontal surface of the overflowing cylinder is definitely not of the first category. Comparable with

the surface of the free falling film in the falling film apparatus, the surface of the wetting film on the outside of the cylinder is hydrodynamically driven. It will be explained in the next chapter that in the presence of surface active components this wetting film causes a surface tension gradient driven flow of the liquid at the top of the cylinder. So in essence the dilational surface deformation of the overflowing cylinder is a combination of a hydrodynamically- and a surface tension gradient driven deformation. This is indeed different from the operation of all other surface dilational techniques which were mentioned in chapter 1.

References Chapter 2

[1] M.J. Boussinesq, Ann. Chim. Phys., 29 (1913) 349.

[2] D.J.M. Bergink-Martens, H.J. Bos, A. Prins and B.C. Schulte, J. Coll. Int. Sc., 138 (1990) 1.

[3] A. Prins and D.J.M. Bergink-Martens, in E. Dickinson and P. Walstra (Eds.), Food Colloids and Polymers: Stability and Mechanical Properties, Royal Society of Chemistry, Cambridge, (1993), pp. 291 - 300.

[4] F. van Voorst Vader, Th.F. Erkens and M. van den Tempel, Trans. Faraday Soc., 60 (1964) 1170.

[5] A.D. Ronteltap, Beer Foam Physics, Ph.D. thesis, Agricultural University Wageningen, (1989).

Chapter 3

Theoretical aspects

The fluid dynamical behaviour of pure liquids in the overflowing cylinder has been analyzed numerically, whereas the behaviour of surfactant solutions has been studied by deriving an algebraic expression for the relation between the relative surface expansion rate and the surface tension gradient (§3.1). The behaviour of surfactant solutions can also be approached from the point of view of transport of surfactant from the bulk fluid to the expanding surface by means of diffusion and convection. Both the dynamic surface tension and the excess surface tension can be related to transport parameters (§3.2). The height of the overflowing meniscus above the rim of the cylinder is for the greater part determined by the value of the dynamic surface tension. The value of the excess height of the overflowing meniscus compared to the situation of zero flow, is probably no proper measure for the relative surface expansion rate (§3.3). In the last paragraph of this chapter the separate theoretical elements are joined in an overall description of the physical mechanism of operation of the overflowing cylinder technique, which is put forward as a hypothesis (§3.4).

3.1 Fluid dynamics

The fluid dynamical behaviour of Newtonian liquids in the overflowing cylinder will be studied theoretically by analyzing and calculating the physical parameters in their dependence on the boundary conditions at the free surface. For this purpose the following overflowing cylinder configuration is considered.

Formulation of the problem

A semi-infinite cylindrical tube is cut perpendicular to its axis. The cylinder is positioned vertically in the gravitational field, and hence the axis of the cylinder coincides with the direction of the acceleration of gravity. A Newtonian liquid is pumped upward through the cylinder under atmospheric

pressure p_0 at room temperature T_0. In this cylinder geometry a cylindrical polar coordinate system is introduced. The axis of the coordinate system coincides with the axis of the cylinder and the origin of the coordinate system is chosen at an arbitrary distance below the rim of the cylinder. At the "entrance" of the cylinder ($z = 0$) a parabolic velocity profile is imposed on the Newtonian fluid. Because of the symmetry of the flowfield only half of the velocity field has to be considered, as indicated in Fig. 3.1. The fluid rises in the cylinder at a relatively low but constant rate till slightly above the rim. Next the fluid flows over the edge and falls as a thin film downward along the outside of the cylinder. The flowfield of the cylinder is assumed to be completely laminar (see chapter 4).

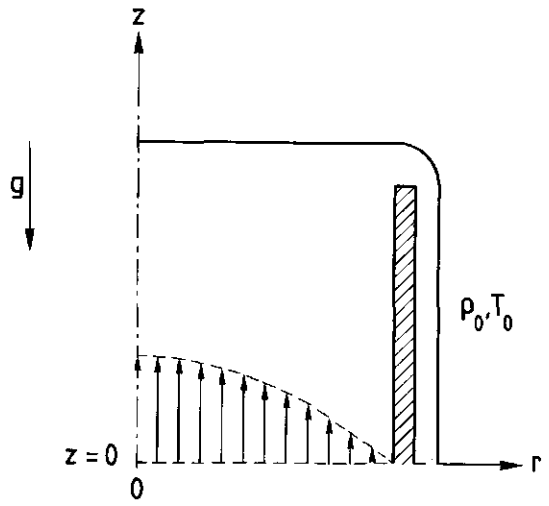

Figure 3.1: *Half of the velocity field in a crossplane through the axis of the cylinder geometry.*

The incompressible viscous flow in the cylinder is governed by the conservation equation of mass

$$\frac{\partial v_r}{\partial r} + \frac{\partial v_z}{\partial z} + \frac{v_r}{r} = 0 \,, \tag{3.1}$$

and by the three equations for the conservation of linear momentum: the

Navier-Stokes equations. Since the geometry is axially symmetrical and the flow is stationary, the Navier-Stokes equations reduce to

$$v_r \frac{\partial v_r}{\partial r} + v_z \frac{\partial v_r}{\partial z} = -\frac{1}{\rho}\frac{\partial p}{\partial r} + \nu\left(\nabla^2 v_r - \frac{v_r}{r^2}\right)$$

$$v_r \frac{\partial v_z}{\partial r} + v_z \frac{\partial v_z}{\partial z} = -\frac{1}{\rho}\frac{\partial p}{\partial z} + \nu \nabla^2 v_z - g. \qquad (3.2)$$

In these equations v_r and v_z are respectively the radial and vertical velocity components, p is the pressure, ν the kinematic viscosity, ρ the fluid density, and g is the acceleration due to gravity. The symbol ∇^2 indicates the Laplace operator

$$\nabla^2 = \frac{\partial^2}{\partial r^2} + \frac{1}{r}\frac{\partial}{\partial r} + \frac{\partial^2}{\partial z^2}. \qquad (3.3)$$

The flowfield in the overflowing cylinder is quantitatively described by equations (3.1) and (3.2). If a proper set of boundary conditions is specified, it is in principle possible to solve these equations.

Boundary conditions

The first boundary condition follows from the no slip condition which applies to the inside and outside of the solid wall so

$$v_r = v_z = 0 \quad for \quad r = R \ \wedge \ r = R + D_w, \qquad (3.4)$$

where D_w is the thickness of the wall. The second boundary condition follows from a free slip condition which is imposed on the axis of symmetry. The free slip condition implies that both the velocity normal to the axis of symmetry and the normal derivative of the velocity tangential to the axis of symmetry are zero:

$$(v_r)_{r=0} = 0 \quad \wedge \quad \left(\frac{\partial v_z}{\partial r}\right)_{r=0} = 0 \,. \tag{3.5}$$

What remains are the boundary conditions to be applied at the free surface. If surface active components are present in the overflowing liquid, a surface tension gradient may operate at the free surface. It is to be expected that in this practical situation the surface tension gradient will depend on r. Because of the fact that this is a complex configuration, two simpler systems will be considered here first:

i) a system in which no surface tension is taken into account, and

ii) a system in which a constant surface tension is incorporated (the surface tension gradient equals zero).

A constant surface tension

With respect to the systems i) and ii) Bos [1] obtained a numerical solution of equations (3.1) and (3.2). He analyzed and calculated the form of the fluid-air interface, the velocity field in the fluid, and the pressure distribution on a finite domain. In the solution procedure he made a choice for an explicit time dependent strategy. This implied that time dependent terms which were deleted in equations (3.2), had to be added again, yielding the time dependent Navier-Stokes equations. These unsteady equations were solved by an explicit Eulerian finite difference scheme on an orthogonal nonuniform Cartesian grid. The Newtonian liquid considered was pure water. At the start of the procedure the cylinder was filled to the rim with fluid and at time t=0 the flow was switched on by imposing the velocity profile already indicated in Fig. 3.1. Next the displacement of the free surface was tracked and the velocity field was calculated till after some time the flow converged into a steady state. He performed this type of calculation for several mass fluxes with and without surface tension. Some of the results of pure water at a temperature of 20 °C are presented below for a cylinder of radius R = 4 cm having a wall thickness of 2 mm.

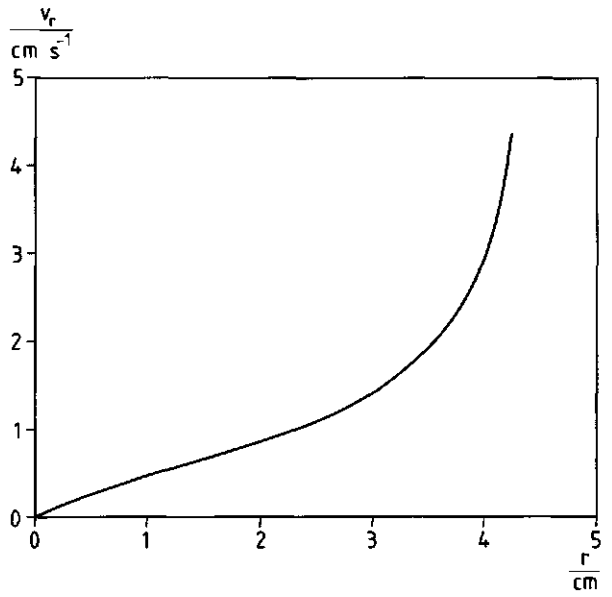

Figure 3.2: *The velocity distribution in the surface of pure water; Q = 33.3 cm^3/s.*

Fig. 3.2 shows the velocity distribution in the surface of pure water for a typical mass flow rate. In the vicinity of the centre of the circular meniscus the radial velocity appears to be linearly dependent on r. Consequently in this area the relative surface expansion rate given in eq. (2.2) can be simplified to

$$\mathrm{d}\ln A/\mathrm{d}t = \frac{v_r}{r} + \frac{\partial v_r}{\partial r} = 2\frac{v_r}{r} . \qquad (3.6)$$

Based on Fig. 3.2 the value of dlnA/dt in the vicinity of the centre equals 0.89 s^{-1} for Q = 7.6 cm^3/s. In Fig. 3.3 the relative surface expansion rate at the centre of the surface is presented as a function of the mass flow rate.
In Fig. 3.4 the overall radial velocity distribution in pure water is given. It is noticed from the figure that in the neighbourhood of the rim of the cylinder the maximum radial velocity occurs below the free surface. This implies that the bulk fluid drives the free surface and the surface layer via viscous forces. Further, in Fig. 3.5 Bos calculated the height of the centre of the meniscus above the rim of the cylinder, h_{dyn}, as a function of the mass flow rate with

surface tension switched on and surface tension switched off. He noted that h_{dyn} is strongly dependent on the value of the surface tension.

Figs. 3.2, 3.3, and 3.5 will be compared with experiments in chapter 5.

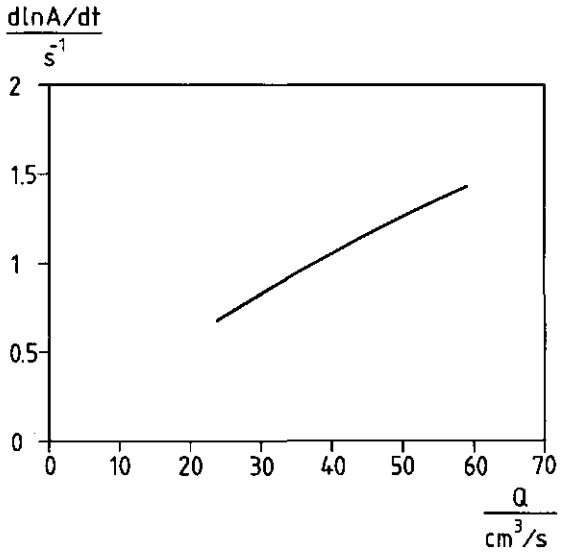

Figure 3.3: *The relative surface expansion rate of pure water at the centre of the surface as a function of the mass flow rate.*

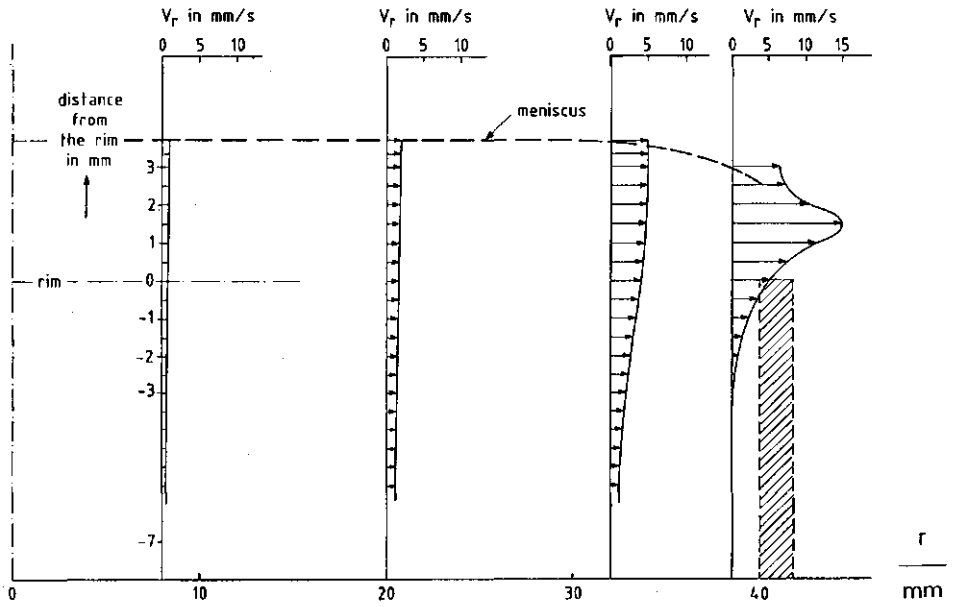

Figure 3.4: *The velocity distribution in pure water; Q = 7.6 cm³/s.*

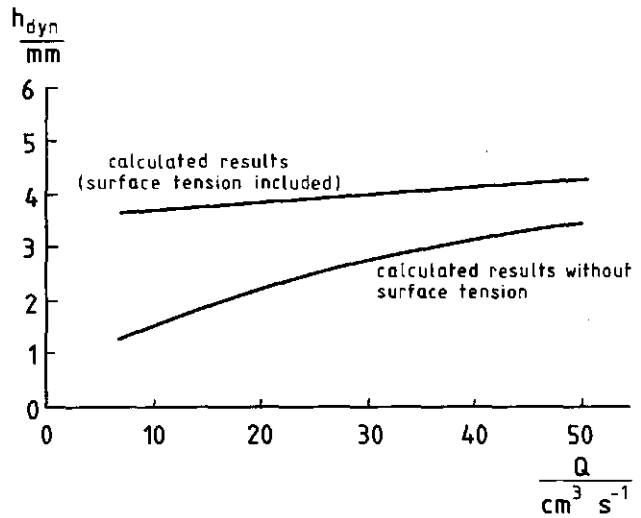

Figure 3.5: *The height of the centre of the meniscus above the rim of the cylinder as a function of the mass flow rate through the cylinder with surface tension switched on and surface tension switched off.*

A surface tension gradient incorporated

So far only the relatively simple systems i) and ii) have been considered. The latter system refers to pure liquids having a constant surface tension. In the overflowing cylinder the free surface of pure liquid systems is passive and the surface velocity distribution is dominated by the bulk flow. Due to the bulk flow the top surface is stretched nonuniformly. Near the rim of the cylinder the surface dilation is larger than in the centre. Hence, when liquids containing surface active components are introduced in the overflowing cylinder, the dynamic surface tension near the rim may be higher than in the centre. The creation of the surface tension gradient over the top surface may be strengthened by the condition of mechanical equilibrium with the vertical film surface (see §3.4). The resulting surface tension gradient changes the surface flow completely. The surface tension gradient influences a thin liquid layer on top of the bulk flow. Due to the surface tension gradient the thin surface layer is accelerated moving from the centre of the surface towards the rim of the cylinder. In this steady state situation the resulting surface velocity will be considerably higher than in the absence of surfactants.

In order to obtain a quantitative insight in the region of influence of the interaction between the surface tension gradient and the surface flow Bos [2] performed a simplified analysis. In the analysis the stretching of the surface by the surface tension gradient was assumed to be the propulsion mechanism of the free surface flow. The influence of transport of surface active components to the expanding surface was left out of the analysis.

One of the intrinsic properties of the liquid flow in the overflowing cylinder is the existence of a stagnation point. The stagnation point is located in the free top surface at the intersection with the axis of symmetry. It was noticed from Fig. 3.2 that in the vicinity of the stagnation point the calculated radial surface velocity of pure water is linearly proportional to the distance from the stagnation point. The experimental results of chapter 5 will show that this behaviour is not only found for pure water, but also for aqueous surfactant solutions. However, a large quantitative difference between the two systems is the constant of proportionality, since for surfactant solutions this constant is a multiple of the constant for pure water. In a first approximation to a description of the complete flow in the overflowing cylinder Bos analyzed the flow in the vicinity of the stagnation point, where due to the linear relationship between the surface velocity and the radial coordinate according to eq. (3.6) dlnA/dt is a constant. His analysis of the uniformly stretched surface was based upon the conservation equation of mass (3.1) and the Navier-Stokes eqs. (3.2). In the local area near the stagnation point Bos assumed a similarity solution. The vertical coordinate z was non-dimensionalized by defining a new coordinate η. Also a stream function $f(\eta)$ was introduced, and the velocity components v_r and v_z were related to $f(\eta)$ in such a way that the conservation equation of mass (3.1) was satisfied. In a next step Bos expressed the Navier-Stokes equations (3.2) and the boundary conditions [2] in terms of $f(\eta)$ and its derivatives. The Navier-Stokes equation for the radial momentum flux was solved by means of a 4^{th} order Runge-Kutta scheme. The final solution showed the stream function $f(\eta)$ and its derivatives as a function of η.

When a surfactant solution generates a surface tension gradient, a tangential shear stress is present in the free surface. The tangential shear stress is balanced by the viscous shear stress, yielding at the surface

$$\frac{d\gamma}{dr} = \eta_b \left(\frac{\partial v_r}{\partial z}\right), \tag{3.7}$$

where η_b is the dynamic viscosity coefficient of the bulk fluid. After having related v_r to the stream function $f(\eta)$ and having found a solution for $f(\eta)$, Bos was able to rewrite eq. (3.7) as

$$\frac{d\gamma}{dr} = 0.415\ r\ \sqrt{\eta_b \rho}\ (d\ln A/dt)^{\frac{3}{2}}. \tag{3.8}$$

The validity of this equation is limited to the vicinity of the stagnation point. There dlnA/dt is a constant implying according to eq. (3.8) that, like v_r, also $d\gamma/dr$ is linearly dependent on r in this area. Upon rewriting eq. (3.8) again the relative surface expansion rate can be expressed in terms of the surface tension gradient. Because of the fact that also for a zero surface tension gradient a non-zero expansion rate exists, it seems plausible to add a term $\{d\ln A/dt\}_0$ symbolizing the relative surface expansion rate of the pure liquid:

$$d\ln A/dt = \left(0.415\ r\ \sqrt{\eta_b \rho}\right)^{-\frac{2}{3}} \left(\frac{d\gamma}{dr}\right)^{\frac{2}{3}} + \{d\ln A/dt\}_0. \tag{3.9}$$

In the analysis mentioned above the surface tension gradient was assumed to influence a thin layer on top of the bulk flow. Bos found for the thickness δ_Q of this layer

$$\delta_Q = \frac{3\sqrt{2\nu}}{\sqrt{d\ln A/dt}}. \tag{3.10}$$

Summarizing, due to the presence of a surface tension gradient for surfactant solutions in the overflowing cylinder the behaviour of the surface differs

considerably from the behaviour when dealing with pure liquids. The surface itself contributes to the surface flow and the magnitude of the resulting relative expansion rate is directly related to the magnitude of the surface tension gradient.

3.2 Transport phenomena

In this paragraph the behaviour of surfactant solutions in the overflowing cylinder will be approached from another point of view. Here the transport of surfactant from the bulk fluid to the expanding surface will be studied.

Formulation of the problem

The radial movement of the surface over the top rim of the cylinder leads to a constant discharge of surface active material. Assuming for the sake of simplicity that both the relative expansion rate dlnA/dt and the adsorbed amount of surfactant Γ are uniform over the surface, the amount of surfactant, n_s, discharged per unit area A and unit time t is given by

$$\frac{1}{A}\frac{dn_s}{dt} = \Gamma \, d\ln A/dt. \qquad (3.11)$$

At the same time surface active material is supplied from the bulk solution by means of diffusion and convection. Generally the system will not succeed in restoring the equilibrium situation, and consequently due to the surfactant depletion in the expanding area, the dynamic surface tension will be higher than the equilibrium one, as has already been noticed in chapter 2. However, because of the fact that the expanding surface is in a steady state, the amount of surfactant transported to the surface equals the amount that flows away over the rim of the cylinder. This situation forms the basis of the overflowing cylinder transport problem.

The surface Fourier number

Prins [3] approached this problem by defining a dimensionless surface Fourier number, Fo_s, being the ratio of the potential supply rate of surfactant diffusing to the surface to the discharge rate of surfactant from the surface. He took the fraction Γ/t as an order of magnitude of the potential transport rate of surfactant to the expanding surface. He obtained an expression for Γ/t on the basis of the penetration theory, implying that only the diffusion part of the transport was taken into account. The penetration theory gives the distance l over which a substance, having a diffusion coefficient D, is transported in a time t:

$$l = \sqrt{\pi D t} \; . \tag{3.12}$$

Prins suggested that in the overflowing cylinder a surfactant, which is present in the bulk fluid to the concentration c_b, has to travel over a distance $l = \Gamma/c_b$ in order to accomplish an adsorption Γ at the surface. It follows from the equation of the two length scales that

$$\frac{\Gamma^2}{c_b^{\,2}} = \pi D t. \tag{3.13}$$

Now the expression for the potential transport rate easily follows from eq. (3.13):

$$\frac{\Gamma}{t} = \frac{c_b^{\,2} \pi D}{\Gamma}. \tag{3.14}$$

According to eq. (3.14) the potential transport rate increases proportional to the square of the concentration in the bulk. Using eqs. (3.11) and (3.14) Prins introduced the surface Fourier number

$$Fo_s \equiv \frac{potential\ supply\ rate}{discharge\ rate} = c_b^{\,2} \frac{\pi D}{\Gamma^2 \mathrm{d}\ln A/\mathrm{d}t}. \tag{3.15}$$

For high values of Fo_s the dynamic surface tension of the expanding surface

will be relatively low, or even approximate to the equilibrium value. Prins calculated the value of Fo_s for various concentrations of a commercially available Teepol solution in water. He noticed that both γ_{dyn} and the foamability of the dilutions are related to the value of Fo_s to the effect that with increasing Fo_s the foamability increases, whereas γ_{dyn} decreases. In this way the surface Fourier number is a measure for the diffusion efficiency of a surfactant to the expanding surface of the overflowing cylinder and a parameter in describing the value of its dynamic surface tension.

The magnitude of the excess surface tension

Starting from basically the same problem as Prins, Van Voorst Vader [4] studied the magnitude of the excess surface tension $\Delta\gamma$ ($= \gamma_{dyn} - \gamma_e$) during continuous expansion of a liquid surface. Experimentally he accomplished a continuous surface expansion by means of moving barriers in a Langmuir trough. Theoretically he succeeded in relating the resulting deviation in surface tension, $\Delta\gamma$, with the relative rate of expansion of the surface, dlnA/dt. He considered solutions of non-ionic, non volatile surfactants, and both diffusion and convection of the surfactant were taken into account. Further, he assumed instantaneous equilibrium between the surface and the sub-surface layer. The final expression Van Voorst Vader obtained, is based upon eq. (3.11) as well as upon the following four equations.

i) The Szyszkowski equation

$$\gamma_L - \gamma_e = RT\,\Gamma_\infty \ln(1 + \frac{c_b}{a}), \tag{3.16}$$

where γ_L is the surface tension of the pure solvent, Γ_∞ symbolizes the saturation adsorption of the surfactant, a is a constant, and R and T are the gas constant and the absolute temperature respectively.

ii) The Langmuir equation

$$\Gamma = \Gamma_\infty \frac{c_b}{a + c_b} \tag{3.17}$$

gives the relative surfactant adsorption Γ at the bulk concentration c_b. The surfactant adsorption at the expanding surface is also given by this equation provided that the sub-surface concentration c_0 is substituted for c_b.

iii) The diffusion equation

$$\frac{1}{A}\frac{dn_s}{dt} = D\frac{\partial c}{\partial z} \tag{3.18}$$

with z again the coordinate perpendicular to the horizontal top surface. This equation reflects that the increase in the amount of surfactant adsorbed at the surface is caused by diffusion.

iv) The so called equation of convective diffusion. By changing the surface area, convection is introduced, and this convection must be accounted for in the diffusion equation. For an incompressible fluid in a steady state the equation of convective diffusion reads

$$D\nabla^2 c = \vec{v}\,\nabla c \tag{3.19}$$

with $\vec{v}$ the liquid velocity vector and the symbol ∇^2 indicating the Laplace operator. Van Voorst Vader neglected horizontal components of the concentration gradient, yielding the following simplification of equation (3.19)

$$D\frac{\partial^2 c}{\partial z^2} = v_z\frac{\partial c}{\partial z}. \tag{3.20}$$

In a Langmuir trough the z-component of the liquid velocity in a thin layer immediately below the surface equals

$$v_z = -d\ln A/dt \cdot z, \tag{3.21}$$

and consequently eq. (3.20) can be rewritten as

$$D\frac{\partial^2 c}{\partial z^2} = -d\ln A/dt \cdot z\frac{\partial c}{\partial z}. \tag{3.22}$$

By repeated integration of eq. (3.22) Van Voorst Vader obtained an expression for the difference in concentration between the bulk and the sub-

surface layer. The excess surface tension was found by combining this expression with eq. (3.11) and the equations under i) up to and including iv). The final result was

$$\Delta\gamma = RT\,\Gamma_\infty \ln\left\{\frac{2(1+Q)}{(1+Q-P)+\sqrt{(1-Q+P)^2+4Q}}\right\}, \qquad (3.23)$$

where the dimensionless quantities Q and P have been introduced to simplify the equation;

$$Q = \frac{c_b}{a}\,; \qquad P = \frac{\Gamma_\infty}{a}\sqrt{\frac{\pi \cdot d\ln A/dt}{2D}}. \qquad (3.24)$$

Van Voorst Vader obtained a good fit between experimentally observed values of the excess surface tension and those calculated by eq. (3.23). So he concluded that the theory he developed is essentially correct.

The question is whether this theory may be applied to the expanding surface of the overflowing cylinder as well. Of course, the validity of the equations under i), ii), and iii) are not limited to a specific apparatus. The equation of convective diffusion, eq. (3.19), reads for the cylindrical polar coordinate system of the overflowing cylinder

$$D\left\{\left(\frac{\partial^2}{\partial r^2}+\frac{1}{r}\frac{\partial}{\partial r}+\frac{\partial^2}{\partial z^2}\right)c\right\} = v_z\frac{\partial c}{\partial z}+v_r\frac{\partial c}{\partial r}, \qquad (3.25)$$

where eq. (3.3) for the Laplace operator has been used. Also in this case the horizontal components of the first- and second derivative of the concentration may be neglected compared to the vertical components, again yielding the simplified eq. (3.20). Further, from a combination of eq. (3.1) of the conservation of mass and the expression for the relative surface expansion rate eq. (2.2) it easily follows that eqs. (3.21) and (3.22) are also applicable to the expanding surface of the overflowing cylinder. The conclusion may be

drawn that the relations which led to the final expression Van Voorst Vader obtained for the Langmuir trough, are valid for the expanding surface of the overflowing cylinder as well, implying that also the final result itself, expressed by eqs. (3.23) and (3.24), can be applied to the overflowing cylinder.

Summary

Now two approaches to discussing experimental results of the overflowing cylinder within the framework of the transport phenomena at the expanding surface are available. Firstly the magnitude of the dynamic surface tension can be studied in its relationship with the surface Fourier number Prins defined, and secondly the obtained value for the excess surface tension can be compared to the theoretical value which follows from the theory Van Voorst Vader developed. In chapter 5 both approaches will be used to discuss the experimental data.

3.3 The height of the meniscus

For pure liquids in the overflowing cylinder Bos [1] is able to calculate the form of the fluid-air interface from the numerical solutions of the Navier-Stokes equations (see §3.1). He noted that the height of the centre of the meniscus above the rim of the cylinder, h_{dyn}, is strongly dependent on the value of the surface tension. For surfactant solutions in the overflowing cylinder no calculated values of h_{dyn} are available. However, despite realizing that the horizontal velocity profile in the meniscus differs from the one of pure liquids, analogous to the case of pure liquids the value of h_{dyn} may expected to be dependent on the value of the surface tension of the expanding surface. In this paragraph a simple relation between h_{dyn} and γ_{dyn} will be deduced.

The equilibrium meniscus

First consider the cylinder to be filled till above the rim on condition that just no overflow takes place. In this equilibrium situation the curvature of the meniscus gives rise to an overpressure in the fluid meniscus to the extend of the Laplace pressure difference ΔP:

$$\Delta P = \left(\frac{1}{R_a} + \frac{1}{R_b} \right) \cdot \gamma_e. \tag{3.26}$$

Here R_a and R_b are the principal radii of curvature of the equilibrium meniscus.

If this were a situation of capillary rise, the Laplace pressure difference would equal the pressure of the fluid risen to height h in the capillary, according to

$$\Delta P = \rho g h. \tag{3.27}$$

In fact analogous to capillary rise the height of the equilibrium meniscus of the overflowing cylinder is such that the pressure of fluid in the meniscus equals the Laplace pressure difference. So eq. (3.27) is also valid for the height h_e of the meniscus above the rim of the cylinder, when just no overflow takes place. Combining eqs. (3.26) and (3.27) gives the following expression for the height of the equilibrium meniscus

$$h_e = \frac{1}{\rho g} \left(\frac{1}{R_a} + \frac{1}{R_b} \right) \cdot \gamma_e. \tag{3.28}$$

The overflowing meniscus

When the liquid is allowed to flow over the rim of the cylinder, the curvature of the meniscus will change. In Fig. 3.6 the principal radii of curvature of the overflowing meniscus, R_1 and R_2 , are shown for the axially symmetrical configuration of the overflowing cylinder. Besides that the value of the surface tension of the continuous expanding surface will generally be higher than the equilibrium value. By adding to eq. (3.28) a term Δh_{flow} representing

the excess height due to the flow of liquid and by replacing γ_e by γ_{dyn}, and R_a and R_b by R_1 and R_2 respectively, the following expression for h_{dyn} is obtained:

$$h_{dyn} = \frac{1}{\rho g}\left(\frac{1}{R_1} + \frac{1}{R_2}\right) \cdot \gamma_{dyn} + \Delta h_{flow}. \qquad (3.29)$$

The first term on the right hand side of eq. (3.29) is the height of the imaginary meniscus of zero flow, not to be confused with the equilibrium meniscus. The principal radii of curvature of the equilibrium meniscus are R_a and R_b and its surface tension is the equilibrium surface tension, whereas the meniscus of zero flow is supposed to have the same curvature and dynamic surface tension as the overflowing meniscus.

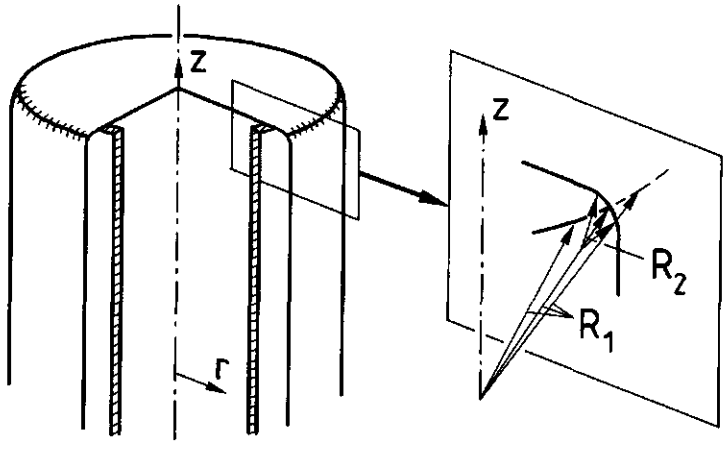

Fig. 3.6: The principal radii of curvature of the fluid meniscus, R_1 and R_2.

It has to be noted that possible effects on h_{dyn} of a surface tension gradient present on the surface have not explicitly been accounted for in eq. (3.29) assuming that these effects are small.

The relation between h_{dyn} and γ_{dyn} will be studied experimentally in chapter 5 for different surfactant solutions at a fixed flowrate in order to verify eq. (3.29).

The excess height

Joos [5] used the value of the excess height, Δh_{flow}, as a measure for the relative expansion rate of the expanding surface of his overflowing funnel. Similar to eq. (3.29) he defined Δh_{flow} as

$$\Delta h_{flow} = h_{dyn} - h_0, \tag{3.30}$$

however, without giving an expression for the height of the meniscus of zero flow, h_0. Joos stated that the volume of liquid, V, flowing over the rim of the funnel equals

$$V = A \cdot \Delta h_{flow}, \tag{3.31}$$

and consequently the flowrate through the funnel can be given by

$$Q = \Delta h_{flow} \cdot \frac{dA}{dt}, \tag{3.32}$$

resulting in the following relation between the relative surface expansion rate and Δh_{flow}:

$$\mathrm{d}\ln A/\mathrm{d}t = \frac{Q}{A \cdot \Delta h_{flow}}. \tag{3.33}$$

This relation has been based on two assumptions which are both invalid for the overflowing cylinder according to the information given in this chapter. Firstly Joos attributes the transport of fluid only to the excess height Δh_{flow}, whereas Fig. 3.3 shows that the entire meniscus contributes to the transport. Even the radial velocity of the fluid below the level of the rim of the cylinder has a finite value. Secondly Joos assumes that the radial velocity of the fluid in the entire volume of height Δh_{flow} equals the velocity of the surface. This may approximately be the case for pure liquids in the overflowing cylinder, but is invalid for surfactant solutions, when a surface tension gradient is present over the surface. In that case, according to eq. (3.7), the tangential shear stress at the surface is balanced by the viscous shear stress yielding a normal derivative of the radial velocity which is definitely not zero at the

surface. So eq. (3.33) is unlikely to be accurate enough for Δh_{flow} to serve as a measure for the value of the relative expansion rate of the surface of the overflowing cylinder.

3.4 Physical mechanism of operation

In the last paragraph of this theoretical chapter an overall description of the physical mechanism of operation of the overflowing cylinder technique will be put forward as a hypothesis. The various elements which have been dealt with seperately in the previous paragraphs will be joined here, and their mutual relationschips will be described. So this paragraph will try to give an answer to the question how and why the fluid flows over the rim of the overflowing cylinder.

Surfactant solutions in the overflowing cylinder behave fundamentally different from pure liquids, because only a fluid containing surface active material is able to create a surface tension gradient, which may have enormous effects on the fluid behaviour. For that reason the two systems will be elucidated here separately.

Pure liquids

In the case of pure liquids the dynamic surface tension of the continuous expanding surface equals the equilibrium value. This value is assumed to determine, for the greater part, the value of h_{dyn}, as has been stated in the previous paragraph. Since the free surface is not able to create a surface shear stress, a viscous shear stress can not be compensated for. Consequently according to eq. (3.7) the normal derivative of the radial velocity of the surface is zero:

$$\left(\frac{\partial v_r}{\partial z}\right) = 0. \tag{3.34}$$

Apart from the pumping action, the only force driving the overflowing liquid is the gravitational force. During the steady state of flowing the meniscus must be slightly higher in the centre than near the rim of the cylinder, so that the fluid is forced into the direction of the rim in the gravitational field. The wetting film on the outside of the cylinder falls in the gravitational field as well. Since according to eq. (3.34) the radial velocity of the sub-surface layer equals the velocity of the surface, the velocity profiles must be as indicated in Fig. 3.7. The velocity profile of the horizontal top surface is similar to the one calculated in Fig. 3.4. Both the horizontal top surface and the film surface are driven by the sub-surface layers via viscous forces. The conclusion may be drawn that in the case of pure liquids in the overflowing cylinder the bulk drives the surface. Consequently the continuous expansion of the top surface can be categorized as a hydrodynamically driven surface deformation.

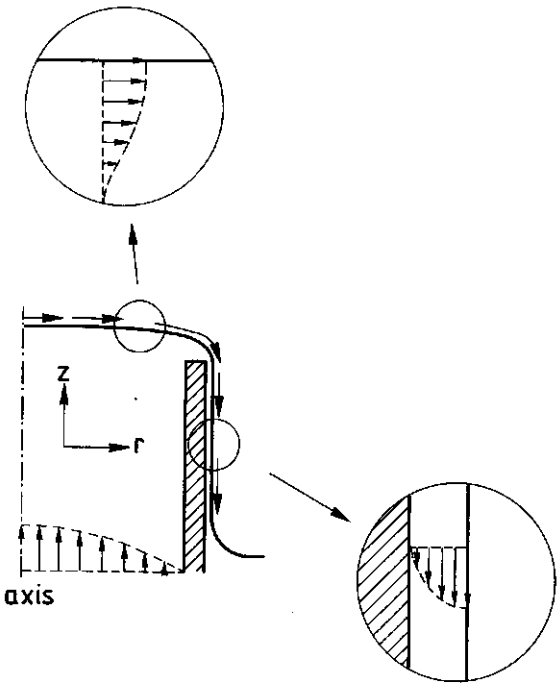

Fig. 3.7: Illustration of the physical mechanism of operation of the overflowing cylinder for pure liquids.

Surfactant solutions

If a surfactant is added to the liquid in the overflowing cylinder, the free surface will be able to generate a surface shear stress which compensates for a viscous shear stress. This implies that eq. (3.7) has to be used, and consequently at the surface the normal derivative of the radial fluid velocity may deviate from the zero value. In order to be able to explain how the overflowing cylinder operates in this situation, it is necessary to go into more details about the wetting film first.

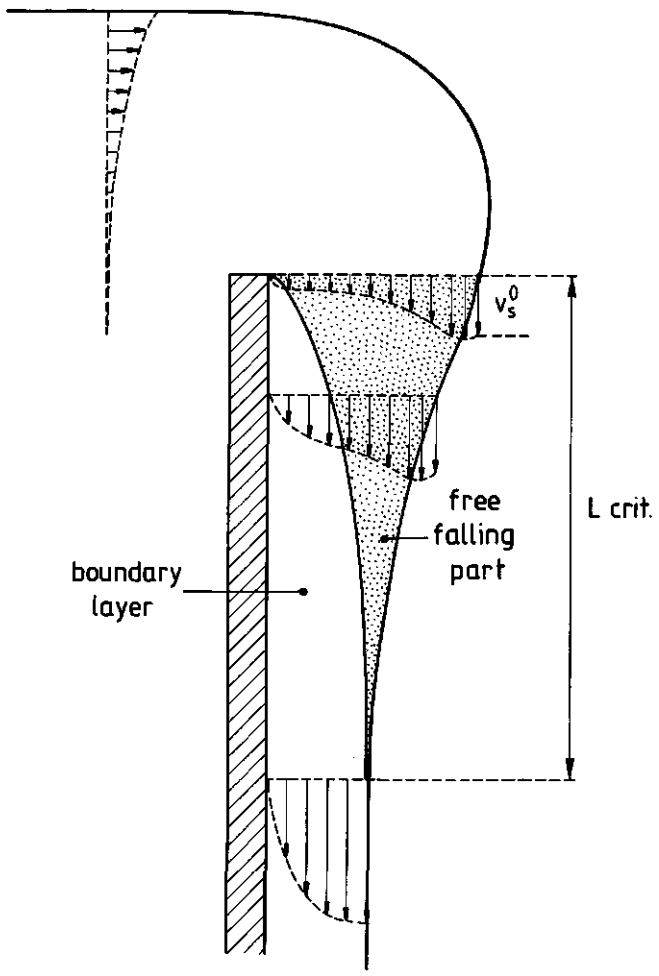

Fig. 3.8: Cross-section of the wetting film indicating the boundary layer and velocity profiles at various heights (not to scale).

The downward flow of liquid in the wetting film on the outside of the cylinder is influenced by a boundary layer which is built up along the wall. The boundary layer gradually covers a bigger part of the film, until the boundary layer reaches the film surface at a length L_{crit}. At this length the boundary layer has become of the same thickness as the wetting film. In one of the papers preceding this thesis Bos [6] derived the following expression for L_{crit}:

$$L_{crit} = \frac{\left(v_s^0\right)^2}{2g}\left[\left(\frac{\delta_0^2\ \rho g}{\eta_b\ v_s^0}\right)^{\frac{2}{3}} - 1\right], \tag{3.35}$$

where v_s^0 and δ_0 are respectively the surface velocity and the thickness of the wetting film near the rim of the cylinder as defined in Fig. 2.3. The order of magnitude of L_{crit} is a few centimeters. Fig. 3.8 shows which velocity profiles may be present in the wetting film at various heights. Following the wetting film on its way down, the boundary layer gradually influences a bigger part of the velocity profile. From the length L_{crit} on the presence of the boundary layer determines the velocity of the wetting film completely resulting in a half parabolic velocity profile. In Fig. 3.8 the shaded part of the wetting film may be considered the free falling part of the film. As long as the length L of the wetting film is smaller than L_{crit}, the volume, and consequently also the weigth, of the free falling part can be varied by changing L. The length L can be imposed on the liquid in the overflowing cylinder by changing the total amount of fluid present in the system, as has been explained in chapter 2. While L is increased to values larger than L_{crit} the weight of the free falling part of the wetting film stays the same. The weight of the free falling part of the wetting film is assumed to determine the behaviour of the expanding top surface via the creation of a surface tension gradient in the following way.

The free falling part of the film exerts a gravitational force on the vertical surface, which is expanded very rapidly, causing the dynamic surface tension to be higher near the rim of the cylinder than at a distance L_{crit} from the rim.

The horizontal top surface has to be in mechanical equilibrium with the vertical film surface. There the dynamic surface tension at the rim of the cylinder will be higher than in the centre of the surface. For a fixed length of the wetting film the magnitude of the created surface tension gradient depends on the transport properties of the applied surfactant(s). The surface tension gradient of the horizontal surface induces a steady state acceleration of the free surface in the direction of the area having the highest surface tension. So, compared with pure liquids, the surface of the surfactant solution moves towards the rim of the cylinder with an increased velocity. The relative surface expansion rate will correspondingly be larger as well. In turn the relative surface expansion rate gives rise to a dynamic surface tension which is generally higher than the equilibrium surface tension. Its absolute steady state value is again determined by diffusion and convection of the surfactant(s). The height of the meniscus above the rim of the cylinder will be strongly influenced by γ_{dyn}. Because of the fact that in this situation the surface tension gradient is the driving force of the surface deformation, in the centre of the surface the meniscus does not have to be as convex as for pure liquids.
In this way the weight of the free falling part of the wetting film is assumed to determine the behaviour of the expanding top surface. However, the weight of the free falling part, and consequently the magnitude of the created surface tension gradient, are dependent on the length of the wetting film. So for example the relative expansion rate of the top surface of the overflowing cylinder can be deminished via the magnitude of its surface tension gradient simply by decreasing the length of the wetting film on the outside of the cylinder.

For surfactant solutions the mechanism of operation of the overflowing cylinder is illustrated by the velocity profiles in Fig. 3.9. Due to the surface tension gradient the horizontal top surface drives the bulk fluid, and consequently the maximum radial velocity can be found in the free surface. In the

wetting film the opposite is the case. A liquid driven surface tension gradient is present over the surface of the free falling part of the film, and the highest surface tension is found near the rim of the cylinder. So the surface will try to slow down the film fluid. From the length L_{crit} on, however, the boundary layer determines the velocity profile of the wetting film completely, and in the absence of a surface tension gradient the surface moves freely with the same velocity as the sub-surface layer.

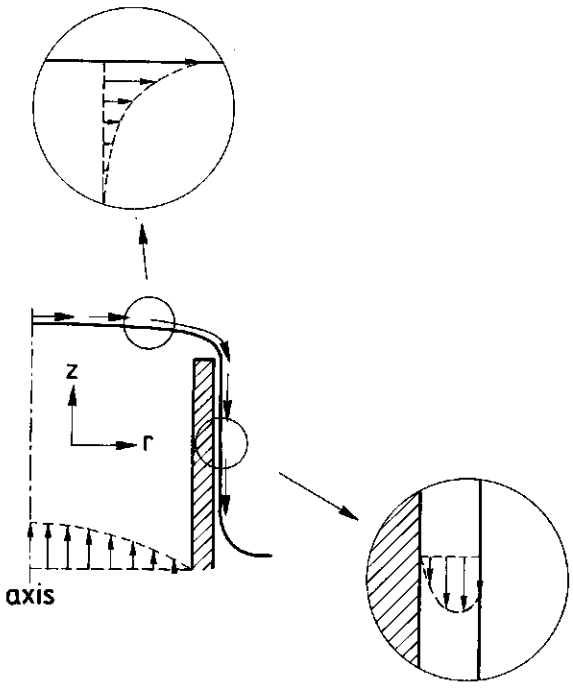

Fig. 3.9: *Illustration of the physical mechanism of operation of the overflowing cylinder for surfactant solutions.*

Summarizing, for surfactant solutions in the overflowing cylinder the free falling part of the wetting film is supposed to pull the horizontal surface and the adhering liquid over the rim of the cylinder via the creation of a surface tension gradient. The continuous expansion of the top surface can therefore be categorized as a surface tension gradient driven surface deformation.

References chapter 3

[1] D.J.M. Bergink-Martens, H.J. Bos, A. Prins and B.C. Schulte, J. Coll. Int. Sc., 138 (1990) 1.

[2] D.J.M. Bergink-Martens, H.J. Bos, A. Prins, submitted for publication in J. Coll. Int. Sc.

[3] A. Prins and D.J.M. Bergink-Martens, in E. Dickinson and P. Walstra (Eds.), Food Colloids and Polymers: Stability and Mechanical Properties, Royal Society of Chemistry, Cambridge, (1993), pp. 291 - 300.

[4] F. van Voorst Vader, Th.F. Erkens and M. van den Tempel, Trans. Faraday Soc., 60 (1964) 1170.

[5] P. Joos and P. de Keyser, The Overflowing Funnel as a Method for Measuring Surface Dilational Properties, Levich Birthday Conference, Madrid, (1980).

[6] D.J.M. Bergink-Martens, C.G.J. Bisperink, H.J. Bos, A. Prins and A.F. Zuidberg, Coll. and Surf., 65 (1992) 191.

Chapter 4

Methods and materials

In this research project a sophisticated overflowing cylinder set-up which also provided the equipment to measure the physical parameters introduced in chapter 2, was used (§4.1). Extra attention was paid to the radial surface velocity by developing various methods to determine its value. Also the differential laser Doppler anemometer was succesfully applied to the overflowing cylinder surface (§4.2). Some rheological instruments were used to measure bulk viscosities (§4.3). In the overflowing cylinder both solutions of commercially available (mixtures of) surfactants and rather pure surface active components were studied (§4.4).

4.1 The overflowing cylinder set-up

Experiments have been carried out on a temperature controlled metal cylinder having a diameter of 8 cm and a wall thickness of 1 mm. In order to prevent pumping vibrations from disturbing the horizontal top surface, the pump was uncoupled from the overflowing cylinder in a way shown in Fig. 4.1.
During an experiment the pump continuously sucks liquid out of the smaller glass vessel which is closely connected to the overflowing cylinder. With this liquid the hydrostatic pressure difference which exists between the fluid level in the bigger glass vessel and the top surface of the overflowing liquid, is kept constant. From the bigger vessel the fluid flows into the overflowing cylinder. In order to ensure a laminar flowfield in the cylinder, the fluid first passes through a conical tube having a small slope (1:10), before it reaches the cylindrical part. Next the liquid is allowed to flow over the horizontal top rim of the vertical cylinder forming a wetting film on the outside wall of the cylinder. When the cylinder is in a perfect vertical position, at its top surface a purely axially symmetric velocity distribution with zero velocity in the centre of the circular meniscus, is created. From the outer cylinder the fluid flows into the smaller vessel, out of which it is pumped upward again. In this way

the overflowing cylinder forms a closed system which contains about 3.8 liters of fluid. The total height of the overflowing cylinder, the conical part included, is about 70 cm.

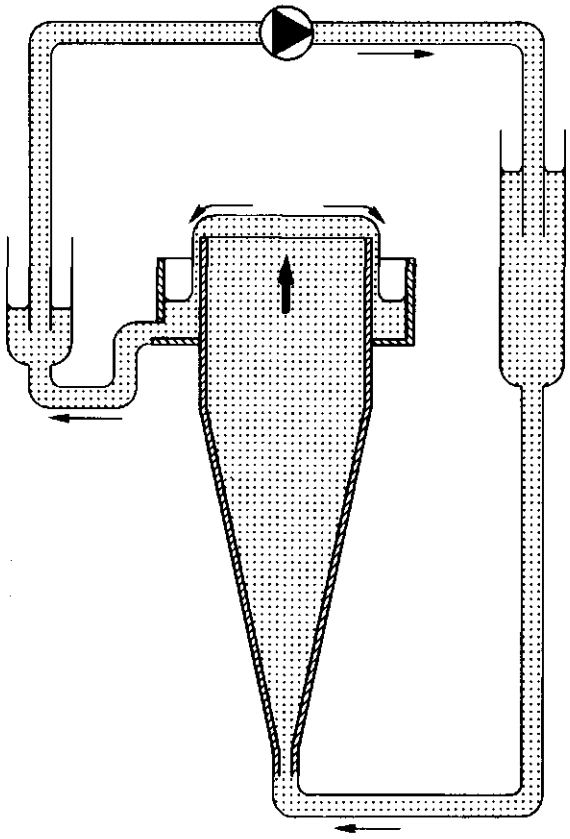

Fig. 4.1: Circulation of fluid through the overflowing cylinder system.

Measurement of the parameters

The flow through the cylinder can be adjusted and determined by means of a needle valve and a flowmeter. Care must be taken that the outside wall of the cylinder is completely wetted by the falling film. For aqueous solutions this condition requires a minimum flow rate of about 3 cm^3/s. The maximum flow rate used was 61.3 cm^3/s. Correspondingly the mean value of the vertical velocity in the cylinder could be varied between 0.6 and 12.2 mm/s.

The length L of the wetting film on the outside of the overflowing cylinder was adjusted by changing the total amount of fluid present in the system. L was varied from 0.7 till 6.0 cm with an accuracy of 0.1 cm.

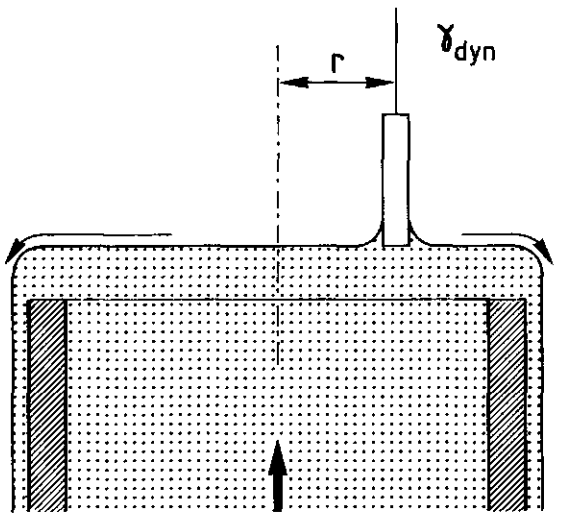

Fig. 4.2: Experimental set-up for the measurement of the dynamic surface tension γ_{dyn} as a function of the radial distance r.

The dynamic surface tension, γ_{dyn}, was measured according to the Wilhelmy plate technique. However, instead of the usual plate solid glass cylinders with diameters ranging from 1.2 to 5.2 mm were used. A cylinder has the advantage over a plate that 'point' measurements can be performed. Fig. 4.2 shows how a roughened glass cylinder was used to measure the dynamic surface tension as a function of the radial distance. In this way it was possible to study the surface tension gradient over the expanding surface of the overflowing cylinder. The glass cylinders have been calibrated at 25 °C in the centre of the circular meniscus by means of the expanding surface of pure water having a surface tension of 72.0 mN/m. At the same place, where the surface velocity equals zero, the dynamic surface tension of an arbitrary surfactant solution was measured. The result appeared to be independent of the diameter, d, of the applied Wilhelmy cylinder. Experiments were also carried out at radial distances r = 2 cm and r = 3 cm, in order to study the

influence of the surface velocity on the dynamic surface tension measurement. If the velocity affects the measured value, the effect is supposed to be more manifest the bigger the diameter of the Wilhelmy cylinder. Fig. 4.3 shows that no such trend is visible, implying that the surface velocity does not perceptibly influence the surface tension measurement. The accuracy of the measurement was estimated to be 0.3 mN/m. So within the accuracy margins the measured γ_{dyn} appears to be independent of the diameter of the Wilhelmy cylinder for all three radial distances studied.

The equilibrium surface tension, γ_e, was measured separately in a petri dish by means of the same Wilhelmy method.

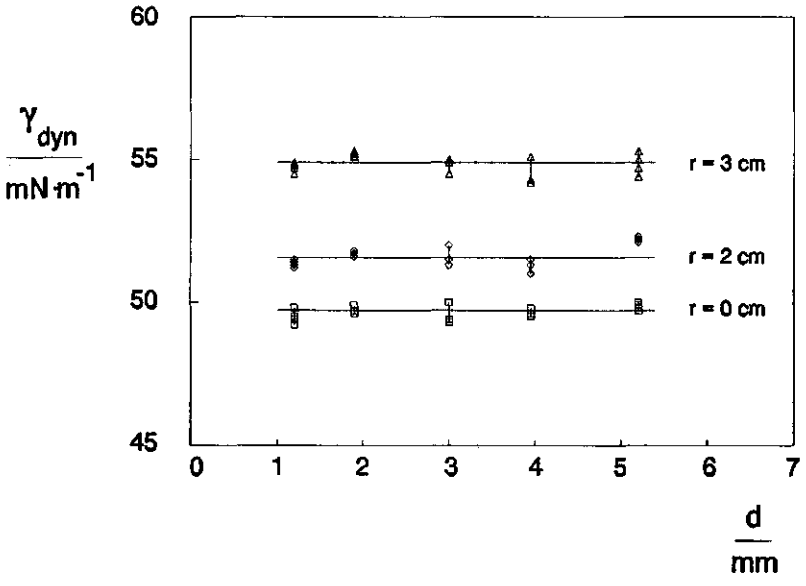

Fig. 4.3: The dynamic surface tension of an arbitrary surfactant solution as a function of the diameter, d, of the Wilhelmy cylinder at various radial distances.

Both the height of the centre of the meniscus above the rim of the cylinder, h_{dyn}, and the thickness of the wetting film near the rim, δ_0, were measured by means of a screw micrometer as accurately as ± 0.005 and ± 0.01 mm respectively.

In order to determine the value of the radius of curvature, R_2, photographs were taken of the meniscus of the overflowing liquid. Each photo was enlarged and the curvature of the enlarged meniscus was compared with the curvature of circles with rising radii. R_2 was defined to be the radius of the biggest circle which fitted the curvature of the meniscus. In Fig. 4.4 this circle and its radius have been indicated on the meniscus of an arbitrary surfactant solution. The maximum absolute error in the value of R_2 was experienced to be 0.2 mm.

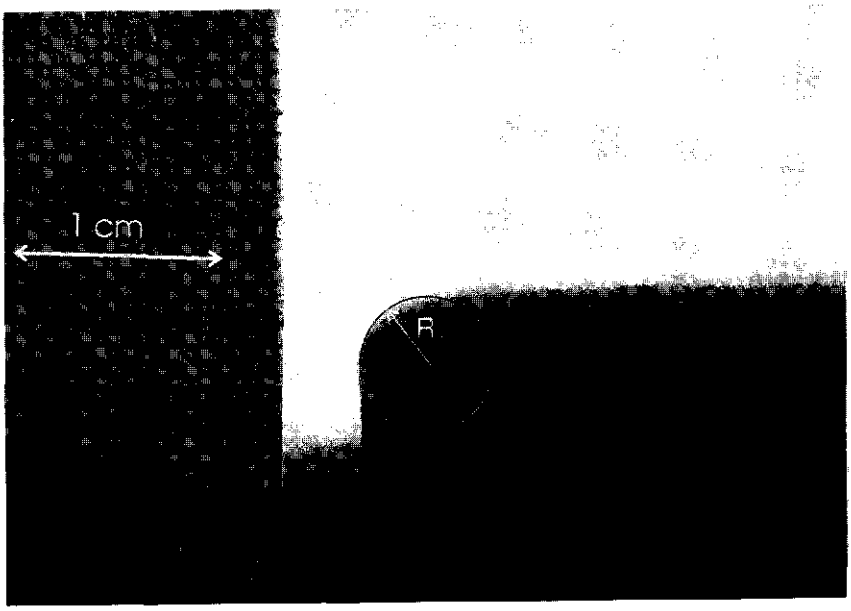

Fig. 4.4: *Photograph of a part of the overflowing meniscus of an arbitrary surfactant solution; the best fitting circle, its radius of curvature, and the scale have been indicated.*

For convenience the equipment which was used to measure the surface tension and the parameters h_{dyn} and δ_0, was attached to the main frame of the overflowing cylinder.

Besides the sophisticated overflowing cylinder which has been described in this paragraph, a large variety of other overflowing cylinders of different sizes is present in the laboratories where this research work has been carried out.

Most of these cylinders are made of glass and built according to the simple scheme given in Fig. 2.1. Since these overflowing cylinders are not the purpose of the investigation, but a tool in studying surfactant solutions, generally there is no need to uncouple the pump from the overflowing cylinder. The measured dynamic surface tension is namely experienced to be insensitive to pumping vibrations. So for most practical applications a simple overflowing cylinder set-up will do.

Laminar flow

The beginning of this paragraph described how the fluid in the overflowing cylinder first passes through a conical tube before reaching the cylindrical part, in order to ensure a laminar flowfield in the cylinder. No turbulence has ever been experienced, neither in the cylinder nor in the wetting film. No ripples have ever been noticed at the horizontal top surface. Particles which were used for the determination of the surface velocity (see next paragraph) have always been observed to move in straight lines radiating from the centre. All experimental results were so well reproducible, that even considering turbulent flow seems out of the question. Therefore the conclusion is drawn that the stationary flowfield of the overflowing cylinder is completely laminar for all solutions studied.

4.2 Measurement of the surface velocity

Various methods have been used to determine the value of the radial velocity, $v_r(r)$, of the expanding surface of the overflowing cylinder. The different methods provided different details and different accuracy.

Following a particle in time

A rough idea of the magnitude of v_r , was obtained by means of polypropylene particles (Shell, diameter $<$ 1.5 mm). Experimentally it was

found that these particles do not influence the equilibrium surface tension of water. One of these particles was placed on the expanding surface near its geometrical centre. This particle was visually followed in time on its way floating on the surface from the position at radial distance r = 1 cm to the rim of the cylinder. For each determination of the radial velocity the measurement was repeated at least 25 times with particles of various arbitrary diameters. In this easy way a mean surface velocity over the interval from r = 1 cm till r = 4 cm was obtained with an accuracy of 10% - 20%.

Taking photographs

In a more laborious experiment polyethylene particles with a diameter ranging from 90 - 130 μm and a density of 900 $kg.m^{-3}$ were used. These particles did not influence the equilibrium surface tension of water either. At the start of an experiment the polyethylene particles were sprinkled uniformly on the surface of the overflowing liquid. A split second later a photo of the expanding surface was taken, using two flashes with a fixed time interval. Both the time interval and the exposure time were chosen in such a way that the photo showed two sharp images of each particle. The radial velocity of the surface, $v_r(r)$, is obtained from the distance between the positions of a particle in the two images $r_2 - r_1$ and the time lapse between the two flashes Δt according to

$$v_r(r) = \frac{r_2 - r_1}{\Delta t} . \qquad (4.1)$$

The calculated velocity is joined to a radial coordinate r which, in a first appoximation, is the mean distance

$$r = \frac{r_2 + r_1}{2} . \qquad (4.2)$$

Although this method is rather time-consuming, because all distances are measured manually, the advantage is that rather detailed information about

the dependence of the surface velocity on the radial coordinate r can be obtained.

Laser Doppler anemometry (LDA)

In a more efficient and sophisticated experiment the surface velocity was determined by means of the differential laser Doppler technique. This technique is the most commonly used method of laser Doppler anemometry, and applications are found in a wide field of flow measurements on fluids and gases. A thorough description of the theory of differential laser Doppler anemometry and characteristics of the method are given by among others Drain [1] and Durst et al [2]. Basically in a differential laser Doppler set-up (see also Fig. 4.6) two coherent light beams are crossed in a probe volume. Particles intersecting the probe volume scatter light from both beams in all directions. A detector viewing the probe volume measures the intensity of the scattered light. The frequency of light scattered by the moving particles is shifted due to the Doppler effect. However, the Doppler shift with respect to the two beams is not the same, thus causing a fluctuating intensity on the detector. The frequency of the fluctuation, f_D, equals the difference between these Doppler shifts, and is given by

$$f_D = \frac{2v_x \sin(\theta/2)}{\lambda}, \tag{4.3}$$

where λ is the wavelength of the laser light, θ is the angle between the two intersecting beams, and v_x refers to the velocity of the particles concerning the component lying in the plane of the beams, perpendicular to the bisector of the two beam directions. The same relation is found, when the interference pattern of the two beams in the probe volume is considered. The interference pattern may be imagined to consist of parallel light and dark planes (often called fringes) which are parallel to the bisector of the beams. The distance d between the light fringes is

$$d = \frac{\lambda}{2 \sin(\theta/2)}. \qquad (4.4)$$

When a particle passes through this interference pattern, the frequency fluctuation resulting on the detector equals $f_D = v_x/d$, yielding the same expression as given in eq. (4.3). The relation between the Doppler frequency and the velocity of the particle is linear, and determined by optical and geometrical parameters only.

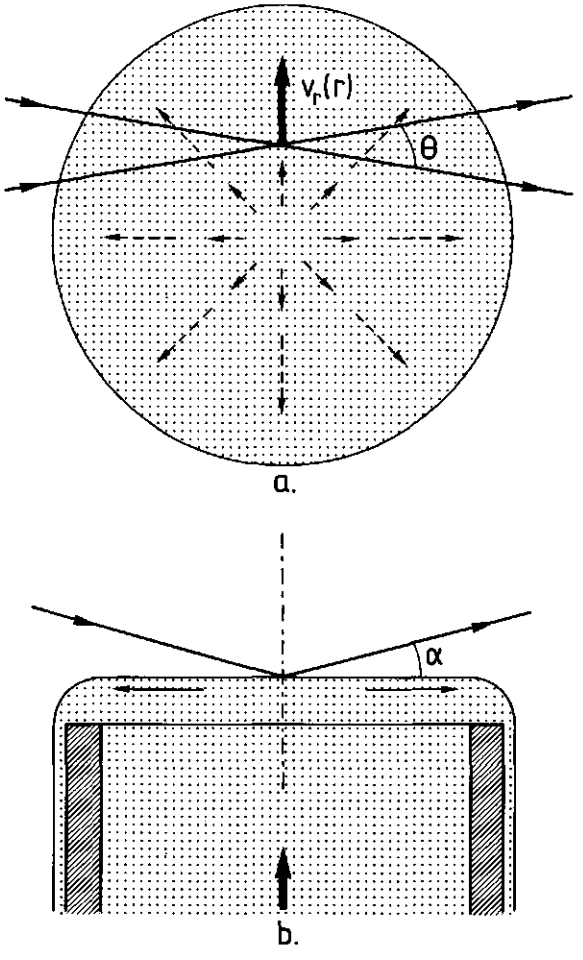

Fig. 4.5: *a. Topview of the expanding surface indicating the position of the probe volume.*
b. Part of the cross-section of the overflowing cylinder showing the reflection of the laser beams in the surface.

Fig. 4.5 shows how the differential laser Doppler technique has been applied to the overflowing cylinder. The light beams are crossed exactly in the expanding surface in such a way that the bisector of the beam directions is perpendicular to the surface velocity. Consequently applying eq. (4.3) to the overflowing cylinder surface, v_r may directly be substituted for v_x. When moving the probe volume over the imaginary line radiating from the centre of the meniscus, the dependency of v_r on the radial distance can be studied. The light beams reflect from the surface in the probe volume. Dealing with surfactant solutions, just below the surface the radial velocity decreases very rapidly (see Fig. 3.9), since in the surface the normal derivative of the radial velocity has its maximum value. Usage of the Doppler anemometer in the specified way guarantees that only velocity information of the surface will be obtained. Experimental results proved that the angle of incidence, α, does not influence the value of the detected Doppler frequency. The Doppler frequency experimentally showed to be dependent on the angle between the two beam directions, θ, in a way as predicted by eq. (4.3).

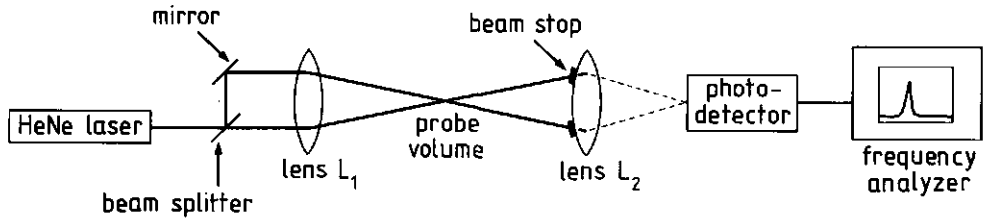

Fig. 4.6: Schematic representation of the differential laser Doppler anemometer; topview.

The total differential laser Doppler set-up used is drawn schematically in Fig. 4.6. Light from a HeNe laser (Melles Griot, 632.8 nm, 5 mW) is divided into two parallel coherent light beams by means of a beam splitter and a mirror (both Spindler & Hoyer). The light beams are crossed in the expanding surface by a positive lens (focal lenght L_1 = 16 cm). The scattered light is

focussed on the detector by a second lens (focal length L_2 = 7 cm), while the reflected beams are stopped by two beam stops attached to the lens. The fluctuating intensity of the scattered light is detected by a photodetector (HLD, TAM), and finally frequency spectra obtained with a Fast Fourier Transform analyzer (SR 760 FFT) are displayed.

The application of talc powder particles to LDA

Talc powder particles were experienced to cause very good forward scattering of the laser light. Besides that the talc powder (Talcum Ph. Eur. from OPG Farma) did not influence the surface tension of pure water. Eq. (4.3) was verified with respect to the correctness of the calculated velocity resulting from a LDA-measurement on talc powder in the following way. A petri dish was filled with water and put on a wheel which rotated with an adjustable angular velocity. Talc powder particles which had been sprinkled on the water surface, moved around having a known velocity. Next the velocity of the particles was determined by means of the differential laser Doppler anemometer at a fixed radial distance from the centre of the surface for various angular velocities of the rotating wheel. Good agreement was found between the results of the measurements and the actual values of the velocity. It was concluded that the calculated result of eq. (4.3) represents the correct value of the velocity of the talc powder particles.

The talc powder particles were brought upon the surface of the overflowing cylinder by means of a vibrating gutter. The number density of the particles on the surface had to be high enough for sufficient particles to pass through the probe volume. In the case of pure water the talc powder was dropped in the centre of the circular surface. Dealing with surfactant solutions having a much higher velocity, the same action resulted in a very low amplitude of the detected signal, because of the fact that too few particles went through the probe volume. In order to get a better signal-to-noise ratio particles were brought upon the surface at a position 1 - 1.5 cm away from the scattering volume in the upstream direction. Since the surface flow is stationary, the

velocity could be averaged out over a long period of time. However, near the centre of the surface this strategy was not profitable, for the centre appeared to drift about a little. The method of instantaneous exposure of particles by means of two successive flashes, which was described before, was more suitable for measuring the temporary surface velocity so close to the centre.

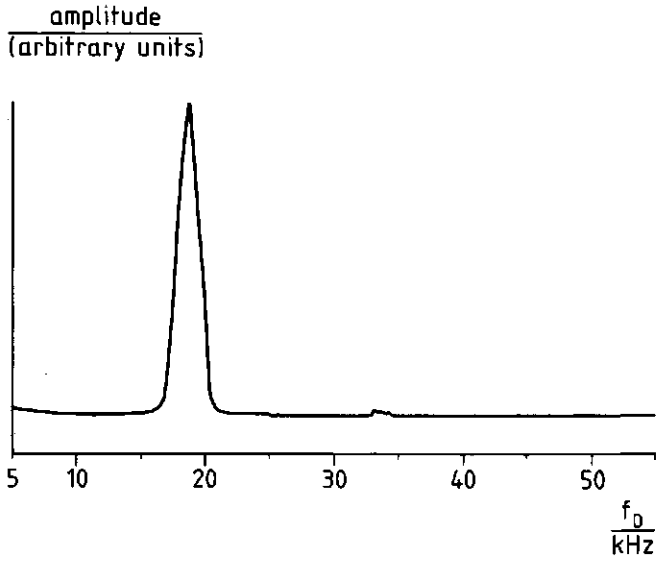

Fig. 4.7: Amplitude spectrum of light scattered by talc powder passing through the probe volume in the expanding surface of a surfactant solution.

Fig. 4.7 is an example of a frequency spectrum displayed for an arbitrary surfactant solution. The peak frequency equals 18.5 kHz. With $\theta = 11°$ according to eq. (4.3) this Doppler frequency yields $v_r = 6.1$ cm/s. For all solutions investigated the peak frequency was experienced to be very reproducible. Variations of only 500 Hz were observed, implying that the accuracy of the velocity calculated from the peak frequency was ca. 0.1 cm/s. However, generally the width of the peak was at least ten times larger than the variation in the peak frequency, viz. 5 kHz. Peak broadening may have various origins. While moving through the probe volume the velocity of the particle increases. Dependent on the chosen sampling-time in relation to

the extensiveness of the volume, the particle may be sampled more than once. If so, and this was practically possible, different Doppler frequencies will be detected giving rise to peak broadening. If particles accidentally move through the volume obliquely, the measured velocity will be smaller than the actual value. Particles which are relatively slow have the same effect on the Doppler frequency. Moreover, these particles are present in the probe volume for a relatively long period, and therefore they have a bigger change than other particles of being sampled twice or even more, thus lowering the mean Doppler frequency extra. On the other hand particles passing through one of the two edges of the volume have already gained a higher velocity than particles going through the middle. These particles give rise to a higher Doppler frequency. It is sensible to keep these causes for peak broadening in mind, but there is no reason for concluding that the detected peak frequency must definitely be lower or higher than the desired frequency, which corresponds with the velocity of the particles in the middle of the probe volume. Therefore calculating the velocity of the particles the peak frequency has always been used.

Now the conclusion has been drawn that the velocity calculated from eq. (4.3) on the basis of the detected peak frequency, equals the velocity of the particles moving on the overflowing cylinder surface, another question comes into consideration. Is the velocity of the particles identical to the velocity of the surface? This is a very important question, for it is not inconceivable that a particle is not able to gain the velocity of the surface on its way from the position where is was dropped, to the probe volume. Moreover when dealing with surfactant solutions a particle may be slowed down by the fluid layer just below the surface having a much smaller velocity than the surface itself (cf. Fig. 3.9). In order to be able to answer the question the forces acting on a particle have to be studied.

Consider a spherical particle floating on the surface with half of its volume below the surface level. The actual ratio of volume above and below the

surface level depends on both the density difference between the particle and the fluid and the contact angle of the liquid onto the surface of the particle. With respect to the wetting properties experiments have been carried out on divers solutions. Dealing with pure water and some surfactant solutions the particles behaved as hydrophobic particles. At very small flow rates the particles caused rupture of the wetting film on the outside of the overflowing cylinder, and consequently at these flow rates no LDA-measurements could be performed. On the other hand at very high concentrations of particular surfactants the talc powder particles were even engulfed by the solution, simply leaving no particles for LDA-measurements. The particle size distribution of the talc powder was determined by sifting. The diameter of about 90% of the particles was smaller than 70 μm, while 40% of the particles even passed through the 30 μm sieve.

The inertia of the particle works against its necessary acceleration from zero radial velocity at the position where the particle is dropped, to the velocity of the surface. The inertial force, F_{ma}, acting on the particle can be expressed by

$$F_{ma} = \frac{4}{3}\pi R_p^3 \cdot \rho_p \cdot \frac{\partial v_r}{\partial t}, \tag{4.5}$$

where R_p and ρ_p are respectively the radius and the density of the particle. Since in the vicinity of the centre of the circular meniscus the radial velocity appears to be linearly dependent on the radial distance, the simplification of the expression for dlnA/dt in eq. (3.6) may be used to rewrite $\partial v_r/\partial t$

$$\frac{\partial v_r}{\partial t} = \frac{\partial v_r}{\partial r}\cdot\frac{\partial r}{\partial t} = \frac{\partial v_r}{\partial r}\cdot v_r = \frac{v_r^2}{r} = \frac{1}{4} r(\mathrm{dln}A/\mathrm{d}t)^2. \tag{4.6}$$

Combining eqs. (4.5) and (4.6) gives

$$F_{ma} = \frac{1}{3}\pi R_p^3 \cdot \rho_p \cdot r(\mathrm{dln}A/\mathrm{d}t)^2. \tag{4.7}$$

Talc powder on the surface of pure water

Dealing with pure water the measured radial velocity of the particles appeared to be substantially lower, when the particles were not dropped in the centre of the surface, but only 1 cm away from the probe volume which was situated at radial distance r = 2.8 cm. So then the influence of the inertia of the particles was noticed. Reckoning with the inertial force a particle must get enough time, and correspondingly sufficient radial distance, to be able to obtain the velocity of the surface.

According to eq. (4.7) the volume of the particle influences the magnitude of its inertia. However, various particle fractions of different mean particle size, which were all brought upon the surface in the centre, yielded the same Doppler peak frequency. Therefore it may be concluded that for LDA-measurements on pure water the inertia of the particles does not play an important role in the sense that particles have gained the surface velocity before reaching the probe volume, provided that the particles are brought upon the surface in the centre.

Just imagine the particle velocity to differ from the surface velocity in the probe volume with only 1% to the amount of Δv_r. The velocities of the water surface and the fluid layer just below the surface are the same, since in the surface of pure water the normal derivative of the radial velocity is zero (see eq. (3.34)). If the velocity of the particle equals this velocity, no viscous shear stress will be experienced by the particle. However, if the particle velocity is smaller than this velocity, a viscous shear stress will act on the surface πR_p^2 of the cross-section of the spherical particle trying to undo the velocity deviation. The deviation Δv_r of the particle is noticed by the fluid over a depth to the extent of the radius of the particle. The fluid exerts a viscous force, F_{vis}, on the particle which may approximately be expressed by

$$F_{vis} = \pi R_p^2 \cdot \eta_b \cdot \frac{\Delta v_r}{R_p}. \qquad (4.8)$$

The value of the relative surface expansion rate which may be applied here, is 1 s^{-1} (see §5.1) implying that at a radial distance r = 2.8 cm the velocity equals 1.4 cm/s and Δv_r = 0.014 cm/s. Further using $\eta_b = 10^{-3}$ Pa·s, ρ_p = 900 kg/m^3 and R_p = 20 μm, F_{vis} is calculated to be $9 \cdot 10^{-12}$ N. Based upon the same numbers the inertial force of eq. (4.7) equals $2 \cdot 10^{-13}$ N. So, if the particle velocity differs from the surface velocity with only 1%, a viscous force will be exerted on the particle which is already more than 10 times bigger than the inertial force. No doubt that the viscous force will undo the velocity deviation really soon. The conclusion is drawn that the talc powder particles move on the surface of pure water having the velocity of the surface, provided of course that they have had enough time to gain this velocity. If accidentally their velocity is somewhat smaller, the viscous shear stress will immediately undo the arisen velocity deviation.

Talc powder on the surface of a surfactant solution

On the surface of a surface active solution the particle is present in the field of a surface tension gradient. The surface tension gradient additionally accelerates the particle until it has gained the surface velocity. Various particle fractions of different mean particle size were brought upon the surface at a postion 1 - 1.5 cm away from the scattering volume in the upstream direction. Also in this experiment all particles yielded the same Doppler peak frequency. In comparison with pure water the particles do not need as much radial distance, in order to gain the surface velocity, since the inertia of the particles is easily overcome by the force due to the surface tension gradient. When the surface tension gradient of an arbitrary surfactant solution is for instance 0.17 Pa (see Table 5.2), the difference in γ_{dyn} over the diameter of the particle (R_p = 20 μm) amounts to $7 \cdot 10^{-3}$ mN/m. This difference will become much bigger, if the particle is slowed down by the fluid layer just below the surface which exerts a viscous shear stress on the particle. Imagine travelling along with the surface. If the particle stays behind, the surface close to the particle in the upstream direction will be temporarily

compressed, and consequently there the surface tension will decrease. This implies that the difference in γ_{dyn} over the diameter of the particle increases. The next chapter will show that already a very small surface tension gradient gives rise to a considerable acceleration of the surface. So the extra difference in γ_{dyn} over the particle is expected to accelerate the particle in such a way that the velocity of the surface will soon be reached (again).

In a more quantitative approach the velocity of the particle is considered to differ from the surface velocity with again 1% only. The value of the relative surface expansion rate which may be applied here is 9 s^{-1} (see Table 5.2) implying that at a radial distance r = 2.5 cm the velocity equals 11.25 cm/s and Δv_r = 0.11 cm/s. The compressed area is assumed to be present in the upstream direction over a distance being identical to the radius of the particle. The ratio $\Delta v_r/R_p$ = 55 s^{-1} may be a measure for the local compression rate of the surface. This value is bigger than the measured relative expansion rate of the surface. On the surface of the overflowing cylinder the magnitude of the surface tension gradient is directly coupled with the resulting dlnA/dt, as is for instance shown by eq. (3.8). Such a high compression rate induces an extra surface tension gradient which thus may be imagined to give rise to an extra acceleration of the particle in the downstream direction. In this way the extra surface tension gradient will immediately undo a velocity deviation. Of course the particle will not move with greater speed than the surface either, for then the opposite occurs. In that case a compression of the surface close to the particle in the downstream direction will induce a counteracting surface tension gradient which will nullify the extra acceleration of the particle.

Having considered the consequences of both a retardation and an acceleration of the particles referring to the velocity of the surface, the conclusion may be drawn that especially for surfactant solutions the velocity of the talc powder particles must be identical to the velocity of the surface.

A similar study has not been made for the polyethylene particles which were used for a photographic determination of the surface velocity. However,

because of the fact that good agreement was found between the results of the photographic method and the laser Doppler technique, the same conclusion was assumed to be valid for the polyethylene particles.

4.3 Rheological methods

The bulk viscosity was determined using a KPG-Ubbelohde viscometer. Its value followed from the measured efflux time and the capillary constant of the viscometer.
The bulk rheological behaviour was studied by means of a Bohlin VOR constant shear rheometer, equipped with a cup and bob system made of stainless steel. In this apparatus the controlled shear rate is applied to the sample in the outer cylinder and the resulting shear stress on the inner cylinder is monitored.

4.4 Materials

By means of the overflowing cylinder measurements have been carried out on water and on aqueous surfactant solutions. In all these cases tap-water was used. Only when the equilibrium surface tension of pure water was considered, demineralized water was used.
In industry the overflowing cylinder is used to experiment on practical systems which are in general far from being model systems. As has already been stated in the first chapter, the scope of this study has been to research on these 'dirty systems' rather than on model systems. For this reason two commercially available surfactants have been studied extensively, whereas the use of very pure surfactants has been limited. Since in practice all kinds of surfactants are added to the fluid in the overflowing cylinder, here for reasons of diversity an anionic, a cationic, a nonionic and some polymer

fractions were used. These surfactants are specified below:

* The concentrated Teepol solution (FNZ, Arnhem) in water. This is a commercially available anionic detergent which has to be diluted before use. Teepol contains among other components alkylarysulfonate, alcoholethersulfate and alcoholethoxylate. The amount of active material is about 15%. As Teepol is a bulk product, the contents of two batches may sligthly differ.
* Sodium caseinate blend from De Melkindustrie Veghel B.V. The minimum milkprotein contents of this product is 88%, whereas the maximum moisture and the maximum amount of fat and ash were both 6%. This is a commercially available product as well.
* N-Cetyl-N,N,N-trimethylammoniumbromide (CTAB, $C_{19}H_{42}BrN$) from Merck, Darmstadt with a minimum assay of 98.5%. This cationic has a molecular weigth of 364.46.
* The nonionic polyethylene glycol monododecyl ether $C_{12}(EO)_{25}$ with a molecular weigth of 1280. This very pure sample was obtained from the Department of Physical- and Colloid Chemistry of Wageningen Agricultural University.
* Polyethyleneoxide (PEO) fractions of mean molecular weigths 1,000, 20,000 and 600,000. These samples were also obtained from the Department of Physical- and Colloid Chemistry of Wageningen Agricultural University.

No special procedures had to be practised to dissolve these surfactants.

The viscosity of water and of a dilution of the Teepol solution was increased by adding various amounts of dextran. The dextran from BDH Chemicals, England had a minimum assay of 90% (grade A) and the molecular weigth ranged from 200,000 to 275,000.

Acknowledgments. The polypropylene particles were kindly supplied by R.M. Visser, Shell Amsterdam. M.A. Cohen Stuart put the nonionic $C_{12}(EO)_{25}$ and the Polyethylene fractions to the author's disposal. Henri Bijsterbosch succeeded in applying the differential laser Doppler technique to the surface of the overflowing cylinder. With great enthusiasm he built the LDA set-up and accurately performed part of the tests.

References chapter 4

[1] L.E. Drain, The Laser Doppler Technique, John Wiley, Chichester, (1980).

[2] F. Durst, A. Melling and J.H. Whitelaw, Principles and Practice of Laser-Doppler Anemometry, second edition, Academic Press, London, (1981).

Chapter 5

Experimental results and discussion

In this chapter the results of overflowing cylinder measurements are presented and discussed within the framework of the theoretical aspects dealt with in chapter 3. For the physical parameters of pure water good agreement exists between numerical calculations and measurements (§5.1). The addition of a surface active agent raises the surface velocity considerably. Experimental evidence has been obtained in support of the existence of a surface tension gradient which directly determines the magnitude of the relative surface expansion rate (§5.2). The excess surface tension has been studied for various surfactant solutions. Minor components highly influence not only this quantity, but also the magnitude of the surface dilational viscosity (§5.3). The curvature of the overflowing meniscus appears to be a constant for a fixed flow rate, irrespective of the applied surfactant and its concentration (§5.4). An increase in bulk viscosity gives rise to small coherent changes in the behaviour of the overflowing liquid (§5.5).

5.1 Fluid dynamics of pure liquids

The first paragraph of chapter 3 described how Bos [1] obtained a numerical solution of the Navier-Stokes equations for pure liquids. He calculated the position of the free surface and the velocity field in the fluid that would be reached in the steady state. The Newtonian liquid he considered, was pure water. Some of the results of his calculations given in chapter 3, will be compared with experimental results here. The experiments were carried out at room temperature.

The surface velocity distribution of pure water was determined at a certain flow rate from a photograph taken of polyethylene particles which were sprinkled on the surface. The results of the measurement are presented in Fig. 5.1. For reasons of comparison the distribution numerically calculated for the same flow rate, is also plotted in this figure. The radial velocity of the

water surface was measured as a function of the mass flow rate by means of the LDA-technique at a radial distance r = 2.8 cm. Using eq. (3.6) dlnA/dt was obtained in the vicinity of the centre of the surface as a function of the mass flow rate. In Fig. 5.2 the results are compared with the calculated curve of Fig. 3.3. Both the calculated height of the centre of the meniscus of pure water and its experimental value are given in Fig. 5.3 as a function of the mass flow rate.

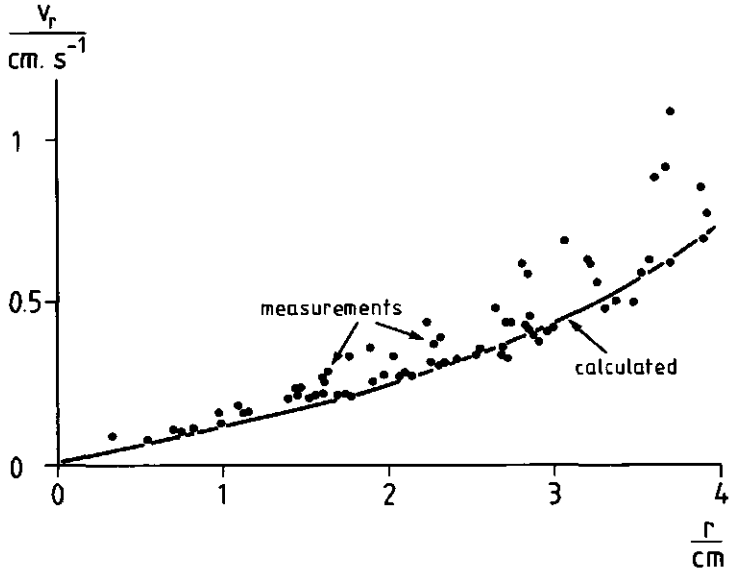

Figure 5.1: *The velocity distribution in the surface of pure water; Q = 7.6 cm^3/s; (measurement by Bart Schulte).*

Figs. 5.1 till 5.3 show that for the parameters of pure water flowing through the overflowing cylinder, a better than qualitative agreement exists between calculations and measurements. This not only demonstrates the accuracy of the numerical solutions, but also pleads for the correctness of the results of the applied experimental methods, like the LDA-technique. Based upon theory in paragraph 3.4 a description of the physical mechanism of operation of the overflowing cylinder technique for pure liquids was put forward as a hypothesis. The validity of this hypothesis is supported by the experienced agreement between the experimental- and calcultated results of pure water.

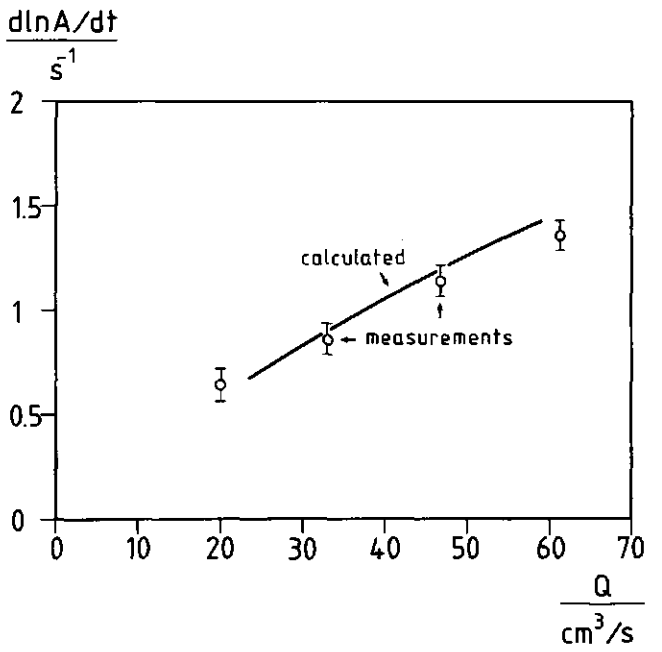

Figure 5.2: *The relative surface expansion rate at the centre of the surface as a function of the mass flow rate.*

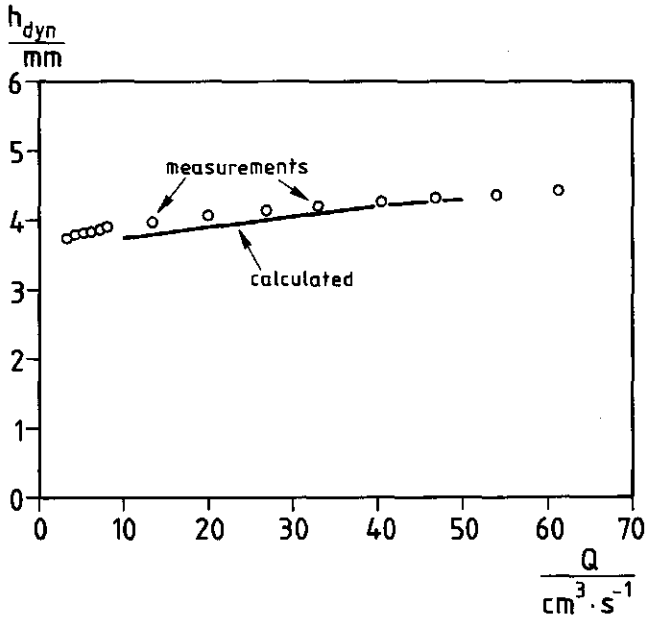

Figure 5.3: *The height of the centre of the meniscus of pure water above the rim as a function of the flow rate.*

5.2 Fluid dynamics of surfactant solutions

When surfactant solutions are introduced in the overflowing cylinder a surface tension gradient may arise at the free surface changing the surface flow completely. In the first paragraph of chapter 3 the surface tension gradient was supposed to accelerate a thin fluid layer on top of the bulk flow in such a way that the resulting surface velocity would be much higher than in the case of pure liquids. The surface velocity distribution of a 1 vol% Teepol solution was determined from a photograph of polyethylene particles which were sprinkled on the surface. The flow rate applied was the same as during the experiment with pure water. The results of the measurement are presented in Fig. 5.4, and for reasons of comparison the velocity distribution in the surface of pure water (Fig. 5.1) has been added.

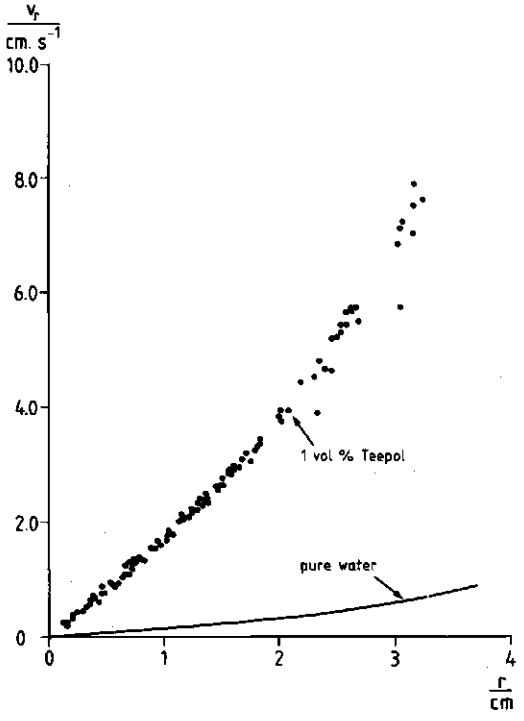

Fig. 5.4: The surface velocity distributions of a 1 vol% Teepol solution and pure water: Q = 7.6 cm^3/s; (measurement by Bart Schultel).

Fig. 5.4 shows that the addition of a surface active agent raises the velocity of the aqueous surface considerably. Besides that it is noticed from Fig. 5.4 that also for surfactant solutions in the vicinity of the centre of the surface the radial surface velocity is almost linearly proportional to the radial distance. The large quantitative difference between a surfactant solution and pure water is the constant of proportionality: for the Teepol solution this constant is almost a factor 10 higher than the constant of pure water. The area of linear proportionality extends as far as about r = 2.5 cm. Consequently according to eq. (3.6) in this area the relative surface expansion rate is a constant. So, although for both systems the relative surface expansion rate is a constant in the vicinity of the stagnation point, the actual value of dlnA/dt of a surfactant solution may be a multiple of the dlnA/dt of pure water.

The presence of a surface tension gradient

A surface tension gradient is held responsible for the observed increase in the magnitude of dlnA/dt. The presence of a surface tension gradient has experimentally been demonstrated for various surfactant solutions.

The dynamic surface tension was for example measured for a 0.3 vol% solution of Teepol as a function of the radial distance. Fig. 5.5 shows that indeed a surface tension gradient exists over the surface of the Teepol solution, for the increase in γ_{dyn} amounts to almost 6 mN/m. Near the centre of the surface the increase in γ_{dyn} is relatively small, but the inclination becomes steeper towards the rim of the cylinder. Eq. (3.8) suggests that in the vicinity of the stagnation point $d\gamma/dr$ is linearly dependent on r, implying that γ_{dyn} must be linearly proportional to r^2. In order to study the practical exactness of this algebraic relation, Fig. 5.5 has been transformed into Fig. 5.6. In both figures the margins of the accuracy in the dynamic surface tension have been indicated.

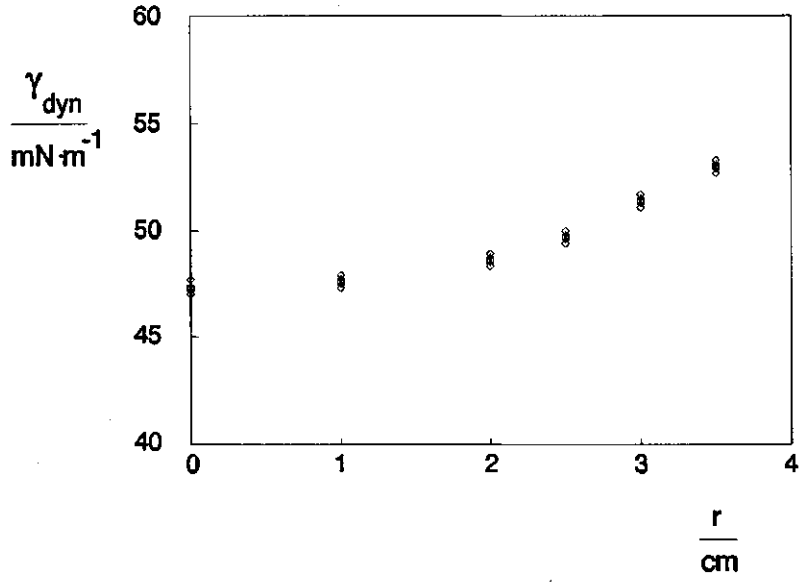

Fig. 5.5: *The dynamic surface tension of a 0.3 vol% Teepol solution as a function of the radial distance; Q = 61 cm^3/s.*

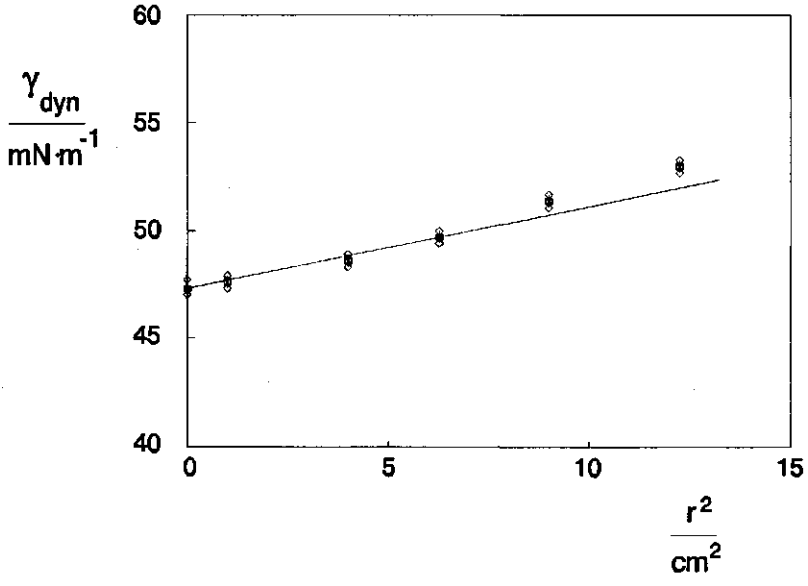

Fig. 5.6: *The dynamic surface tension of a 0.3 vol% Teepol solution versus the square of the radial distance at 61 cm^3/s.*

Owing to the accuracy margins γ_{dyn} may indeed be considered to be linearly proportional to r^2 in the vicinity of the centre of the surface. From the drawn line in Fig. 5.6 the constant of proportionality between $d\gamma/dr$ and r is estimated to be ca. 8. With $\eta_b = 10^{-3}$ Pa·s, $\rho = 10^3$ kg/m^3, and dlnA/dt of the investigated Teepol solution is 10 s^{-1} (see further on), according to eq. (3.8) the constant of proportionality is calculated to equal 13. So the experimental result and the calculated constant are of the same order of magnitude.
It may be concluded that experimental evidence has been obtained in support of the existence of a surface tension gradient over the surface of the overflowing cylinder. In the vicinity of the stagnation point the surface tension appeared to be dependent on the radial distance approximately in a way as predicted by theory.

The resulting relative surface expansion rate

Now the surface tension gradient over the top surface of the overflowing cylinder has shown to be measurable, the relation between the magnitudes of $d\gamma/dr$ and the resulting relative surface expansion rate can be studied. The dlnA/dt data were obtained by measuring the radial surface velocity at r = 2.5 cm by means of the LDA-technique. The value of dlnA/dt then follows from eq. (3.6). All experiments were carried out at fixed values of the mass flow rate and the length of the wetting film, chosen in such a way that for each solution in the overflowing cylinder the highest values of dlnA/dt and $d\gamma/dr$ turned up.

Already a very small surface tension gradient induces a considerable acceleration of the free surface, as can be seen from Fig. 5.7. This figure not only presents dlnA/dt, but also γ_{dyn} at the positions r = 0 cm and r = 3 cm versus the concentration of Teepol. At very small surfactant concentrations γ_{dyn} equals the surface tension of pure water, and in the surface the relative expansion rate of pure water is found. While increasing the concentration of Teepol a relatively small difference between γ_{dyn} at r = 3 cm and r = 0 cm

becomes manifest, giving rise to a marked increase in dlnA/dt. The maximum in dlnA/dt is reached at the concentration where γ_{dyn} decreases most with increasing concentration; in other words where $-d\gamma_{dyn}/d\log c$ is the highest. For even higher concentrations the fluid has less ability to generate a surface tension gradient, and consequently dlnA/dt becomes smaller again.

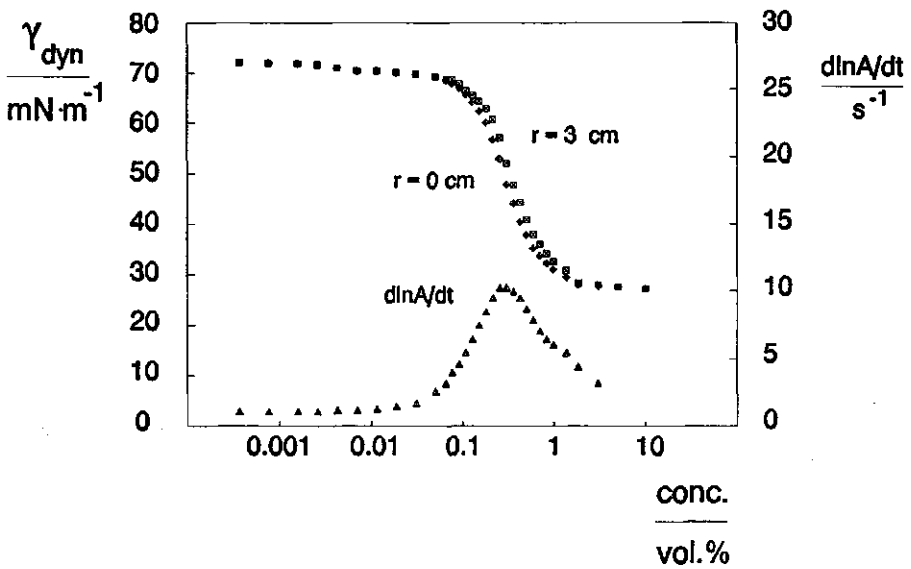

Fig. 5.7: The relative surface expansion rate and γ_{dyn}, both at the position r = 0 cm and r = 3 cm, as a function of the concentration of Teepol.

The mean value of $d\gamma/dr$ over the top surface of the overflowing cylinder was determined from the dynamic surface tensions at the positions r = 0 cm and r = 3 cm, like presented for Teepol in Fig. 5.7. As an approximation this mean value was considered to be the surface tension gradient at the position half-way the interval at radial distance r = 1.5 cm. In this way a surface tension gradient was obtained having an accuracy of 0.02 Pa.

In Figs. 5.8 and 5.9 both dlnA/dt and $d\gamma/dr$ are given as a function of the surfactant concentration of respectively Teepol and CTAB.

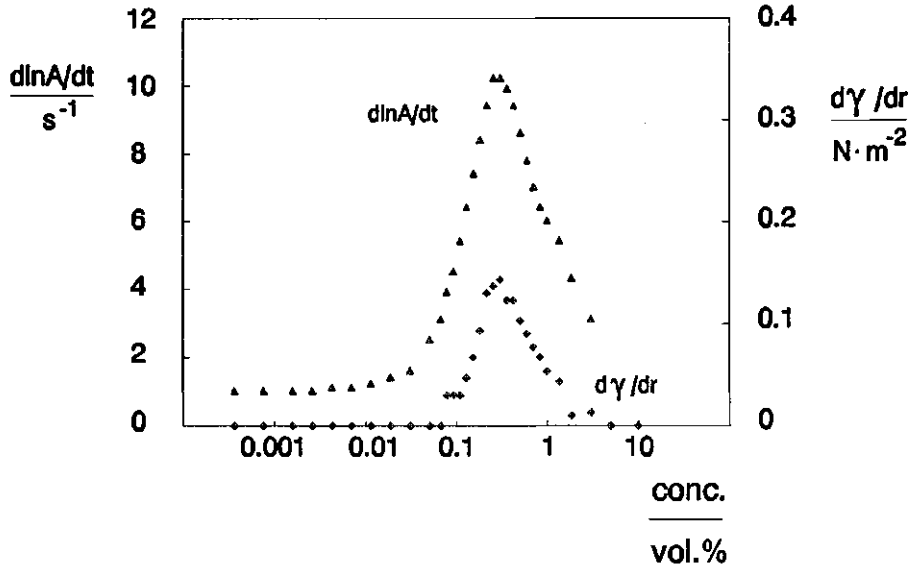

Fig. 5.8: *The surface tension gradient and the relative surface expansion rate as a function of the concentration of Teepol.*

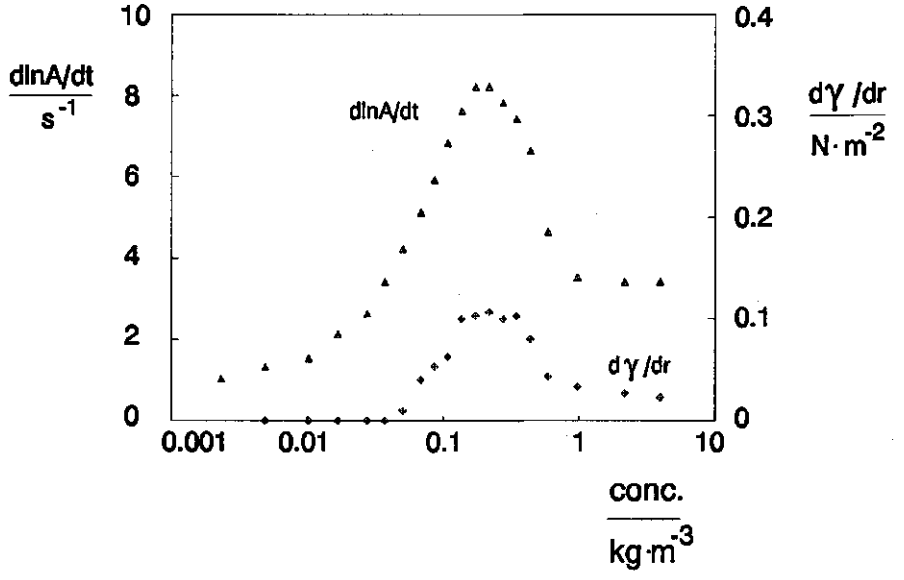

Fig. 5.9: *The surface tension gradient and the relative surface expansion rate as a function of the concentration of CTAB.*

The curves of dlnA/dt and $d\gamma/dr$ in Figs. 5.8 and 5.9 show the same course versus the concentration. The maxima are reached at the same concentration as well, implying that also the maximum in $d\gamma/dr$ is found where $-d\gamma_{dyn}/d\log c$ is the highest. The maximum can be imagined appearing just there, for at this concentration a concentration difference over the top surface gives rise to the relatively largest difference in γ_{dyn}. For a fixed length of the wetting film the absolute magnitude of the surface tension gradient depends on the transport properties of the applied surfactant(s). Teepol happens to be able to create a higher maximum value of $d\gamma/dr$ than CTAB. Correspondingly the maximum value of dlnA/dt is higher as well.

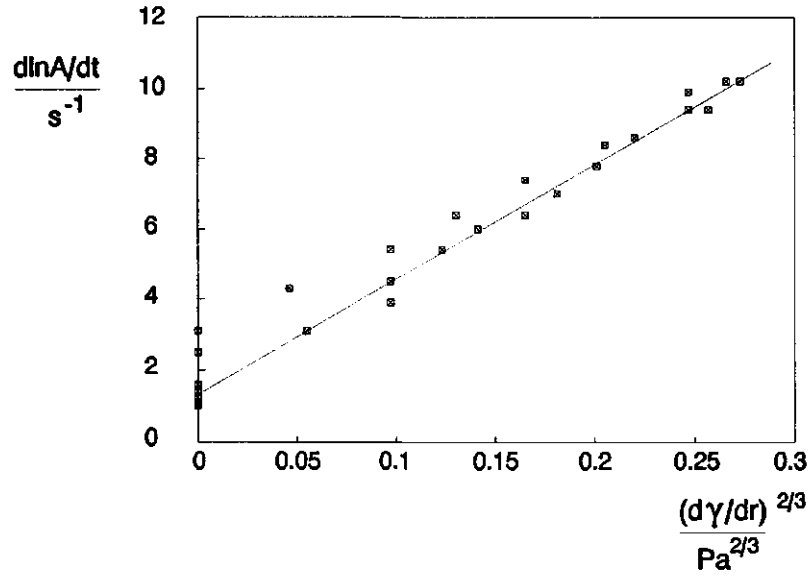

Fig. 5.10: *The relative surface expansion rate as a function of the surface tension gradient to the exponent 2/3 for Teepol; the line is drawn according to the equation:* $dlnA/dt = 32\ (d\gamma/dr)^{2/3} + 1.3$

Eq. (3.9) provides a tool for studying the relation between dlnA/dt and $d\gamma/dr$ quantitatively. Referring to this relation Figs. 5.8 and 5.9 have been transformed into Figs. 5.10 and 5.11. The concentrations of the surfactants

Teepol and CTAB respectively are the implicit variables in these figures. The drawn lines represent the best fits of the experimental results referring to a linear relationship between dlnA/dt and $(d\gamma/dr)^{2/3}$. Figs. 5.10 and 5.11 show that the experimental results are well described by eq. (3.9). The lines cross the y-axis at approximately the relative surface expansion rate of pure water. With r = 1.5 cm and η_b and ρ having the same values as before, the constant of proportionality is calculated from eq. (3.9) to amount to 29.6. The inclinations of the drawn lines in Figs. 5.10 and 5.11 (32 and 30 respectively) are very close to this calculated value, producing evidence in support of the validity and exactness of eq. (3.9).

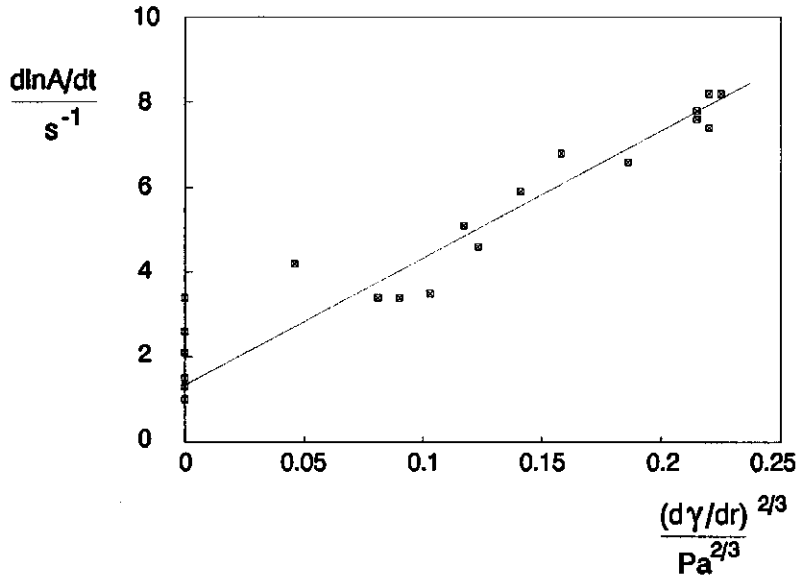

Fig. 5.11: The relative surface expansion rate as a function of the surface tension gradient to the exponent 2/3 for CTAB; the line is drawn according to the equation: $dlnA/dt = 30\ (d\gamma/dr)^{2/3} + 1.3$

These findings prove the hypothesis put forward by Bos [2] (see §3.1) that in the vicinity of the stagnation point the surface tension gradient accelerates a thin layer on top of the bulk flow resulting in an increased velocity of the uniformly stretched surface. Eq. (3.10) gives an expression for the thickness

δ_Q of this layer. As an example δ_Q was calculated for two different dlnA/dt values of Teepol. Using $\nu = 10^{-6}$ m^2/s, the maximum in dlnA/dt (dlnA/dt = 10.2 s^{-1}) and a relatively small value (dlnA/dt = 3 s^{-1}) respectively yielded $\delta_Q = 1.3$ mm and $\delta_Q = 2.5$ mm. So in the vicinity of the centre the surface tension gradient influences a fluid layer on top of the bulk flow which is as thin as a few millimeters.

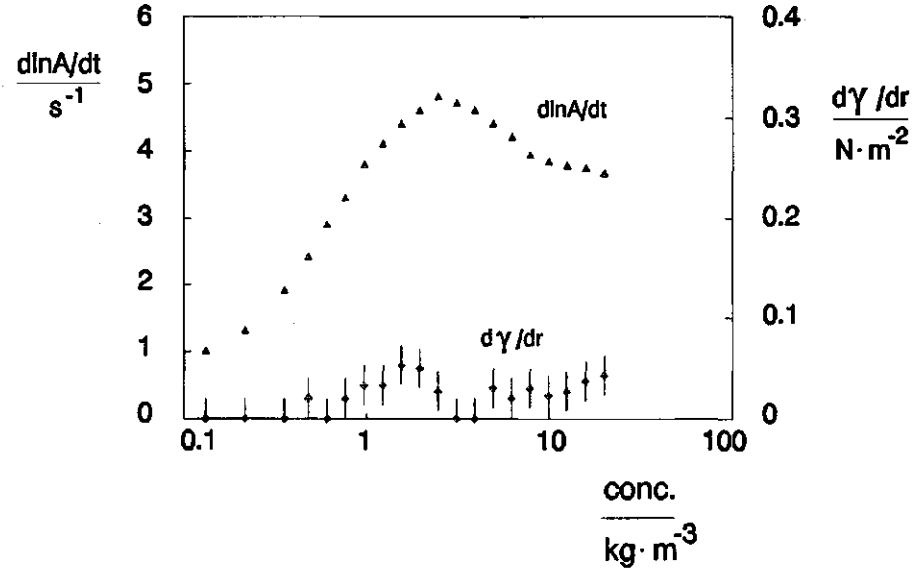

Fig. 5.12: The surface tension gradient and the relative surface expansion rate as a function of the concentration of Sodium caseinate.

Similar to the experiments on Teepol and CTAB also for Sodium caseinate an attempt was made at relating the magnitudes of dlnA/dt and dγ/dr. The results of the measurements on Sodium caseinate are presented in Fig. 5.12. The margins of the accuracy in dγ/dr were the same as in the case of Teepol and CTAB, and have been indicated in this figure. By comparing Fig. 5.12 with Figs. 5.8 and 5.9, it is noticed that Sodium caseinate generates a very small surface tension gradient, giving rise to a relative surface expansion rate which is correspondingly smaller as well. Only half of the concentrations studied yielded a surface tension gradient high enough to exceed the

accuracy margin. Due to these results a distinct relation between dlnA/dt and $d\gamma/dr$, like in eq. (3.9), could not be recognized. Unlike Teepol and CTAB, Sodium caseinate increases the bulk viscosity of pure water to 1.55 mPa·s for the highest concentration studied. This effect results in an extra variable in eq. (3.9). However, §5.5 which reports on the role of the bulk viscosity, will show that such a small increase has no significant influence on the physical parameters of the overflowing cylinder. So the course of $d\gamma/dr$ versus the concentration of Sodium caseinate can not be explained by the rise in bulk viscosity. For the most viscous concentration studied, however, the ratio of the magnitude of dlnA/dt to the magnitude of $d\gamma/dr$ appeared to be well predicted by eq. (3.9). With $d\gamma/dr$ = 0.04 Pa, η_b = 1.55 mPa·s, $\{dlnA/dt\}_0$ = 1 s^{-1}, and r and ρ having the same values as before, dlnA/dt was calculated to equal 4.0 s^{-1}, whereas experimentally dlnA/dt = 3.7 s^{-1} was obtained. Besides this, owing to a combination of a small surface tension gradient and relatively large accuracy margins no further conclusion can be drawn about the relation between dlnA/dt and $d\gamma/dr$ for Sodium caseinate.

The magnitude of the generated surface tension gradient

It has been stated before that the transport properties of the applied surfactant(s) are responsible for the absolute magnitude of the generated surface tension gradient. One may speculate why for instance Teepol creates a surface tension gradient which is substantially larger than the one Sodium caseinate is able to generate. Teepol contains a mixture of various low molecular surfactant components. The concentrations of the single components in the bulk may differ. Consequently the concentrations of these components at the surface and in the sub-surface layer will vary as well. Imagine travelling along with a continuously expanding surface element and its adhering sub-surface layer. Instantaneous equilibrium between the surface and the sub-surface layer is assumed. On its way to the rim of the cylinder the sub-surface layer may get 'exhausted' with respect to the low

concentrated components, and consequently only high concentrated components will be able to adsorp at the surface. So travelling along with the surface element the fractions of the surface active components may change in favour of the high concentrated ones. If the low concentrated components are highly surface active, a 'shortage' of these components will give rise to an increase in dynamic surface tension. This effect, which is of course most prominent at the surfactant concentration where $-d\gamma_{dyn}/d\log c$ is the highest, may explain the existence of a marked surface tension gradient over the expanding surface of a Teepol solution.

Dealing with Sodium caseinate the assumption of instantaneous equilibrium between the surface and the sub-surface layer is no longer valid. Even when no further deformation of the freshly created surface takes place, the surface tension of a solution of β-casein, the main component of Sodium caseinate, changes over an extended period of time. Graham and Philips [3] assigned this behaviour principally to slow rearrangement in the surface and conformational changes in the adsorbed layer. They found that the derivative $-d\gamma/dt$ is the highest just after having created the surface. The Sodium caseinate blend used here is, like Teepol, a commercially available product which may contain low concentrated components which are highly surface active. Travelling along with a continuously expanding surface element the effect of the 'exhausted' components would increase the dynamic surface tension. However, on their way to the rim of the cylinder the protein molecules at the surface have some time available for rearrangement and conformational changes. These alterations at the freshly created surface may lead to a decrease in surface tension. So the effect of the 'exhausted' components on the dynamic surface tension may be counteracted by the consequence of the rearrangement and conformational changes of the proteins. This may explain why the surface tension gradient over the expanding surface of a Sodium caseinate solution is so small that it can hardly be measured.

This reasoning about the magnitude of the surface tension gradient is all

rather speculative. More attention has been paid to the absolute value of the dynamic surface tension in relation to the equilibrium value. In the next paragraph the experimental results will be discussed within the framework of the theoretical transport aspects dealt with in chapter 3.

5.3 Transport phenomena

The relative surface expansion rate of the horizontal top surface of the overflowing cylinder gives rise to a dynamic surface tension which is generally higher than the equilibrium value. The absolute steady state value of γ_{dyn} in the centre of the surface is determined by the transport properties of the surfactant solution under investigation. The magnitude of γ_{dyn} is also influenced by the magnitude of dlnA/dt, as is illustrated by Fig. 5.13 for the surfactants Sodium caseinate and Teepol.

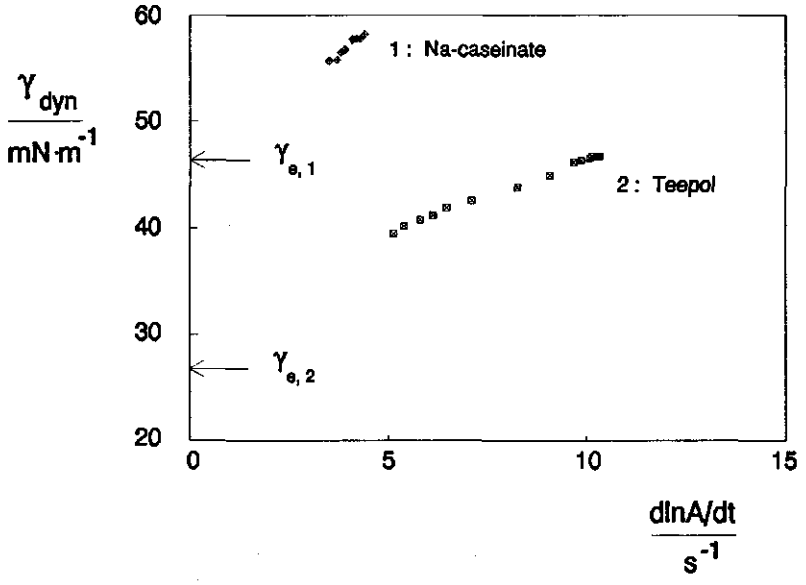

Fig. 5.13: The dynamic surface tension in the centre of the surface of 20 kg/m^3 Sodium caseinate and 0.3 vol% Teepol versus the relative surface expansion rate.

The curves were obtained by changing the mass flow rate, Q. Although the same flow rates were applied, the resulting dlnA/dt values for Sodium caseinate and Teepol were different. It is noticed from Fig. 5.13 that the highest value of dlnA/dt correlates with the highest γ_{dyn} of a particular surfactant solution.

This paragraph reports on dynamic surface tension measurements which were carried out in the centre of the surface at fixed values of the mass flow rate and the length of the wetting film. Q and L were chosen in such a way that for each solution in the overflowing cylinder the highest dlnA/dt value possible was obtained (see also the next chapter). Consequently also the highest value of γ_{dyn} turned up. If under these experimental conditions a surface tension gradient is present, the increase in γ_{dyn} over the top surface will be superimposed on the this value of γ_{dyn}.

The experimental excess surface tension

Figs. 5.14, 5.15 and 5.16 show both the dynamic and equilibrium surface tensions as a function of the concentration of respectively the surfactants Teepol, Sodium caseinate and the nonionic $C_{12}(EO)_{25}$.

The distance between the curves of Teepol amounts to two decades on the concentration axis. The same distance was found for various other low molecular systems which are used in practice, like the plant spray solution of De Ruiter et al [4]. In the laboratories where this research work has been carried out, the same graph was obtained for coffee, except for the part at high concentrations, since coffee appeared not to be concentrated enough for γ_{dyn} to reach the low plateau value of γ_e. These so called dirty systems have in common that minor components may be present in the system. Minor components generally lower the equilibrium surface tension, especially at low total surfactant concentrations. In the concentration region where γ_e starts to decrease, however, the concentration of the minor components is so low that

they can not diffuse to the expanding surface during the time scale of the experiment. Consequently in this region γ_{dyn} still approximates the surface tension of pure water. When γ_e reaches its low plateau value, the concentration of surfactants in the sub-surface layer is apparently such that γ_{dyn} starts to decrease. In this region the excess surface tension has its maximum value. At high concentrations the surfactant concentration in the sub-surface layer is also so high, that enough molecules are able to diffuse to the expanding surface during the time scale of the experiment, in order to maintain the equilibrium surface tension.

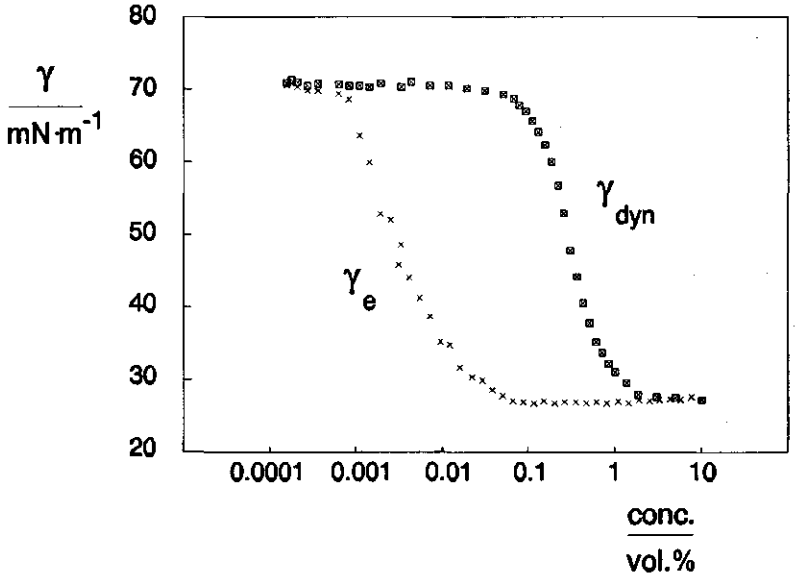

Fig. 5.14: The dynamic and equilibrium surface tensions as a function of the concentration of Teepol.

The distance between the equilibrium curve and the dynamic curve of Sodium caseinate amounts to far more than two decades on the concentration axis. Much higher amounts of Sodium caseinate than applied were not soluble any more. The same graph was obtained for other proteins, like whey protein [5], and in the laboratories where this research work has been carried out, also different beers showed the same behaviour. Besides possible effects of

present minor components, two characteristics of proteins may influence the position of the curves on the concentration axis. Firstly the high-affinity character results in low values of the equilibrium surface tension already at very low surfactant concentrations. Secondly during continuous expansion of the surface hardly any time is available for rearrangement and conformational changes of protein molecules in the surface. For this reason γ_{dyn} in the centre of the surface only starts to decrease at relatively high concentrations. The high-affinity character and the lack of time for rearrangement and conformational changes may cause the excess surface tension of proteins to be relatively high over a large range of concentrations.

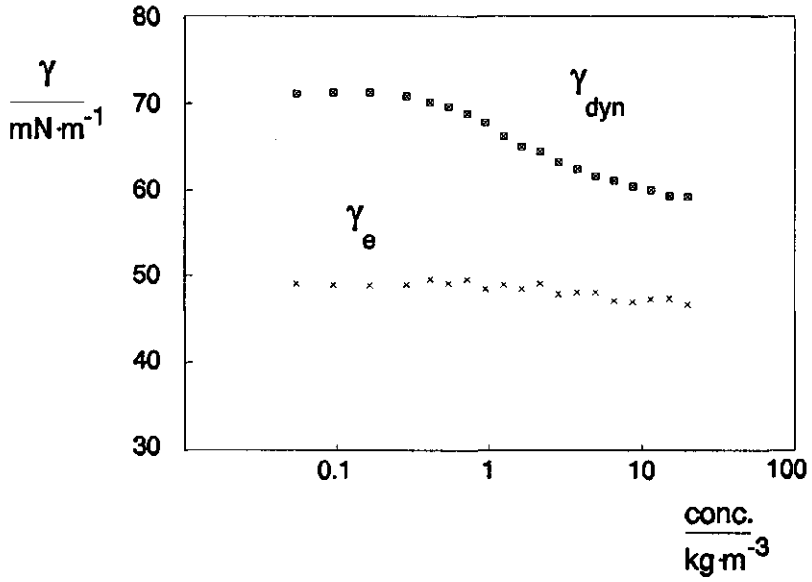

Fig. 5.15: The dynamic and equilibrium surface tensions as a function of the concentration of Sodium caseinate.

Fig. 5.16 presents the results of a very pure sample of the low molecular nonionic $C_{12}(EO)_{25}$. The minimum in the γ_e versus concentration curve shows that the sample still contained a small amount of impurities. However, compared to Figs. 5.14 and 5.15 the position of the dynamic curve on the concentration axis is close to the equilibrium curve. Only in the concentration

region where γ_e starts to decrease, the dynamic surface tension is substantially higher than the equilibrium one. At these bulk concentrations the surfactant concentration in the sub-surface layer may be too low to result in a dynamic surface tension which is close to the equilibrium value. Another possible explanation is that in this concentration region the impurities lower the equilibrium surface tension and give rise to a higher value of the excess surface tension. In comparison with the curves of Teepol the results of this rather pure surfactant suggest that for low molecular surfactants the excess surface tension is small, provided that minor components are not present in the system.

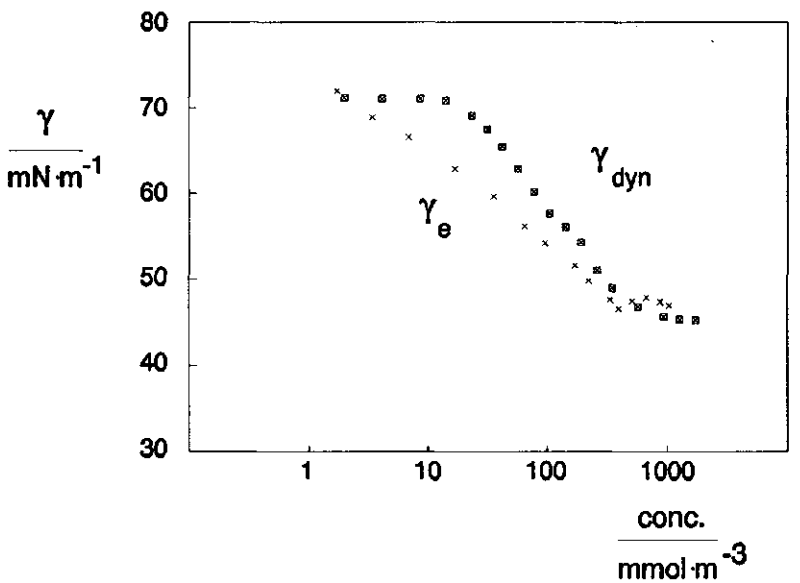

Fig. 5.16: The dynamic and equilibrium surface tensions as a function of the concentration of $C_{12}(EO)_{25}$; (measurement of γ_e by Marcel Böhmer).

This suggestion is supported by the results which were obtained with the cationic N-Cetyl-N,N,N-trimethylammoniumbromide (CTAB). Prins et al [6] carried out equilibrium surface tension measurements on various concentrations of CTAB. The sample they used was prepared in the laboratory and no impurity could be detected by any of the usual procedures.

The experimental γ_e-curve Prins obtained, was well represented by the Szyszkowski equation (3.16), yielding for the parameters $\Gamma_\infty = 12.1 \cdot 10^{-6}$ mol/m^2 and a = 0.368 mol/m^3. Here Γ_∞ is a hypothetical quantity symbolizing the saturation adsorption at infinite bulk concentration. Both Γ_∞ and a are computational constants serving to represent the relation between the equilibrium surface tension and the bulk concentration of CTAB. Using these constants the equilibrium surface tension of CTAB was calculated from the Szyszkowski equation as a function of the concentration and added to the experimental γ_e- and γ_{dyn}-curves in Fig. 5.17.

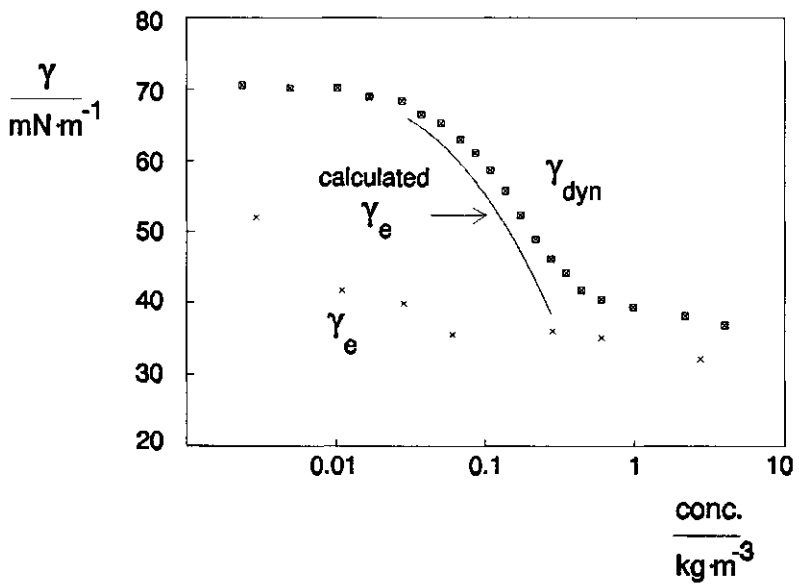

Fig. 5.17: *The dynamic and equilibrium surface tensions, as well as the calculated equilibrium surface tension as a function of the concentration of CTAB; (measurement of γ_e by Stephanie Ágoston).*

It is remarkable that the calculated γ_e-curve is so close to the experimental γ_{dyn}-curve, whereas the experimental γ_e-curve has moved to far lower concentrations on the concentration axis. Apparently the sample used for the experiments was contaminated by minor components which lowered the equilibrium surface tension considerably. During expansion of the surface,

however, the extension is such that these minor components have no allowance to adsorp at the surface and consequently the value of γ_{dyn} is determined by the transport properties of the pure CTAB. So the relatively high value of the experimental excess surface tension is in fact caused by a decrease in γ_e rather than by an increase in γ_{dyn}.

In accordance with these experiences Joos [7] stated that it is very hard to obtain a pure surfactant. Almost every sample, even if it has been purified very carefully, will still contain some minor components, resulting in an equilibrium surface tension which is too low. He concluded that his overflowing funnel was also useful for measuring the surface tension of Sodium dodecyl sulfate (S.D.S.) starting from an impure sample. He got excellent agreement between the surface tension of the expanding surface of the overflowing funnel and literature values of the equilibrium surface tension. So in other words one of the functions of his overflowing funnel was getting rid of impurities. Although the same ability is observed at the expanding surface of the overflowing cylinder, dealing with CTAB the experimental values of γ_{dyn} do not equal the equilibrium values of the pure sample, like in the case of S.D.S. in the overflowing funnel. The deviation will be studied within the framework of the theory of Van Voorst Vader further on.

Diffusion or convection?

Surface active material can be transported to the expanding surface by means of convection and diffusion. The question is which aspect is in general the most important. The dynamic behaviour of different Polyethyleneoxide (PEO) fractions has been studied experimentally in order to answer this question. If the process is diffusion controlled, of course at equal concentration gradients the smallest molecules have the advantage over the bigger molecules of more quickly reaching the surface. However, if the process is convection controlled, bigger molecules will benefit from their extensiveness, and gain a higher vertical velocity on approaching the

expanding surface, for according to eq. (3.21) in a thin layer immediately below the surface the vertical component of the velocity is linearly dependent on the distance from the surface. Assuming instantaneous equilibrium between the surface and the sub-surface layer, the first option implies that the lower the mean molecular weight of the PEO fraction, the less high the dynamic surface tension of low concentrated systems will be. The second option, however, implies that rather the highest molecular weight fractions will be able to lower the surface tension of pure water under dynamic conditions.

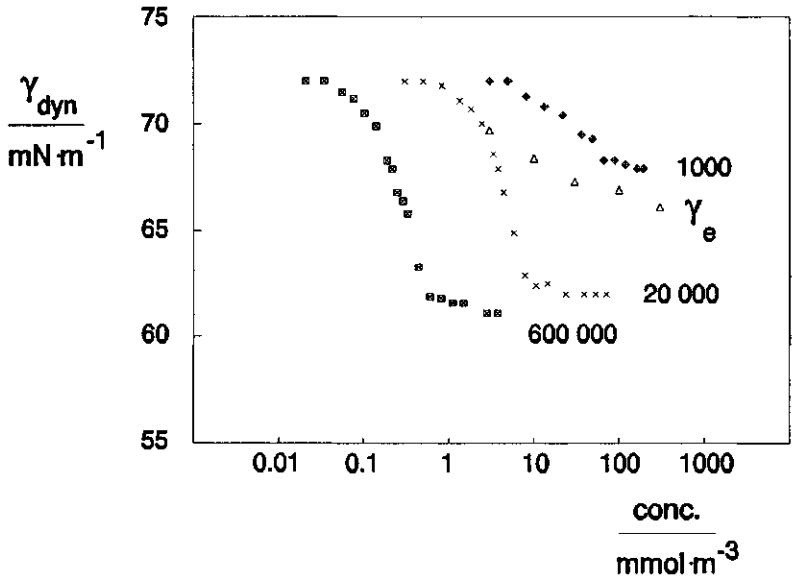

Fig. 5.18: The dynamic surface tensions of the PEO fractions of mean molecular weights 1,000, 20,000 and 600,000, along with the equilibrium surface tension of the fraction of mean molecular weight 1,000 as a function of the concentration in mmol/m^3; (measurement of γ_e by M.A. Cohen Stuart).

In Fig. 5.18 the dynamic surface tensions of three PEO fractions of different mean molecular weights are presented as a function of the concentration given in mmol/m^3. The γ_e-curve of the fraction of M = 1,000 has also been added. Similar to other low molecular surfactant systems without minor

component contaminants the γ_e-curve is positioned close to the γ_{dyn}-curve on the concentration axis. Because of the high affinity character of PEO fractions of high molecular weight, the γ_e- curves of M = 20,000 and M = 600,000 have moved to far lower concentrations. In the concentration region studied, for M = 20,000 and M = 600,000 γ_e was still a constant which was measured to equal the low plateau value of γ_{dyn}.

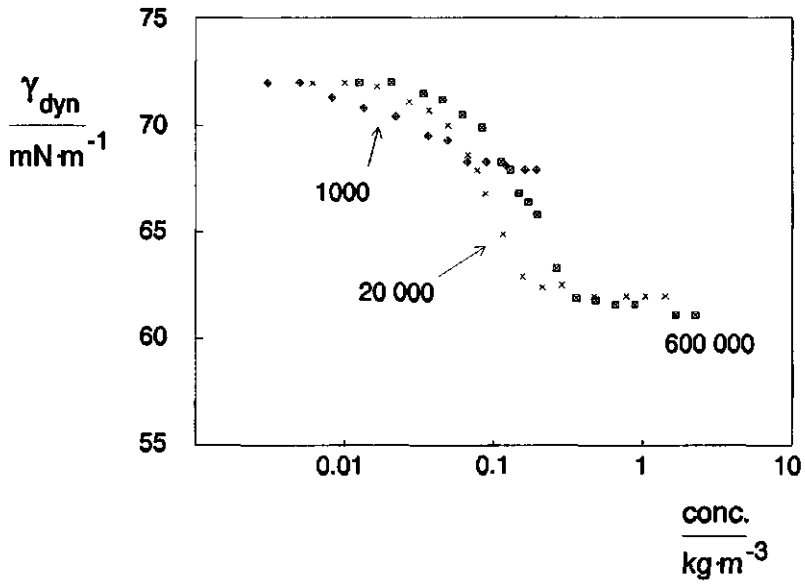

Fig. 5.19: The dynamic surface tensions of the PEO fractions of mean molecular weights 1,000, 20,000 and 600,000 as a function of the concentration in kg/m^3.

Fig. 5.19 shows the dynamic surface tensions of the PEO fractions versus the concentration given in kg/m^3. Here the decrease in γ_{dyn} of the different molecular weight fractions occurs in the same concentration region. By comparing with Fig. 5.18 the conclusion may be drawn that the dynamic surface tension is not determined by the amount of molecules in solution, but by their total mass, that is by the total amount of present monomer segments. This is in agreement with literature reports on the dependency of the surface behaviour of polymers in solution on the total mass dissolved.

Vander Linden et al [8], for instance, experimented on linear polystyrene samples with a narrow molecular weight distribution. They found that above a certain molecular weight the amount of monomer segments adsorbed was independent of the molecular weight. These results have theoretically been predicted by Scheutjens and Fleer [9].

Besides that Fig. 5.19 shows that the lower the mean molecular weight, the less high the dynamic surface tension is at relatively low surfactant concentrations. In other words the PEO fraction of the lowest molecular weight has the greatest ability to lower the surface tension of pure water under dynamic conditions. This means that in the investigated range of molecular weights the transport process at the expanding surface of the overflowing cylinder is diffusion controlled. These findings suggest that at least up to and including M = 600,000 convection plays no important role at the expanding surface of the overflowing cylinder. Extending these results to other surfactant systems the conclusion may be drawn that in general dealing with low molecular surfactant solutions the transport process at the expanding surface is governed by diffusion.
Since the low plateau value of γ_e decreases with increasing molecular weight, the γ_{dyn}-curves of Fig. 5.19 have to cross.

The surface Fourier number

The experiments on solutions of PEO showed that for low molecular surfactant systems the transport process at the expanding surface of the overflowing cylinder must mainly be diffusion controlled. Assuming instantaneous equilibrium between the surface and the sub-surface layer, the value of the dynamic surface tension is correspondingly determined by the diffusion properties of the surfactant. Since Prins [10] (see also §3.2) defined the surface Fourier number, Fo_s, being a measure for the transport efficiency of a surfactant diffusing to the expanding surface, it is now readily understood why he concluded that the surface Fourier number is an

important parameter in describing the dynamic surface tension. He calculated the value of Fo_s for various concentrations of Teepol by means of eq. (3.15). At low concentrations of Teepol, where γ_{dyn} equals the surface tension of pure water, Fo_s was as low as $5 \cdot 10^{-3}$. The dynamic surface tension started to decrease at about the concentration, where the potential supply rate was 10 times larger than the discharge rate. In the concentration region where γ_{dyn} has reached its low plateau value, Fo_s was as high as 10^4. Failing detailed information about the dependency of both dlnA/dt and the surfactant adsorption Γ on the concentration, Prins chose these parameters to be constants. With Γ and dlnA/dt being constants, according to eq. (3.15) Fo_s simply increases squarely with the bulk concentration. Because of the fact that γ_{dyn} decreases monotonously with c_b, of course Prins found γ_{dyn} to decrease monotonously with Fo_s as well.

However, in the overflowing cylinder neither the surfactant adsorption at the expanding surface nor the relative expansion rate are constants with respect to the concentration. The dlnA/dt data of the previous paragraph may be used in order to get more accurate results. Here Fo_s has been calculated for various concentrations of CTAB, because of the availability of the surfactant adsorption data [6] of the highly purified CTAB. Dealing with a nonionic the surfactant adsorption at the equilibrium surface is given by the Langmuir equation (3.17). In the case of a cationic like CTAB, however, which is converted into two ions in solution, Γ has to be multiplied by two in order to equal the right hand side of the Langmuir equation (3.17) [6]:

$$2\Gamma = \Gamma_\infty \frac{c_b}{a + c_b}. \qquad (5.1)$$

The surfactant adsorption at the expanding surface is also given by this equation, provided that the sub-surface concentration c_0 is substituted for c_b. The value of c_0 should be used in the calculation of Fo_s, but unfortunately its magnitude as a function of the concentration is unknown. At relatively high concentrations c_0 will almost equal c_b, whereas at low concentrations c_0 will

be smaller than c_b. Using c_b instead of c_0, at low surfactant concentrations the resulting value of Γ, calculated according to eq. (5.1), will be higher than the real value, although the deviation will be small in comparison to the variation in Γ over the whole range of applied concentrations. Combining eq. (3.15) with eq. (5.1), being the best available approximation of Γ, the surface Fourier number was calculated from

$$Fo_s = \frac{4\pi D}{\Gamma_\infty^2} \frac{(a + c_b)^2}{d\ln A/dt}, \qquad (5.2)$$

where for the diffusion constant D = 10^{-9} m^2/s was used. The values of the computational constants Γ_∞ and a are the same as before. Due to the inaccuracy in Γ at low surfactant concentrations, at these concentrations the calculated value of Fo_s is correspondingly too low.

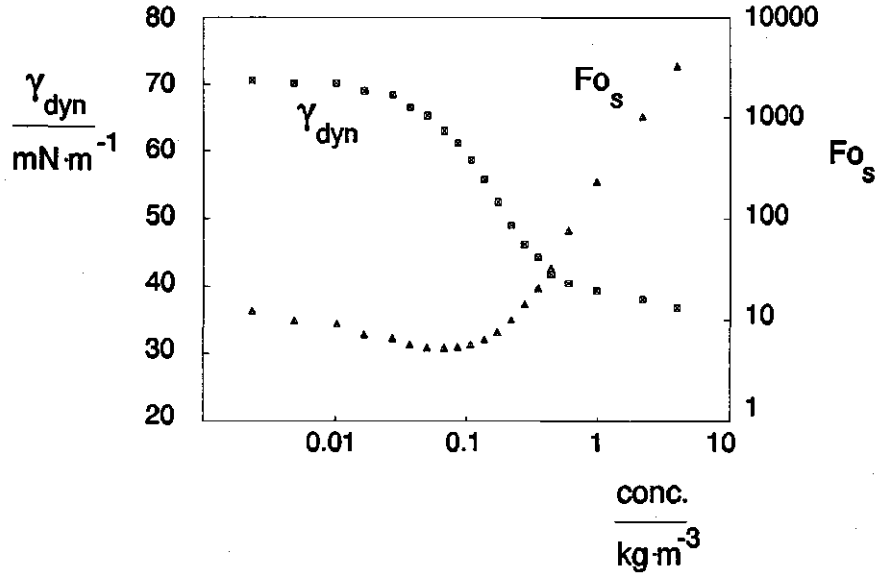

Fig. 5.20: The dynamic surface tension and the surface Fourier number as a function of the concentration of CTAB.

Fig. 5.20 presents both Fo_s and γ_{dyn} as a function of the concentration of CTAB. In this figure the surface Fourier number does not monotonously increase with increasing c_b, and consequently γ_{dyn} will not monotonously decrease with increasing Fo_s. The 'dip' in the Fo_s-curve corresponds with the highest value of dlnA/dt. Like in the case of Teepol at high surfactant concentrations the surface Fourier number approaches the value of 10^4. At low concentrations, however, Fo_s already amounts to ten, although γ_{dyn} still equals the surface tension of pure water. This is not as contradictory with Fo_s of Teepol as it seems. After having reported on the detailed dlnA/dt measurements in the previous paragraph, the dlnA/dt value of the lowest concentrations of Teepol is now known to be 1 s^{-1} instead of the value of 10 s^{-1} Prins used. Moreover, if at these concentrations the value of the surfactant adsorption is actually ten times smaller than the value Prins used, which is not inconceivable, according to eq. (3.15) Fo_s will increase by a factor 1000 in total. This implies that in stead of $5 \cdot 10^{-3}$ the value of 5 is obtained, which is in the same order of magnitude as the value of the surface Fourier number at low concentrations of CTAB.

These findings violate the conclusion of Prins that the surface Fourier number is a measure for the transport efficiency of a surfactant to the expanding surface of the overflowing cylinder. Besides that in the case of CTAB the surface Fourier number has not proved to be appropriate for describing its dynamic surface tension.

The excess surface tension calculated

Van Voorst Vader [11] succeeded in relating the deviation in surface tension, $\Delta\gamma$, with the relative expansion rate of the surface, dlnA/dt. He assumed instantaneous equilibrium between the surface and the sub-surface layer and both diffusion and convection of the surfactant were taken into account. Paragraph 3.2 showed that his theory may also be applied to the expanding surface of the overflowing cylinder. Here the experimental value of the excess surface tension will be compared to the value which follows from the

theory he developed. Because of the fact that the γ_e-curve of the highly purified CTAB in Fig. 5.17 is well described by the Szyszkowski equation using empirical constants, this curve forms the starting-point for the calculation of $\Delta\gamma$.

The theoretical value of the excess surface tension can be calculated according to eqs. (3.23) and (3.24). However, the expressions were deduced for a nonionic, and are based on among others the Langmuir equation (3.17). Since CTAB is a cationic the Langmuir equation (3.17) has to be replaced by eq. (5.1). This implies that in eqs. (3.23) and (3.24) $1/2\Gamma_\infty$ has to be substituted for Γ_∞ . Using the experimental dlnA/dt values of Fig. 5.9, with R = 8.3144 J/mol·K, T = 298 K and all other constants as before, the excess surface tension was calculated for various concentrations of CTAB. The resulting values have been added to the equilibrium surface tensions of the same concentrations of the highly purified CTAB, yielding the calculated γ_{dyn}-curve of CTAB. This curve is compared with the experimental values of γ_{dyn} in Fig. 5.21.

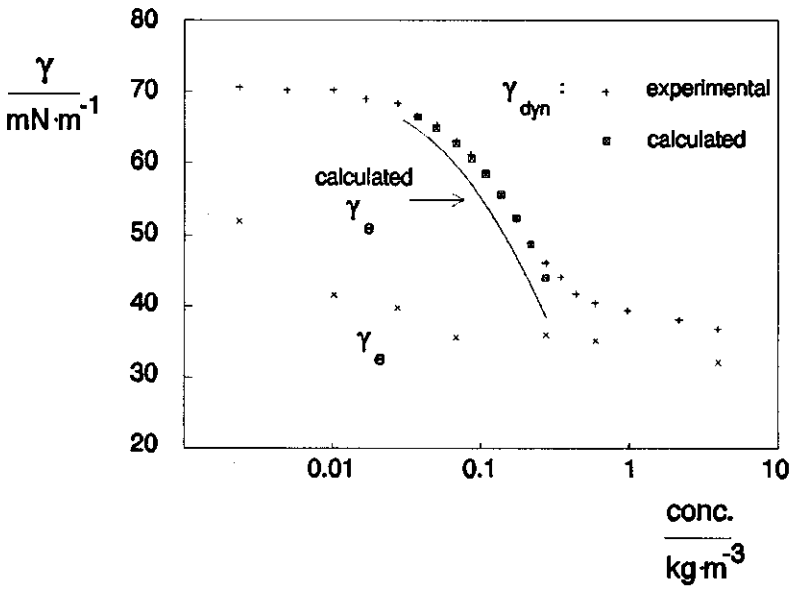

Fig. 5.21: Both experimental and calculated values of γ_{dyn} and γ_e as a function of the concentration of CTAB.

Fig. 5.21 shows that a beautiful fit between experimentally observed values of the dynamic surface tension and those calculated is obtained. These findings support the correctness of the theory Van Voorst Vader developed. Moreover these results prove the dynamic surface tension of the contaminated CTAB to be determined by the transport properties of the pure CTAB. Minor components lower the equilibrium surface tension considerably, but have no allowance to adsorp at the expanding surface, and therefore do not influence the value of the dynamic surface tension.

The surface dilational viscosity

Since both surface tension data and dlnA/dt of various surfactant solutions are now available, the surface dilational viscosity can be calculated according to eq. (2.1). The measurements of the dynamic surface tension and the relative surface expansion rate were carried out at fixed values of the mass flow rate and the length of the wetting film, as has been mentioned before. Q and L were chosen in such a way that for each solution the highest dlnA/dt value possible was obtained. So the resulting value of η_s^d may be attributed to the highest value of dlnA/dt of a particular surfactant solution in the overflowing cylinder.

The surface dilational viscosity has been calculated for various concentrations of Teepol. In Fig. 5.22 both $\Delta\gamma$ (resulting from Fig. 5.14) and dlnA/dt (see Fig. 5.8) are given as a function of the concentration of Teepol. The value of η_s^d is obtained simply by dividing $\Delta\gamma$ by the corresponding value of dlnA/dt. The resulting curve is added to Fig. 5.22.

The maximum in dlnA/dt occurs where the derivative of the dynamic surface tension, $-d\gamma_{dyn}/d\log c$, is the highest (see Fig. 5.7), and the maximum in $\Delta\gamma$ is found where γ_{dyn} starts to decrease with increasing concentration (Fig. 5.14). Consequently the maximum in η_s^d appears at even lower concentrations, where γ_{dyn} still equals the surface tension of pure water. This remark on the position of the maximum in η_s^d also counts for the surfactant Sodium caseinate. Besides that the value of the excess surface tension of the protein

is such, that η_s^d is relatively high over a large range of concentrations. If η_s^d is calculated for CTAB using the equilibrium surface tension of the contaminated sample, the same graph as Fig. 5.22 will be obtained. If, however, the calculation is based upon the equilibrium surface tension of the highly purified sample, the results will be totally different. In that case the excess surface tension is very small and almost independent of the concentration. Consequently the value of η_s^d will also be very small and nearly constant. The maximum η_s^d of the contaminated CTAB amounts to 19 mNs/m, whereas the pure CTAB maximally gives η_s^d = 1 mNs/m only.

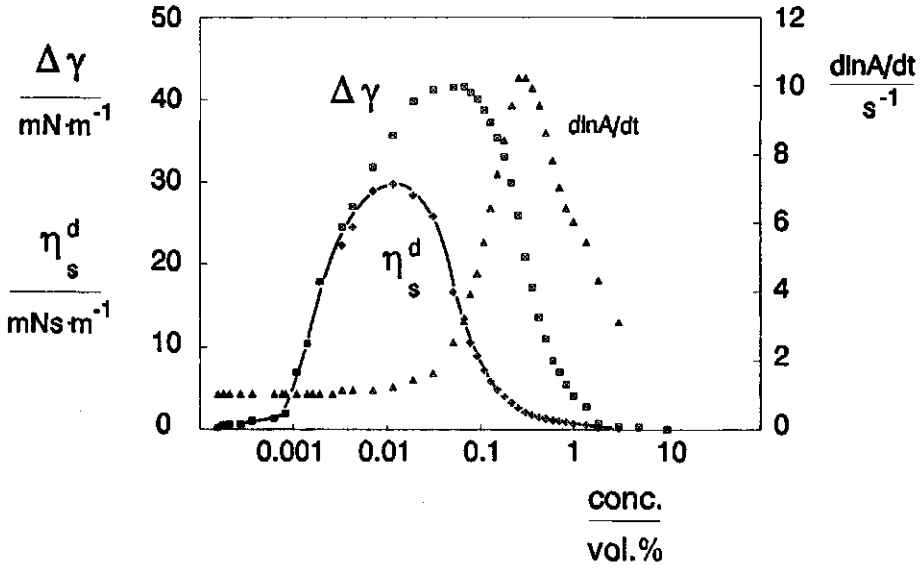

Fig. 5.22: The excess surface tension, the relative surface expansion rate, and the surface dilational viscosity as a function of the concentration of Teepol.

These findings illustrate that the magnitude of η_s^d is highly influenced by the value of the equilibrium surface tension, which is in turn, dealing with low molecular surfactant systems, for the greater part determined by the presence of minor components. In fact the surface dilational viscosity is a measure for the degree of purity of the low molecular surfactant, rather than a tool for describing the behaviour of the continuous expanding surface of

the overflowing cylinder. This does not imply that the surface dilational viscosity is not a relevant property of the surfactant solution either. The surface dilational viscosity, which can be determined from overflowing cylinder measurements, may be an important tool for describing for instance the foaming behaviour, since the foaming behaviour of a contaminated surfactant system may expected to be different from the foaming behaviour when dealing with a pure surfactant solution.

5.4 The height of the overflowing meniscus

The numerical calculations on the height of the overflowing meniscus of pure liquids showed that h_{dyn} is strongly dependent on the value of the surface tension (see Fig. 3.5). In §3.3 the height of the meniscus of surfactant solutions was also expected to be dependent on the value of the surface tension of the continuous expanding surface. Fig. 5.23 gives h_{dyn} as a function of the concentration of the surfactant Teepol at fixed values of the mass flow rate and the length of the wetting film. By comparison with the γ_{dyn}-curve of Fig. 5.14, it is noticed that the course of both parameters versus the concentration is similar. For low surfactant concentrations h_{dyn} equals the height of the overflowing meniscus of pure water. The decrease in h_{dyn} occurs in the same concentration region as the decrease in γ_{dyn}. At high concentrations, like γ_{dyn}, h_{dyn} seems to have reached a low plateau value. So Fig. 5.23 indeed suggests h_{dyn} and γ_{dyn} to be closely related.

Of course the value of h_{dyn} is also influenced by the flow rate. Fig. 5.24 shows the dependency of h_{dyn} on the flow rate for solutions of fixed concentrations of Teepol and Sodium caseinate. For high flow rates, where the magnitude of the flow rate has no effect on the value of γ_{dyn} any more (see chapter 6), the inclination of the curves is relatively small. At low flow rates the inclination of the curves is higher, because there γ_{dyn} acts as an extra variable which increases with increasing flow rate as well.

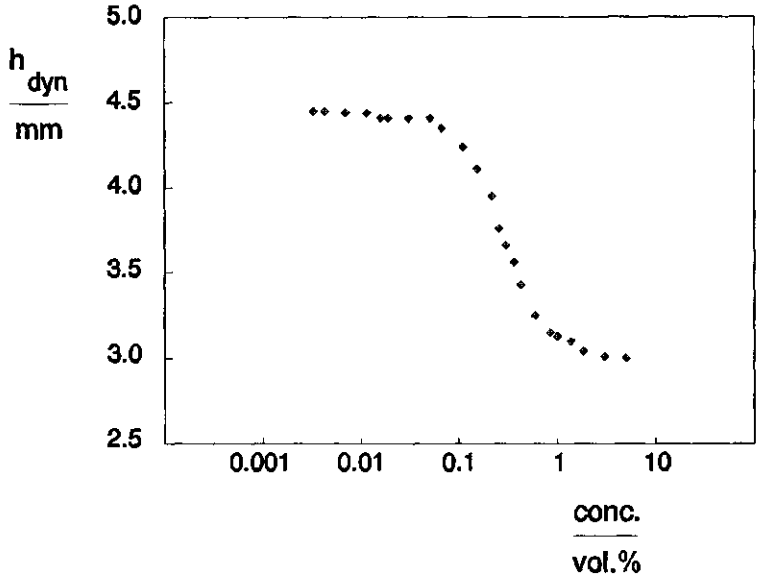

Fig. 5.23: The height of the meniscus above the rim as a function of the concentration of Teepol; Q = 54 cm³/s, L > 4 cm.

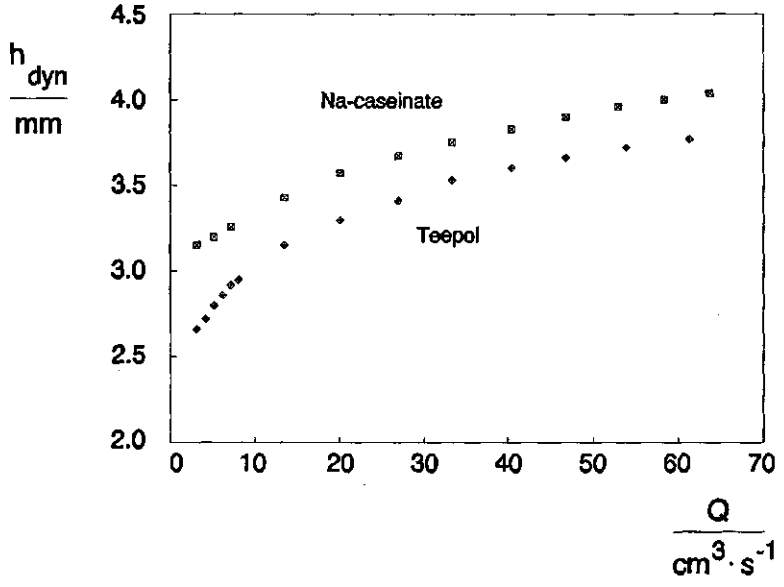

Fig. 5.24: The height of the centre of the meniscus above the rim of the cylinder as a function of the flow rate for 0.3 vol% Teepol and 20 kg/m³ Na-caseinate; L > 4 cm.

A quantitative description

Figs. 5.23 and 5.24 qualitatively demonstrate that the magnitude of h_{dyn} is related to both γ_{dyn} and the flow rate. In §3.3 an expression for h_{dyn} has been deduced stating that h_{dyn} is linearly dependent on the dynamic surface tension. An extra term Δh_{flow} has been included in eq. (3.29) representing the excess height due to the flow of liquid. Possible effects on h_{dyn} of a surface tension gradient present in the surface have not explicitly been accounted for in eq. (3.29).

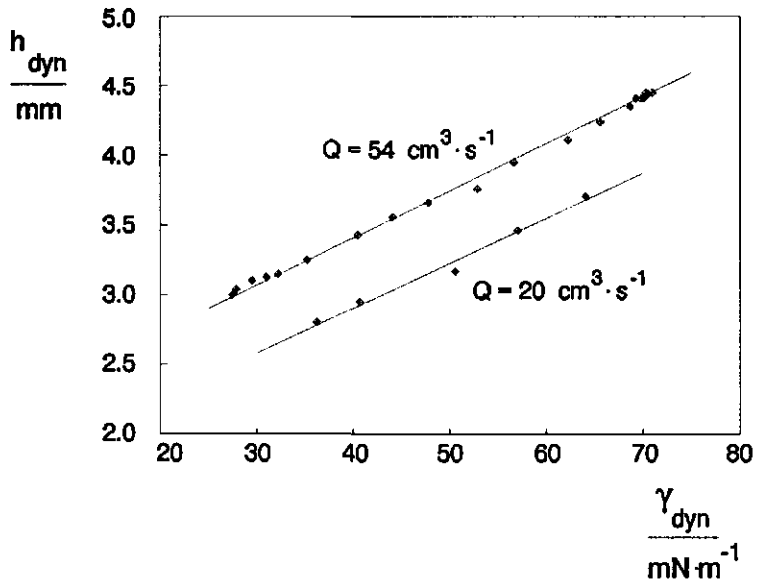

Fig. 5.25: The height of the centre of the meniscus above the rim of the cylinder versus the dynamic surface tension of Teepol at two mass flow rates; the lines are drawn according to the equations:
$h_{dyn} = 3.37 \cdot 10^{-2}\ \gamma_{dyn} + 2.06 \cdot 10^{-3}$, *for* $Q = 54\ cm^3/s$;
$h_{dyn} = 3.21 \cdot 10^{-2}\ \gamma_{dyn} + 1.62 \cdot 10^{-3}$, *for* $Q = 20\ cm^3/s$.

The relation between h_{dyn} and γ_{dyn} is studied experimentally for Teepol at two mass flow rates. The concentration of Teepol was the adjustable variable in the experiments. For each flow rate the drawn line in Fig. 5.25 represents the best fit of the experimental results referring to eq. (3.29):

$$h_{dyn} = \frac{1}{\rho g}\left(\frac{1}{R_1} + \frac{1}{R_2}\right) \cdot \gamma_{dyn} + \Delta h_{flow}. \qquad (3.29)$$

Fig. 5.25 shows that the experimental results are well described by eq. (3.29). Assuming Δh_{flow} to be dependent on the flow rate only, and $1/\rho g$ being a constant, these findings imply that for a fixed flow rate the mean curvature of the meniscus is also a constant, irrespective of the concentration. Besides that the inclination of the line does not change very much with altering flow rate, whereas the value of h_{dyn} at the point of intersection with the y-axis does. This means that the curvature of the meniscus stays nearly unchanged with altering flow rate, whereas of course Δh_{flow} varies with the flow rate.

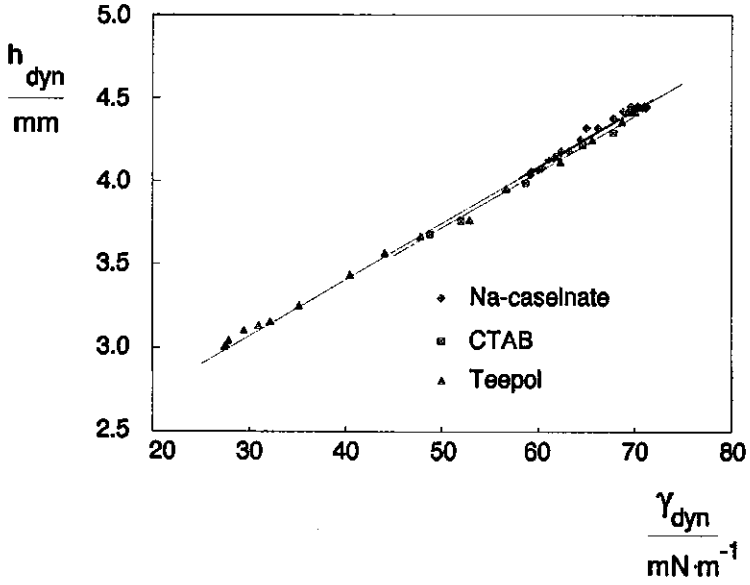

Fig. 5.26: *The height of the centre of the meniscus above the rim of the cylinder versus the dynamic surface tension of various surfactants; Q = 54 cm³/s and the lines are drawn according to the equations:*
$h_{dyn} = 3.43 \cdot 10^{-2}\ \gamma_{dyn} + 2.03 \cdot 10^{-3}$, *for Na-caseinate;*
$h_{dyn} = 3.39 \cdot 10^{-2}\ \gamma_{dyn} + 2.02 \cdot 10^{-3}$, *for CTAB;*
$h_{dyn} = 3.37 \cdot 10^{-2}\ \gamma_{dyn} + 2.06 \cdot 10^{-3}$, *for Teepol.*

In Fig. 5.26 the results of Teepol of Fig. 5.25 obtained at the highest flow rate are presented again. For reasons of comparison the results of the surfactants CTAB and Sodium caseinate referring to the same flow rate have been added. Each surfactant has its own region of possible values of the dynamic surface tension. Where the values of γ_{dyn} are the same, however, both the experimental results and the fitted lines of h_{dyn} almost coincide. The inclination of the lines only varies with $\pm\ 0.03 \cdot 10^{-2}$ m^2/N, and the variation in the value of h_{dyn} at the point of intersection with the y-axis ($\gamma_{dyn} = 0$ mN/m) is even smaller with $\pm\ 0.02 \cdot 10^{-3}$ m. Assuming again Δh_{flow} to be dependent on the flow rate only, and $1/\rho g$ being a constant, according to eq. (3.29) these findings imply that at a fixed flow rate not only Δh_{flow} is a constant, but also the mean curvature of the overflowing meniscus is a constant, irrespective of both the concentration and the applied surfactant. It is rather surprising that the value of h_{dyn} appears to be completely determined by the value of the dynamic surface tension and the imposed mass flow rate, whatever the applied surfactant and its concentration in solution may be.

The curvature of the meniscus

In order to check this reasoning about the curvature of the meniscus being independent of the surfactant and its concentration, photos were taken of the overflowing liquid. From these photos the radius of curvature R_2 was measured for various concentrations of all three surfactants of Fig. 5.26 at the flow rate $Q = 54$ cm^3/s. The radius of curvature R_1 originates in the axis of symmetry of the cylinder, and is situated in the plane perpendicular to the plane of R_2 (see Fig. 3.6). Its magnitude can not be measured directly. Where the tangent of the meniscus is vertical, R_1 has its minimum value which approximates the radius of the cylinder, $R = 4$ cm. At any other position on the meniscus the magnitude of R_1 is larger. Since R_1 is always much bigger than R_2, its contribution to the total value of the curvature of the meniscus will be small. Dealing with very high values of R_1, its effect may even be neglected.

The calculation of R_2 has been based upon the inclinations of the lines fitting the experimental results in Fig. 5.26. With ρ = 1000 kg/m^3 and g = 10 m/s^2 values of R_2 were calculated according to eq. (3.29) using alternately the minimum value of R_1 and $R_1 = \infty$. In Table 5.1 the calculated values are compared with the experimental value resulting from the photo. The measured radius is given for each single investigated concentration of Teepol, whereas the average radius of concentrations of CTAB and Sodium caseinate is reported.

Table 5.1: *Both calculated and experimental values of the radius of curvature R_2 for various surfactants and surfactant solutions, as well as h_{dyn} for various concentrations of Teepol.*

surfactant	R_2 [mm] calculated R_1 = 4 cm	R_2 [mm] calculated $R_1 = \infty$	R_2 [mm] measured ± 0.15	h_{dyn} [mm] measured ± 0.02
CTAB	3.19	2.95	2.9	
Na-caseinate	3.15	2.92	3.1	
Teepol:	3.21	2.97		
0.15 vol%	3.21	2.97	3.0	4.11
0.23 vol%	3.21	2.97	3.1	3.88
0.30 vol%	3.21	2.97	2.6	3.62
0.50 vol%	3.21	2.97	2.4	3.28
0.80 vol%	3.21	2.97	2.7	3.12

Owing to the margins of the accuracy of the experiment rather good agreement exists between the measured and calculated radius R_2 for CTAB, Sodium caseinate and low concentrations of Teepol. The measured values of high concentrations of Teepol, however, are substantially smaller than the calculated value. By comparison with Fig. 5.8 it is noticed that these concentrations generate the highest surface tension gradients, and correspondingly yield high relative surface expansion rates. Since for surfactant solutions the surface tension gradient is the driving force of the

surface deformation, the higher its value, the less convex the meniscus in the centre of the surface has to be. In this situation of the meniscus being more level in the vicinity of the centre, the curvature of the meniscus close to the rim of the cylinder has to increase, resulting in the experimentally observed smaller value of R_2. Besides that, due to the increased relative surface expansion rate, the excess height Δh_{flow} may slightly decrease. Because of the fact that these concentrations of Teepol, too, satisfy the linear relationschip of Fig. 5.26, the effect of the smaller radius may accidentally be neutralized by the effect of a smaller Δh_{flow}. In order to be able to neutralize the effect of the smaller radius of for example 0.5 vol% Teepol, having a dynamic surface tension of 38 mN/m, the quantity of ca. $0.3 \cdot 10^{-3}$ m has to be subtracted from the value of Δh_{flow} in Fig. 5.26. Thus reasoning the influence of the surface tension gradient on the value of Δh_{flow} is comparable to the influence of a change in flow rate (see Fig. 5.24). CTAB only showed the same tendency versus the concentration on a very small scale not exceeding the margins of the accuracy, but there the surface tension gradient of CTAB is also smaller than the one of Teepol. None of these effects were observed for Sodium caseinate, probably because the surface tension gradient of Sodium caseinate is almost immeasurable small.

The conclusion may be drawn that the curvature of the overflowing meniscus of a surfactant solution is independent of the applied surfactant and its concentration, provided that the solution under investigation is not able to generate a relatively large surface tension gradient. Under the same condition the magnitude of Δh_{flow} appears to be determined by the flow rate only.

The form of the meniscus

The values of h_{dyn} of the investigated concentrations of Teepol have been included in Table 5.1. Making a comparison between the radius R_2 and h_{dyn}, R_2 is noticed to be smaller, suggesting that the meniscus is most broad at a certain distance above the rim of the cylinder, like it was drawn in Figs. 2.3 and 3.8. Here the tangent of the meniscus is vertical, whereas at the level of

the rim of the cylinder the inclination of the tangent has a finite value. This idea is confirmed by other experimental results. The thickness of the wetting film near the rim of the cylinder, δ_0, of a 0.3 vol% solution of Teepol was measured to be 0.56 mm, whereas the most extensive part of the meniscus was experienced to be positioned slightly above the rim at a distance of 0.70 mm referring to the wall of the cylinder.

5.5 Influence of the bulk viscosity

The bulk viscosity of the solution in the overflowing cylinder was increased by adding dextran. No surface activity of dextran was observed at the surface of pure water, neither under equilibrium conditions, nor during continuous expansion of the surface in the overflowing cylinder. The dependency of the bulk viscosity on the shear rate was studied by means of the Bohlin VOR constant shear rheometer for a solution containing twice as much dextran (8%) as the most viscous solution investigated in the overflowing cylinder. The bulk viscosity was determined for those shear rates existing in the cylinder and at the expanding surface, when a surface tension gradient is present. The results did not bear evidence of significant non-Newtonian behaviour. Therefore, the investigated systems, being less concentrated, were considered to fully behave Newtonian.

Experiments were carried out at a fixed flow rate on pure water containing sequentially 0, 2, and 4 $^{w}/_{w}$ % dextran. Next the viscosity of a solution of 0.3 vol% Teepol was raised step by step by adding dextran. If a higher viscosity effects a change in behaviour of the overflowing liquid, this is expected to be most manifest for the Teepol concentration of 0.3 vol%, because at this concentration $-d\gamma_{dyn}/dc$ is the highest, yielding the maximum values of $d\gamma/dr$ and $d\ln A/dt$. The surfactant Teepol itself proved not to affect the viscosity of the dextran solution. Table 5.2 reports on the influence of the viscosity on the physical parameters of the overflowing cylinder. The

mean value of the surface tension gradient was calculated from the dynamic surface tensions at the positions r = 0 cm and r = 3 cm. This value was considered to be the surface tension gradient of the position half way the interval at radial distance r = 1.5 cm. The relative surface expansion rate of Teepol has not only been measured by means of the LDA-technique, but was also calculated from eq. (3.8) using the measured value of the surface tension gradient.

Table 5.2: *The influence of the viscosity on the physical parameters for pure water and 0.3 vol% Teepol; Q = 33.3 cm^3/s.*

	pure water			0.3 vol% Teepol				
% dextran	0 %	2 %	4 %	0 %	1 %	2 %	3 %	4 %
η_b (20 °C) ± 0.01 mPas	1.00	1.89	3.25	1.00	1.32	1.89	2.54	3.25
h_{dyn} ± 0.005 mm	4.20	4.18	4.15	3.56	3.54	3.53	3.52	3.46
δ_0 ± 0.01 mm	0.61	0.63	0.67	0.56	0.56	0.57	0.58	0.57
γ_{dyn} ± 0.3 mN/m	72.8	72.3	72.5	49.7	48.5	48.0	48.3	47.4
$d\gamma/dr$ (r = 1.5) ± 0.02 Pa	–	–	–	0.17	0.18	0.19	0.20	0.20
dlnA/dt (exp.) ± 0.1 s^{-1}	1.0	1.0	1.2	9.0	8.4	7.8	7.4	7.1
dlnA/dt (cal.) ± 0.5 s^{-1}				9.1	8.6	7.9	7.4	6.8

Increasing the viscosity of pure water

At the surface of pure water dextran appears not to affect the dynamic surface tension. Besides that dextran shows not to be able to generate a surface tension gradient. So indeed no surface activity of dextran is observed. Since dextran does not create a surface tension gradient, the relative surface expansion rate keeps the minimum level of pure water with

increasing concentrations of dextran. From Table 5.2 it is noticed that the bulk viscosity does influence both the height of the meniscus and the thickness of the wetting film. At higher bulk viscosities the wall of the cylinder is more capable of slowing down the wetting film. It is generally known [12] that the thickness of the boundary layer at the wall of the cylinder increases with increasing bulk viscosity. Consequently the mean velocity of the wetting film decreases. Since the flow rate is fixed, in order to be able to transport the same amount of fluid, the wetting film has to become thicker with increasing bulk viscosity. At the horizontal top surface of the overflowing cylinder the opposite is the case. Due to the higher bulk viscosity, in correspondence with eq. (3.7), the normal derivative of the radial velocity of the surface reduces. Consequently the mean radial velocity in the meniscus increases. This implies that in eq. (3.29) the term Δh_{flow}, representing the excess height due to the flow of liquid, may become smaller, resulting in a decrease of the total height of the meniscus, h_{dyn}.

Increasing the viscosity of a surfactant solution

Increasing the bulk viscosity of the solution of Teepol, a few alterations in the values of the physical parameters are observed which are logically connected. The reasoning starts off with the surface tension gradient which appears to be higher for higher concentrations of dextran. The magnitude of the surface tension gradient depends on the transport properties of the applied surfactant. The higher the bulk viscosity, the less efficient the transport will be. A higher bulk viscosity may be imagined to induce a higher surface tension gradient. This effect may be compared to the observation in §5.3 that the PEO solution of the highest mean molecular weight, containing molecules having the lowest diffusion coefficient, happens to generate the highest surface tension gradient.

The bulk viscosity is a very important parameter in eq. (3.8) which relates the relative surface expansion rate to the surface tension gradient. Generally a higher surface tension gradient leads to a higher value of dlnA/dt, but when

the surface tension gradient is increased by the bulk viscosity, the opposite may occur as is noticed from the calculated values of dlnA/dt in Table 5.2. Although the accuracy of the input parameter $d\gamma/dr$ is small, good agreement exists between calculated and measured values of dlnA/dt.

If the relative surface expansion rate gets smaller, the dynamic surface tension will deviate less from the equilibrium value. The effect of the decrease in transport efficiency is apparently small, for γ_{dyn} is observed to decrease with increasing bulk viscosity. In turn a smaller value of γ_{dyn} directly implies a smaller value of h_{dyn}.

The thickness of the wetting film does not change very much. Following the explanation given above for water, the wetting film is likely to become thicker with increasing viscosity. Although the arguments put forward for water are also valid here, the effects are smaller, because of the film velocity which is much higher for surfactant solutions.

Summarizing, an increase in bulk viscosity appears to give rise to coherent changes in the behaviour of the overflowing liquid, either pure water or a surfactant solution. These effects are logically understood, but are in fact relatively small. When studying various concentrations of a surfactant which does not explicitly raise the bulk viscosity, the influence of the bulk viscosity on the physical parameters of the overflowing cylinder may be neglected.

Acknowledgments. The author wishes to thank M.A. Cohen Stuart from the Department of Physical- and Colloid Chemistry of Wageningen Agricultural University for his assistance in interpreting the experimental results of the Polyethylene fractions. Thanks are also due to mrs. Stephanie Ágoston and mrs. Marjo Geurts for performing the prepatory investigation of respectively the behaviour of solutions of CTAB and the influence of the bulk viscosity. Bart Schulte and Marcel Böhmer accurately contributed to the indicated figures.

References chapter 5

[1] D.J.M. Bergink-Martens, H.J. Bos, A. Prins and B.C. Schulte, J. Coll. Int. Sc., 138 (1990) 1.

[2] D.J.M. Bergink-Martens, H.J. Bos and A. Prins, submitted for publication in J. Coll. Int. Sc.

[3] D.E. Graham and M.C. Philips. J. Coll. Int. Sc., 70 (1979) 403.

[4] H. de Ruiter, A.J.M. Uffing, E. Meinen and A. Prins, Weed Science, 38 (1990) 567.

[5] D.J.M. Bergink-Martens, H.J. Bos, H.K.A.I. van Kalsbeek and A. Prins, in E. Dickinson and P. Walstra (Eds.), Food Colloids and Polymers: Stability and Mechanical Properties, Royal Society of Chemistry, Cambridge, (1993), pp. 376 - 386.

[6] A. Prins, C. Arcuri and M. van den Tempel, J. Coll. Int. Sc., 24 (1967) 84.

[7] P. Joos and P. de Keyser, The Overflowing Funnel as a Method for Measuring Surface Dilational Properties, Levich Birthday Conference, Madrid, (1980).

[8] C. vander Linden, R. van Leemput, J. Coll. Int. Sc., 67 (1978) 48.

[9] J.M.H.M. Scheutjens and G.J. Fleer, in T.F. Tadros (Ed.), The Effect of Polymers on Dispersion Properties: papers presented at the Int. Symp., 21 - 23 Sept. 1981, London, London [etc.], Academic Press, (1982), pp. 145 - 168.

[10] A. Prins and D.J.M. Bergink-Martens, in E. Dickinson and P. Walstra (Eds.), Food Colloids and Polymers: Stability and Mechanical Properties, Royal Society of Chemistry, Cambridge, (1993), pp. 291 - 300.

[11] F. van Voorst Vader, Th.F. Erkens and M. van den Tempel, Trans. Farady Soc., 60 (1964) 1170.

[12] H. Schlichting, Boundary-layer theory, McGraw-Hill Book Company, New York, (1968).

Chapter 6

The magnitude of the surface expansion rate

The relative surface expansion rate is experienced to range from about 1 s^{-1} for pure water to 10 s^{-1} for particular surfactant solutions. The only parameter influencing the relative surface expansion rate of pure water is the flow rate. Dealing with surfactant solutions the capacity for changing the relative surface expansion rate via the flow rate is small. More variation can be accomplished by adjusting the length of the wetting film (§6.1). With respect to the magnitude of the relative surface expansion rate the overflowing cylinder is compared with other techniques bringing about dilational surface deformations. The overflowing cylinder is pre-eminently useful for studying processes which imply expansion of liquid surfaces far from equilibrium (§6.2).

6.1 Factors of influence on the relative surface expansion rate

The radial surface velocity of both pure water and a surfactant solution appears to be almost linearly dependent on the radial coordinate r in the vicinity of the centre of the circular meniscus. In this area, extending as far as about r = 2.5 cm, the simplified expression (3.6) for the relative surface expansion rate may be used:

$$d\ln A/dt = 2\frac{v_r}{r}. \qquad (3.6)$$

The dlnA/dt data presented in this paragraph were obtained by measuring the radial surface velocity at or near the position r = 2.5 cm by means of the LDA-technique, and next calculating the result according to eq. (3.6).

From all the physical parameters describing the operation of the overflowing cylinder technique only the values of the flow rate, Q, and the length of the wetting film, L, can be imposed on the liquid system, as has already been stated in chapter 2. The solution in the overflowing cylinder determines

autonomously the values of all other parameters, the relative surface expansion rate included.

Dealing with pure water in the overflowing cylinder, the dynamic surface tension equals the equilibrium value of pure water, independently of the surface expansion rate. According to the experience, however, it is simply impossible to have the cylinder filled with pure water, for there will always be some surface active impurities present in the system. These contaminants are not being noticed at the expanding top surface, but they do affect the surface tension in the outer cylinder where the surface is continuously compressed. Diminishing the length of the wetting film no alterations in the values of the parameters at the expanding surface occur until L becomes smaller than 1.5 cm. Thereon instabilities arise, because the contaminated surface of the outer cylinder can not be 'separated' from the expanding surface of pure water any more. In this situation undulations are observed at the top surface, and consequently the usual measurements can not be performed. Setting aside the experimental instabilities caused by surface active impurities, the magnitude of the relative surface expansion rate of pure water is independent of the length of the wetting film. This is readily understood considering the assumption (§3.4) that the weight of the free falling part of the wetting film determines the behaviour of the expanding top surface via the creation of a surface tension gradient. Since pure water is not able to generate a surface tension gradient, no influence of L on the surface expansion rate is to be expected. The only parameter influencing the relative surface expansion rate of pure water is the flow rate. Fig. 5.2 has already shown that in the case of pure water $d\ln A/dt$ is a monotonously increasing function of the flow rate.

Dealing with a surfactant solution in the overflowing cylinder both the nature of the applied surfactant and its concentration considerably influence the magnitude of the surface tension gradient which is generated over the hori-

zontal top surface, and thus the magnitude of dlnA/dt, as has been elucidated in §5.2. The bulk viscosity has shown (§5.5) to have a minor effect on the magnitude of dlnA/dt. In this paragraph the influence of the imposed values of respectively L and Q on the relative surface expansion rate of a particular surfactant solution in the overflowing cylinder will be discussed.

The influence of the length of the wetting film

The length of the wetting film of a 0.3 vol% Teepol solution was varied keeping the mass flow rate constant. Fig. 6.1 gives the corresponding γ_{dyn} measured both in the centre of the circular surface and at r = 3.5 cm.

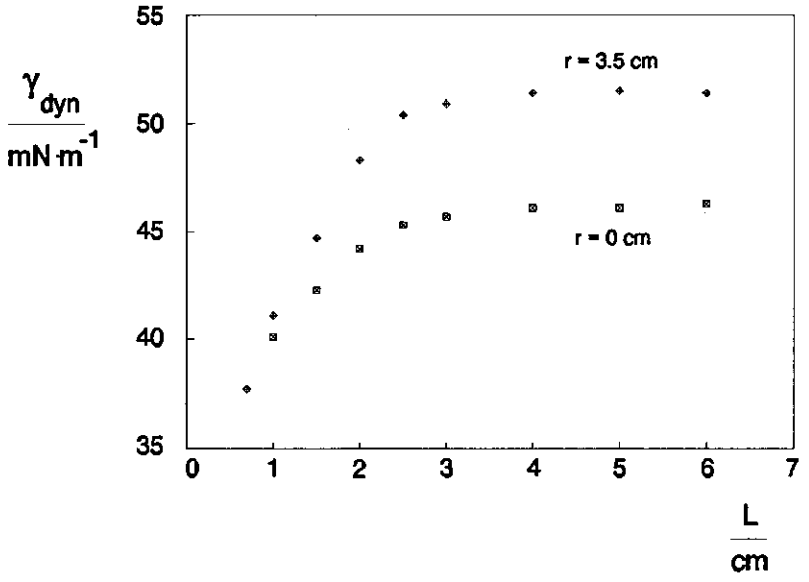

Fig. 6.1: The dynamic surface tensions at r = 0 and r = 3.5 cm as a function of the length of the wetting film for a 0.3 vol% solution of Teepol; Q = 33.3 cm³/s.

At a length of ca. 2.5 - 3.0 cm a change in the behaviour of the overflowing liquid is observed. When the length of the wetting film becomes smaller than this value, the decrease in γ_{dyn} amounts to almost 10 mN/m. In the laboratories where this research work has been carried out the same graph

was obtained for milk and solutions of egg white powder. The dynamic surface tension has always been observed to remain constant for L > 2-3 cm. Dealing with aqueous solutions of egg white powder the decrease in γ_{dyn} below this value was even as large as 25 mN/m.
The parameter h_{dyn} experimentally showed to have the same course versus L as the dynamic surface tension. Since at a fixed flow rate h_{dyn} is completely determined by the value of γ_{dyn}, this is no surprise.

In §3.4 the function of the boundary layer which is built up along the outside wall of the cylinder, was put forward as a hypothesis. The boundary layer reaches the surface of the wetting film at a length L_{crit}. As long as $L < L_{crit}$, the weight of the free falling part of the wetting film can be varied by changing L. While L is increased to values higher than L_{crit} the weight of the free falling part of the film stays the same. It is the weight of the free falling part of the wetting film that is assumed to determine the behaviour of the expanding top surface via the creation of a surface tension gradient.
L_{crit} can be calculated for the 0.3 vol% solution of Teepol by applying equation (3.35) to its parameters. The radial surface velocity was measured to be 15 cm/s at r = 3.0 cm, whereas near the rim of the cylinder v_r was found to have already increased to 25 cm/s. Since in this area v_r increases far more than linearly with r, v_s^0 is estimated to be 35 cm/s. For the applied flow rate the thickness of the wetting film near the rim of the cylinder, δ_0, was measured to be 0.56 mm. The mean film velocity near the rim of the cylinder, V_f^0, is approximately expressed by

$$V_f^0 = \frac{Q}{2\pi R \cdot \delta_0}, \qquad (6.1)$$

and can now be calculated to equal ca. 25 cm/s. The estimate of the surface velocity, v_s^0, appears to be higher than the mean film velocity, and this has been predicted by Fig. 3.8. With $\rho = 10^3$ kg/m^3, $\eta_b = 10^{-3}$ Pa·s and g = 10 m/s^2, the calculated value of L_{crit} from eq. (3.35) is 2.0 cm. Physically this

implies that the boundary layer has become of the same thickness as the wetting film at the point L = 2.0 cm. This calculated value of L_{crit} corresponds well with the value of L = 2.5 - 3.0 cm where in Fig. 6.1 a change in the behaviour of the overflowing liquid is observed. So in accordance with the hypothesis above this value the weight of the free falling part of the film is likely to stay unchanged. This is why in Fig. 6.1 the surface tension gradient is noticed to be a constant for high values of L.

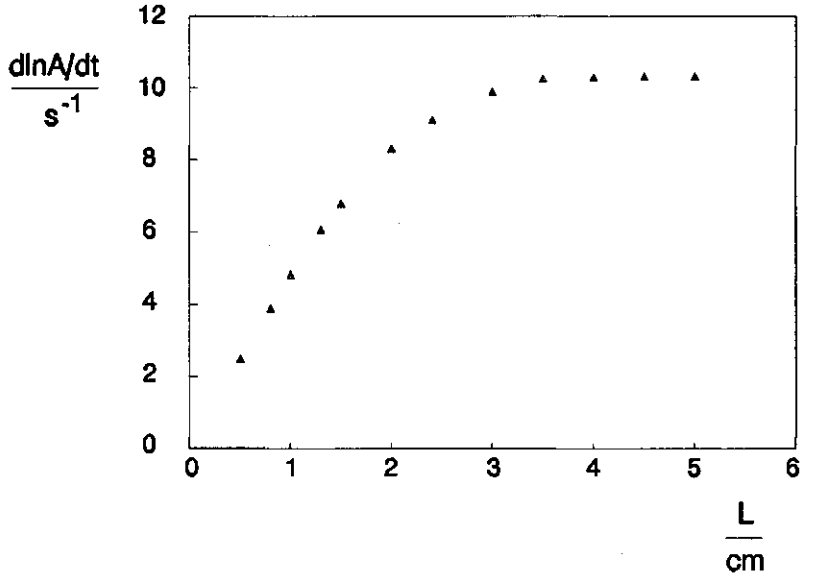

Fig. 6.2: The relative surface expansion rate as a function of the length of the wetting film for a 0.3 vol% solution of Teepol; Q = 33.3 cm^3/s.

Because of the fact that the magnitudes of the surface tension gradient and the relative surface expansion rate are directly coupled, also dlnA/dt is a constant in this region, as is shown by Fig. 6.2. Below the value of L_{crit} the surface tension gradient starts to decrease with decreasing L (see Fig. 6.1). Here by diminishing the total length of the wetting film the weight of the free falling part becomes smaller, and consequently the ability to generate a surface tension gradient is less high. Correspondingly the relative surface expansion rate is observed to decrease in the same region as well.

Dealing with solutions of egg white powder for small values of L a stiff film arose at the top surface of the overflowing cylinder. Probably denatured proteins formed a gel and thus immobilized the surface. Owing to the resulting zero value of dlnA/dt, the decrease in γ_{dyn} was found to be that large as has already been mentioned.

It is concluded that the behaviour of the expanding top surface of the overflowing cylinder is governed by the weight of the free falling part of the wetting film. The free falling part generates a surface tension gradient and in this way influences the magnitude of the physical parameters. As long as L is smaller than L_{crit} at a fixed flow rate the values of dlnA/dt, $d\gamma/dr$, γ_{dyn} and h_{dyn} can be substantially increased by increasing L. For $L > L_{crit}$ the weight of the free falling part of the wetting film stays unchanged, and that is why in this region these parameters are constants.

The influence of the flow rate

The flow rate was varied at a fixed length of the wetting film chosen in such a way that $L >> L_{crit}$, and the corresponding dlnA/dt was measured for solutions of 0.3 vol% Teepol and 20 kg/m^3 Sodium caseinate.

Fig. 6.3 shows a steep increase in dlnA/dt for small values of the flow rate, whereas for higher values the inclination of the curves is relatively small. The first steep increase is connected with an increase in both $d\gamma/dr$ and γ_{dyn}. When in this region a higher flow rate is imposed on the liquid system in the overflowing cylinder, the wetting film becomes thicker causing the free falling part of the wetting film to grow. Due to the rise in weight of the free falling film part the system is able to generate a higher $d\gamma/dr$. In turn this surface tension gradient induces a higher value of dlnA/dt. As a result both v_s^0 and V_f^0, the mean film velocity at the level of the rim of the cylinder, get higher values as well. Along the outside wall of the cylinder a boundary layer is built up. It is a well-known fact [1] that the thickness of a boundary layer is inversely proportional to the square root of the undisturbed fluid velocity

outside the layer. So here the boundary layer along the wall of the cylinder will become less thick, since the velocity outside the boundary layer increases, and the thinner the boundary layer, the bigger the free falling part of the wetting film will be. So, when imposing a higher flow rate on the liquid system in the overflowing cylinder, the effect on the magnitude of dlnA/dt is strengthened by the decrease in boundary layer thickness, for this brings about an additional growth of the free falling part of the wetting film.

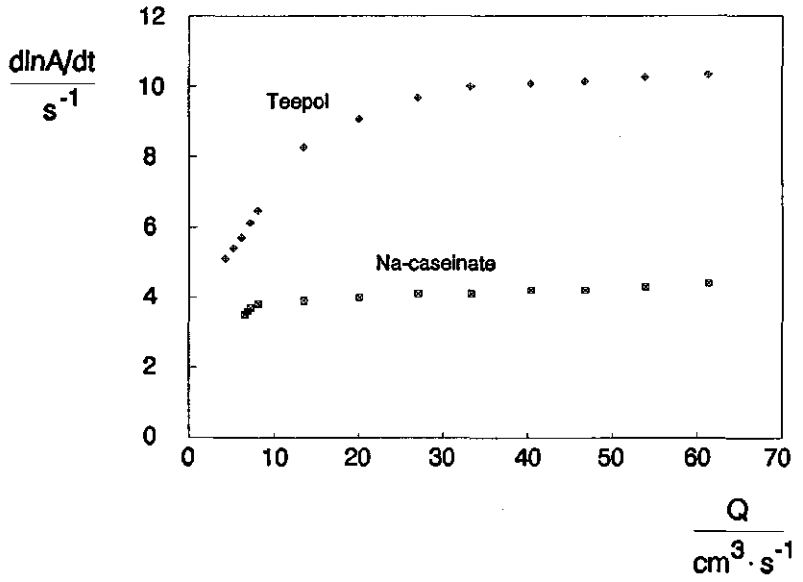

Fig. 6.3: *The relative surface expansion rate of solutions of 0.3 vol% Teepol and 20 kg/m^3 Na-caseinate as a function of the flow rate.*

At a certain flow rate, however, $d\gamma/dr$ has reached its limit. The solution in the overflowing cylinder simply bears no more potential to create a higher surface tension gradient. The flow rate in question differs for different solutions, for its magnitude is determined by the transport properties of the applied surfactant(s). From this flow rate on the origin of the relatively small increase in dlnA/dt with the flow rate is caused by hydrodynamic effects. The inclination of the curve is namely identical to the inclination of the graph of pure water in Fig. 5.2. In this flow rate region the increase in dlnA/dt is

simply caused by an increase of the mean vertical velocity in the cylinder. Like in the case of pure water, the increase in dlnA/dt happens without implying a change in $d\gamma/dr$ and γ_{dyn}. Fig. 6.4 indeed shows that the dynamic surface tension of the Teepol solution does not alter in this flow rate region. The same behaviour was observed for γ_{dyn} of Sodium caseinate.

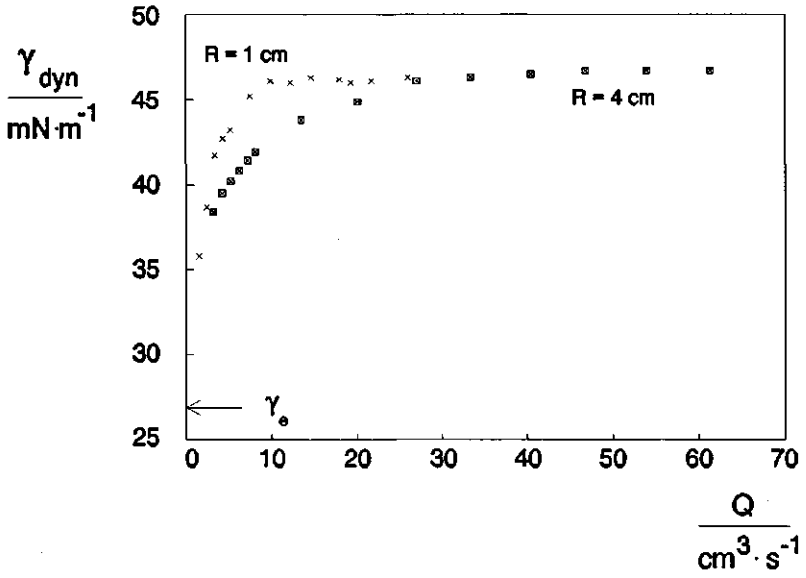

Fig. 6.4: *The dynamic surface tensions of the cylinders of radii R=1 cm and R=4 cm as a function of the flow rate; (measurement concerning R = 1 cm by Marlies Wijnen).*

Fig. 6.4 not only presents the results of the cylinder of Radius R = 4 cm, which was used for all experiments dealt with in this thesis, but also gives the dynamic surface tension as a function of the flow rate for a cylinder of radius R = 1 cm. With respect to the radius R = 1 cm γ_{dyn} reaches its plateau value at ca. Q = 10 cm^3/s, whereas for the cylinder of radius R = 4 cm the same level is reached at a flow rate being almost four times higher. It is noticed that the ratio of these flow rates equals the ratio of the radii. Eq. (6.1) has been rewritten in order to obtain an expression for the flow rate in terms of parameters which refer to the wetting film at the level of the rim of

the cylinder:

$$Q = 2\pi R \cdot \delta_0 \cdot V_f^0. \tag{6.2}$$

Where the maximum value of $d\gamma/dr$ is obtained and γ_{dyn} reaches its plateau value, $Q/2\pi R$ is almost the same for both cylinders, and consequently, according to eq. (6.2), there $\delta_0 \cdot V_f^0$ must be the same as well. For the applied solution of Teepol this constant amounts to ca. $1.6 \cdot 10^{-4}$ m^2/s. On account of the quantity $\delta_0 \cdot V_f^0$ being a constant, it is imaginable that at the point of change in physical behaviour the overflowing cylinders yield the same weight of the free falling part of the wetting film, giving rise to identical maximum values of the surface tension gradient present over the length of the wetting film. One may jump to the conclusion that the same plateau value for γ_{dyn} implies that at the point of change also the dlnA/dt values in the centres of the surfaces have to be the same. The relation between dlnA/dt and $d\gamma/dr$, as expressed by eq. (3.9), is valid for all cylinders, irrespective of the radius, and so it is indeed very tempting to say that both cylinders operate exactly in the same way meaning that also the relation between dlnA/dt and γ_{dyn} is independent of the radius of the cylinder. However, it is also plausible that the latter conclusion is wrong. The mean value of the vertical velocity in the cylinder, V_z, is given by

$$V_z = \frac{Q}{\pi R^2}. \tag{6.3}$$

At the point of change V_z in the cylinder of radius R = 1 cm is four times higher than in the cylinder of radius R = 4 cm. Only taking the hydrodynamics of the overflowing cylinder into consideration a higher vertical velocity leads to a higher relative surface expansion rate in the vicinity of the stagnation point. So it is most probable that in the surface of the smallest cylinder the highest dlnA/dt results. In accordance with eq. (3.9) then over the horizontal surface also a larger $d\gamma/dr$ is present. If the surface tension gradient of the cylinder of radius R = 1 cm is even four times higher, the

total difference in γ_{dyn} over the top surface will be the same for both cylinders. Of course this speculative suggestion needs further investigation.

Generally it is concluded that a higher flow rate raises the relative surface expansion rate via the growth of the free falling part of the wetting film, until at a certain weight of the free falling film part, which is determined by the transport properties of the applied surfactant(s), the generated surface tension gradient has reached its maximum value. Thereon the origin of further increase, being relatively small, is hydrodynamic.

6.2 Comparison with other techniques

In the overflowing cylinder the relative surface expansion rate is experienced to range from about 1 s^{-1} for pure water to 10 s^{-1} for particular surfactant solutions. The relative surface expansion rate can not be imposed on the liquid system in the overflowing cylinder, but is established by the system itself. Dealing with a surfactant solution the value of dlnA/dt is almost completely determined by the magnitude of the generated surface tension gradient. Each solution in the overflowing cylinder bears a limit value of $d\gamma/dr$. Setting aside the relatively small hydrodynamic effects on dlnA/dt, the maximum in $d\gamma/dr$ gives rise to the highest relative surface expansion rate obtainable referring to the surfactant solution under investigation. This maximum can be diminished by adjusting the flow rate. However, since care must be taken that the outside wall of the cylinder is always completely wetted by the falling film, the capacity for lowering dlnA/dt via the flow rate is small, and at best a factor 2. More variation can be accomplished by diminishing the length of the wetting film. A decrease of a factor 5 is easily achieved, and some surfactants are even capable of immobilizing the surface at very small values of L.

So in general the overflowing cylinder creates a surface deformation having a

relative expansion rate of the order of magnitude of 1 - 10 s^{-1}. With respect to this magnitude the overflowing cylinder can be compared to other techniques bringing about dilational surface deformations. A comparison may also reveal information on the applicability of the overflowing cylinder technique for studying relevant dynamic surface behaviour of surfactant solutions in practice.

The Langmuir trough

It counts for all varieties of the Langmuir trough that, of course within the experimental limits, the desired surface expansion rate can be imposed on the liquid system under investigation. Ronteltap [2] carried out experiments by means of a Langmuir trough equipped with a caterpillar belt with several barriers. The relative surface expansion rate of the trough ranged between $2 \cdot 10^{-4}$ and 0.2 s^{-1}. In the Langmuir trough Van Voorst Vader et al [3] used, dlnA/dt could be varied from 0.15 s^{-1} to any lower value. It is noticed that the Langmuir trough operates at much smaller dlnA/dt values than the overflowing cylinder. In fact the dlnA/dt range of the trough is complementary to the range of the overflowing cylinder. The trough may be used to simulate practical processes which imply a continuous surface expansion relatively close to equilibrium. During foaming of surfactant solutions, bubble growth in carbonated beverages, spraying of plants and other processes given as examples in chapter 1, however, surface expansion takes place far from equilibrium. The overflowing cylinder may be more suitable for studying these processes than the Langmuir trough.

The overflowing funnel

Joos [4] calculated the relative surface expansion rate of an arbitrary surfactant solution present in his overflowing funnel according to eq. (3.33). Depending on the flow rate dlnA/dt was found to range from almost zero to about 1 s^{-1}. Referring to the comments made on eq. (3.33) in §3.3 these calculated values are likely to be smaller than the actual values.

The free falling film apparatus

In one of the papers preceding this thesis [5] a comparison was made between the surface dilational behaviour of surfactant solutions in the overflowing cylinder and the free falling film apparatus. The dynamic surface tension could be measured along the height of the free falling film by means of a modified Wilhelmy plate method. In order to be able to compare the results with the overflowing cylinder data of Fig. 5.14, surface tension measurements were carried out on various concentrations of Teepol at a fixed distance from the slit of the vessel. Here the relative surface expansion rate was calculated to be between 5 and 10 s^{-1}, which is of the same order of magnitude as the surface expansion rate of the Teepol solutions in the overflowing cylinder. However, the continuous expansion of the vertical film surface is, in contrast with the radial expansion of the top surface of the overflowing cylinder, a hydrodynamically driven surface deformation. Although the free falling film apparatus and the overflowing cylinder create expanding surfaces in different ways, the dynamic surface tension data obtained with these two techniques appeared to be nearly the same. Consequently the physical mechanism that underlies the operation of these techniques must also be the same. This is no surprise, since in the previous paragraph the behaviour of the expanding top surface of the overflowing cylinder has showed to be governed too by a falling film, in this case wetting the outside of the cylinder. Because of the fact that the expanding liquid surfaces of the two apparatuses generate the same value of the dynamic surface tension, the overflowing cylinder is as suitable as the free falling film apparatus for studying the rapid drainage in the early stages of a freshly made foam. This conclusion can also explain the good correlation which shows to exist between the stability of these liquid films under dynamic conditions during the process of foaming and the surface tension data obtained with the overflowing cylinder technique [5,6]. This is illustrated by Fig. 6.5 for the surfactant Teepol. The foam volume, resulting from shaking the aqueous solution in a glass cylinder for then seconds, is compared to the

equilibrium and dynamic surface tensions. All three quantities are given as a function of surfactant concentration. Fig. 6.5 shows that, in the region where the equilibrium surface tension has reached its low plateau value, the foamability still increases considerably. The greatest increase in foamability correlates with the decrease in the measured dynamic surface tension. These data also qualitatively demonstrate that the process of foaming benefits from a low surface tension during expansion, which is in agreement with the results of Prins [7] who showed that a high surface tension is probably unfavourable for foam stability.

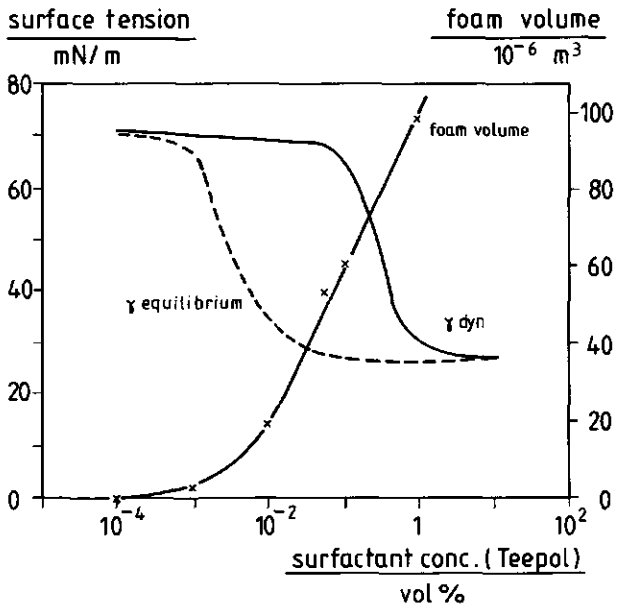

Fig. 6.5: The equilibrium and dynamic surface tensions measured by the overflowing cylinder technique, and the foam volume as a function of the concentration of Teepol.

The maximum-bubble-pressure-method

Maximum bubble pressures can be measured for bubble intervals ranging from hours to ca. 0.1 s [8]. Although the bubble growth indeed implies a continuous expansion of a liquid surface, the process does not take place

under steady-state conditions. However, an approximate idea of the mean value of the relative surface expansion rate of the bubble can be formed by assuming the radius of the capillary and the radius of the bubble at the moment of detachment from the capillary to be 50 μm and 500 μm respectively. Using these values dlnA/dt is roughly estimated to range between 10^{-2} and 10^{3} s^{-1}, dependent on the applied bubble interval. So the relatively small dlnA/dt interval of the overflowing cylinder is included in this range, and both substantially higher and lower dlnA/dt values can be accomplished by the maximum-bubble-pressure-method, though not as low as the Langmuir trough is able to provide. The question is whether the extension to high surface expansion rates reveals additional information on the dynamic surface behaviour of surfactant solutions applied in practical processes. The following example concerning spin finishes may illustrate this question.

The spinning of high-tech yarns essentially relies on the properties of spin finishes [9]. A high rate of spreading is a pre-condition for an even wetting of the yarn with the spin finish. Engels et al [9] studied the effect of increasing amounts of a wetting agent on the performance of the spin finish. They measured γ_e by means of the Wilhelmy plate method and determined γ_{dyn} from maximum-bubble-pressure experiments at 7 Hz (order of magnitude dlnA/dt = 10^{3} s^{-1}). The resulting graph representing the surface tensions versus the concentration of the wetting agent closely resembled the concentration curves of Teepol and the contaminated CTAB in Figs. 5.14 and 5.17. Rather than the equilibrium surface tension the dynamic surface tension showed a strong correlation with the spreading ability of the spin finish. The spreading was drastically enhanced by lowering the dynamic surface tension via the addition of the wetting agent.

The maximum-bubble-pressure-method operating at a much higher surface expansion rate than the overflowing cylinder and the free falling film apparatus, appears to produce similar dynamic surface tension data. This is no surprise considering the liquid systems studied. Not only solutions of

Teepol and the contaminated CTAB, but also solutions of the wetting agent of the spin finish are low molecular dirty systems. Like in many other 'dirty' surfactant solutions used in practice, minor components are present in these systems. Minor components generally lower the equilibrium surface tension, but have no allowance to adsorp at a surface which is continuously expanded far from equilibrium. At expansion rates high enough for getting rid of surface active impurities the surface tension of the expanded surface almost equals the equilibrium surface tension of the pure sample, as has been shown for CTAB in Fig. 5.17. Thereon increasing the relative surface expansion rate only causes the dynamic surface tension to become a few mN/m higher. This is readily seen by reviewing the positions of the term dlnA/dt in eq. (3.23).

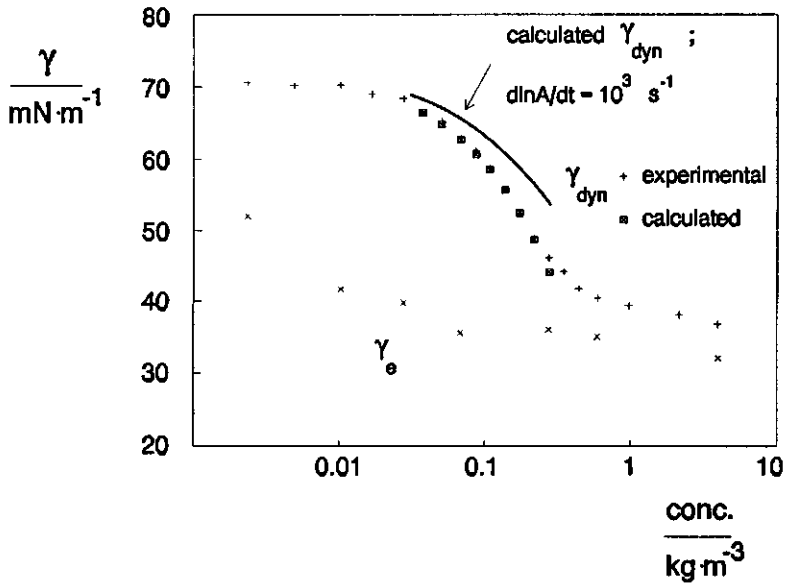

Fig. 6.6: The experimental dynamic and equilibrium surface tensions, as well as calculated dynamic surface tensions based upon respectively experimental dlnA/dt values and dlnA/dt = 10^3 s^{-1} as a function of the CTAB concentration.

As an example the excess surface tension was calculated again for various concentrations of CTAB in the way specified in §5.3. This time instead of the actual relative surface expansion rate of the overflowing cylinder surface the

value dlnA/dt = 10^3 s^{-1} was filled in. In Fig. 6.6 the new calculated γ_{dyn}-curve has been added to the original curve of Fig. 5.21.

In comparison with the difference between γ_{dyn} and the experimental γ_e, the calculated γ_{dyn}-curve based upon dlnA/dt = 10^3 s^{-1} only slightly deviates from the γ_{dyn}-curve referring to the experimental dlnA/dt which was 100 - 1000 times smaller. Due to the presence of minor components the first step from the equilibrium situation to dlnA/dt = ca. 1-10 s^{-1} gives rise to the major increase in surface tension, whereas the next step increasing dlnA/dt to 1000 s^{-1} only brings about a small effect. So dealing with low molecular 'dirty' systems, after the first step has been taken, extension to higher relative surface expansion rates only results in a small additional increase in the dynamic surface tension of the surfactant solution.

Concluding remarks

The application of surfactants in processes often implies the creation of liquid surfaces. During these processes the liquid surfaces may be expanded so far from equilibrium that present minor components have no ability to play any role of importance at the surface. The maximum-bubble-pressure-method, the falling film apparatus and the overflowing cylinder operate at relative surface expansion rates which are high enough for getting rid of these minor components. So all three techniques are useful for studying processes which imply expansion of liquid surfaces far from equilibrium, like foaming, painting, coating etc. It is not even necessary to know precisely the actual relative surface expansion rate of both the process under investigation and the applied technique, in order to get good correlations. Knowing that in both cases dlnA/dt is sufficiently high, will be enough.

In this respect there is no reason for giving preference to one of the techniques. However, the maximum-bubble-pressure-method suffers from the disadvantage that the surface expansion does not take place under steady-state conditions. Compared to the falling film apparatus the expanding surface the overflowing cylinder creates, is very smooth. Besides that, at the

horizontal top surface the overflowing cylinder accomplishes a pure dilation without any shear-components, which is not the case for the expanding surface of the free falling film. The simple way in which the dynamic surface tension of the top surface can be measured, is also in favour of the overflowing cylinder technique.

In order to be able to simulate practical processes implying expansion rates not sufficiently high for minor components to be absent from the expanding surface, the length of the wetting film of the overflowing cylinder can be reduced. In that case the applied value of dlnA/dt has to be relevant for the process under investigation. Dealing with applications in which a surface is expanded relatively close to equilibrium the capacity of the overflowing cylinder may be inadequate, and the Langmuir trough may be more suitable to use. However, in comparison with the Langmuir trough, the advantage of the overflowing cylinder is that no problems with leakage along barriers exist, being almost always the problem for users of the trough [3].

Summarizing, the overflowing cylinder is pre-eminently useful for studying processes which imply expansion of liquid surfaces far from equilibrium.

Acknowledgments. J.A. Garritsen kindly permitted publication of some of his results on solutions of egg white powder. Marlies Wijnen accurately contributed to the indicated figure.

References Chapter 6

[1] H. Schlichting, Boundary-layer theory, McGraw-Hill Book Company, New York, (1968).

[2] A.D. Ronteltap, Beer Foam Physics, Ph.D. thesis, Agricultural University Wageningen, (1989).

[3] F. van Voorst Vader, Th. F. Erkens and M. van den Tempel, Trans. Farady Soc., 60 (1964) 1170.

[4] P. Joos and P. de Keyser, The Overflowing Funnel as a Method for Measuring Surface Dilational Properties, Levich Birthday Conference, Madrid, (1980).

[5] D.J.M. Bergink-Martens, C.G.J. Bisperink, H.J. Bos, A. Prins and A.F. Zuidberg, Coll. and Surf. 64 (1992) 191.

[6] D.J.M. Bergink-Martens, H.J. Bos, H.K.A.I. van Kalsbeek and A. Prins, in E. Dickinson and P. Walstra (Eds.), Food Colloids and Polymers: Stability and Mechanical Properties, Royal Society of Chemistry, Cambridge, (1993), pp. 376-386.

[7] A. Prins, in R.J. Akers (Ed.), Foams, Academic Press, London, (1976), pp. 51 - 60.

[8] K.J. Mysels, Coll. Surf., 43 (1990) 241.

[9] T. Engels, T. Forster, R. Mathis and W. von Rybinski, Characterization of Spin Finishes by Physical-Chemical Parameters, Poster (A3/P-22) presented on the 7th Int. Conf. on Surface and Colloid Science, July 7 - 13, 1991, Compiègne, France.

Chapter 7

The water-oil overflowing cylinder

A new dimension is given to the overflowing cylinder technique by creating the possibility of expanding a water-oil interface. This extension of the known overflowing cylinder technique is elucidated (§7.1). The behaviour of the expanding water-oil interface is compared to the behaviour of the expanding surface of the liquid-air overflowing cylinder and the results are discussed (§7.2). The technique shows to be very promising when the preparation of emusions is considered (§7.3).
Part of this chapter has already been published in one of the papers preceding this thesis [1].

7.1 The creation of an expanding water-oil interface

A few alterations have been made to the concept of the liquid-air overflowing cylinder, resulting in a design for an apparatus suitable for studying an expanding water-oil interface. This extension of the known overflowing cylinder technique has only recently been explored. A prototype water-oil overflowing cylinder has been built, and experiments were carried out by means of this model. The total set-up consisted of separate parts which were attached to several frames. This situation was not favourable for the stability of the equipment. Therefore, in comparison with the sophisticated liquid-air overflowing cylinder, the accuracy of the measurements was less, though trends in the experimental results were clearly noticed.

The experimental set-up

The water-oil overflowing cylinder consists of an inner glass cylinder (diameter 6 cm, height 50 cm, and wall thickness 3.3 mm) through which water or an aqueous surfactant solution is pumped upwards. The outer glass cylinder (diameter 9.5 cm) is higher than the inner cylinder, in order to create

the possibility of pumping the aqueous phase 'against' an oil phase, like it is shown in Fig. 7.1.

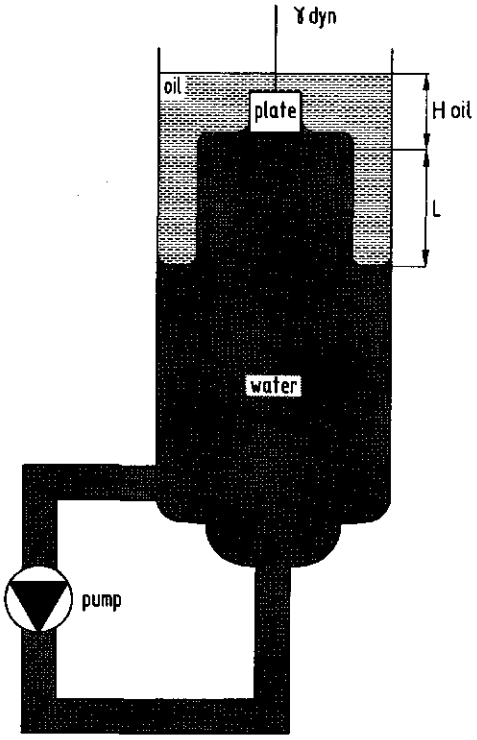

Fig. 7.1: Cross-section of the water-oil overflowing cylinder (not to scale); the arrows indicate the direction of the circulation of fluid through the system.

At the start of an experiment the system is filled with water till above the rim of the inner cylinder. After having poured some oil on top of the water phase, the flow is switched on. By reducing the total amount of water present in the system and adding oil, on the outside of the overflowing cylinder a wetting water film is formed. A new parameter, H_{oil}, is introduced, denoting the height of the oil layer above the rim of the inner cylinder. The flow through the cylinder was adjusted and determined by means of a needle valve and a flowmeter. The range of applicable flow rates was smaller than in the case of the liquid-air overflowing cylinder. A relatively high minimum flow rate was

required for preventing the outside of the overflowing cylinder from being wetted by the oil phase, whereas at high flow rates instabilities arose over the interface of the wetting film, and the water phase started to emulsify the oil in the compressed surface of the outer cylinder.

The closed overflowing cylinder system contains about 4 litres of water and 400 ml of oil. The length L of the wetting water film was increased by again reducing the total amount of water and meanwhile adding some extra oil. In the same way, L was decreased by increasing the amount of water, and, if necessarily, reducing the amount of oil. The resulting expanding water-oil interface has the same steady state velocity profile as has already been drawn for the liquid-air cylinder in Fig. 2.2. The mean radial velocity, v_r, of the interface was determined using high density polyethylene particles (Janssen Chimica, density 950 kg/m^3, diameter $<$ 1.5 mm). These particles did not affect the surface tension of pure water. One of the particles was brought upon the interface near the geometrical centre. The particle was visually followed in time on its way moving on the interface from the position at radial distance r = 1 cm to the rim of the cylinder. For each determination of the mean radial velocity the measurement was repeated several times with particles of various arbitrary diameters.

The interfacial tension under these dynamic conditions, γ_{dyn}, was again measured by means of the Wilhelmy plate technique. This time, however, a roughened glass plate was used, having a perimeter of 52.9 mm. The height of the oil layer, H_{oil}, has always been such that during an experiment the Wilhelmy plate was immersed in oil. The equilibrium interfacial tension, γ_e, was measured separately in a beaker according to the same Wilhelmy method. The thickness of the wetting film near the rim of the cylinder, δ_0, was again measured by means of a screw micrometer.

Materials

The oil phase was either soya oil (η_b = 59 mPa·s) or sunflower oil (η_b = 57 mPa·s). Both oils were commercially available products (Reddy) having a

density of 920 kg/m^3. Some experiments were carried out with soya oil which had been purified by means of silicagel (Merck, R_p = 32 - 100 μm). Silicagel is an adsorbens for various surface active components, like mono-glycerides, which may be present in the commercially available soya oil. The aqueous phase was either tap water or a solution of the surfactant Teepol.

7.2 Experimental results and discussion

In the previous chapter the expansion of the liquid-air surface of the overflowing cylinder appeared to be governed by the falling film on its outside. At a length of 2.5 - 3.0 cm a change in behaviour of the overflowing surfactant solution was observed. When the length of the wetting film becomes smaller than this value, the decrease in γ_{dyn} amounts to ca. 10 mN/m. A physical explanation was proposed by considering the boundary layer which is built up along the outside wall of the overflowing cylinder. The explanation showed that it is in fact the weigth of the free falling part of the wetting film which determines the behaviour of the expanding circular surface.

The question now is whether the behaviour of the water-oil interface is governed by the wetting water film on the outside of the overflowing cylinder in the same way? When a liquid is pumped against air, the driving force of the system is the body force

$$f_{body} = \rho_w g, \tag{7.1}$$

where ρ_w (10^3 kg/m^3) is the density of the water phase. When water is pumped against oil, the body force changes to

$$f_{body} = (\rho_w - \rho_o)\, g \equiv \rho_w\, g^*, \tag{7.2}$$

where ρ_o ($0.92 \cdot 10^3$ kg/m^3) is the density of the oil phase. From eq. (7.2) it follows that the two experimental systems are comparable, where the newly defined constant g^* for the water-oil system amounts to g^* = 0.08 g.

Therefore, in the water-oil overflowing cylinder, the gravitational constant may be considered to have less than one tenth of its actual value.

Varying the length of the wetting water film

In Fig. 7.2 data are presented for the water-soya oil system. It should be noted here that the soya oil used had not been purified, and so water-soluble impurities from the oil phase could dissolve in the aqueous phase during pumping. Therefore, instead of pure water, the aqueous phase was a dilute surfactant solution. The length L of the wetting water film was varied keeping the mass flow rate constant, and γ_{dyn} was measured in the centre of the circular interface. Fig. 7.2 shows that at almost the same length L as in Fig. 6.1 a change in the behaviour of the expanding interface is observed. And again, when the length of the wetting film becomes smaller than 2.5 - 3.0 cm, the decrease in γ_{dyn} amounts to ca. 10 mN/m.

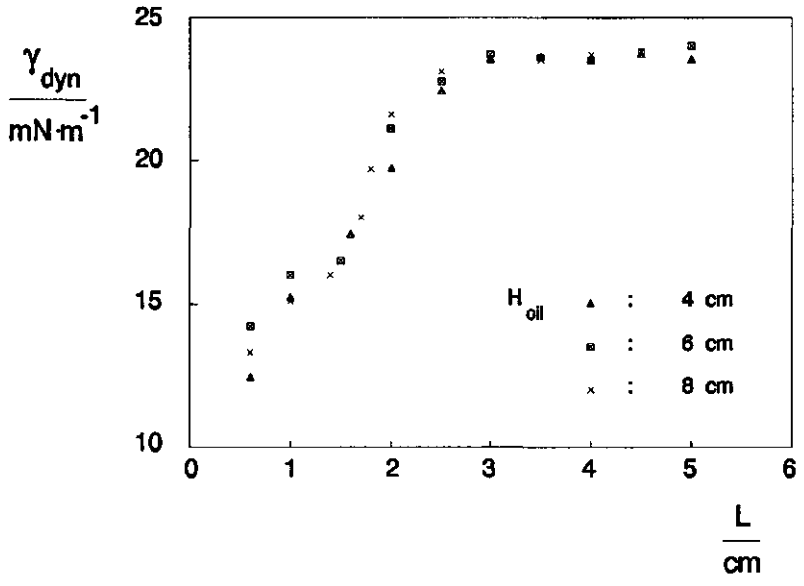

Fig. 7.2: The dynamic interfacial tension of water pumped against soya oil, as a function of the length of the wetting water film for various oil heights; Q = 51 cm^3/s; (measurement by Arne van Kalsbeek).

These results are surprisingly close to the results of the liquid-air overflowing cylinder. Besides that the results appear not to be influenced by the thickness of the oil layer on top of the expanding interface for $H_{oil} \geq 4$ cm. Since during a measurement the Wilhelmy plate was immersed in oil, the minimum oil height applicable was 4 cm. The experiment of Fig. 7.2 was repeated with sunflower oil, and an identical graph was obtained.

So far the behaviour of the overflowing liquid in the water-oil cylinder resembles the behaviour of a surfactant solution in the liquid-air overflowing cylinder. The two experimental systems appear to be comparable. However, the mean radial velocity of the water-oil interface was measured to be 0.2 cm/s, which is more than a factor 50 smaller than the value for the liquid-air surface. Since near the rim of the cylinder v_r increases far more than linearly with r, good estimates of $v_r(r = 3$ cm) and v_s^0 are considered to be 0.5 cm/s and 2 cm/s respectively. For the applied flow rate the thickness of the wetting film near the rim of the cylinder, δ_0, was found to be 2.5 mm, which is nearly a factor 5 bigger than the value for the liquid-air cylinder. Knowing these quantities the mean velocity of the wetting film near the rim of the cylinder, V_f^0, can be calculated by means of eq. (6.1). V_f^0 approximately equals 10 cm/s, which is 5 times higher than the estimated velocity of the interface, implying that the wetting film is enormously slowed down by the oil phase. Also the value of L_{crit} can be calculated for the water-oil system by applying eq. (3.35) to its parameters. With $\rho = \rho_w$, $\eta_b = 10^{-3}$ Pa·s and g^* substituted for g, eq. (3.35) gives $L_{crit} \approx 1$ cm. The calculated value of L_{crit} is of the same order of magnitude as the value of L where, in Fig. 7.2, the change in behaviour of the expanding interface is observed. This indicates that the boundary layer explanation given for the liquid-air system is also plausible for the water-oil system. Consequently, also in the case of a water-oil overflowing cylinder, the dynamic interfacial tension is dependent on the weigth of the free falling part of the wetting water film.

The experiment of Fig. 7.2 was repeated for two other flow rates. The length L where a change in course of γ_{dyn} was observed, became somewhat smaller, the higher the imposed flow rate. This tendency is qualitatively understood by realizing that a higher flow rate causes an increase in the thickness of the wetting film, implying that the free falling part of the wetting film becomes thicker as well. It was concluded in §6.1 that at a certain weight of the free falling film part, the generated surface tension gradient reaches its limit, giving rise to the maximum value of γ_{dyn}. Assuming that this weight is independent of the applied flow rate, the thicker the free falling part of the wetting film, the less length is needed for accomplishing the limit value of $d\gamma/dr$. Thus reasoning for higher flow rates the change in the behaviour of the expanding interface is likely to be observed at smaller values of L. These experiments have not yet been performed for the liquid-air overflowing cylinder. Further investigation is necessary for a quantitative analysis of the observed tendency.

The course of γ_{dyn} versus L was also studied for a pure water-oil system. Here pure water was pumped against soya-oil which had been purified by means of silicagel. Diminishing the length of the wetting water film no alteration in the value of γ_{dyn} occurs. The measured interfacial tension equals the equilibrium interfacial tension being 29 mN/m. Only when L becomes smaller than 0.5 cm undulations arise hindering the measurement. Setting aside these instabilities, the magnitude of the interfacial tension of the pure water-oil system is independent of the length of the wetting water film. So regarding this aspect the behaviour of the pure system in the water-oil overflowing cylinder is similar to the behaviour of pure water in the liquid-air overflowing cylinder.

Summarizing, for both the contaminated water-oil system and the pure water-oil system the results of an experiment in which the wetting water film is varied, resemble the results of the same experiment for the corresponding

systems in the liquid-air overflowing cylinder. These findings support the statement that the water-oil and liquid-air overflowing cylinders operate according to the same physical principle.

The addition of a surfactant

The aqueous phase of the impure water-oil system has shown to be in fact a dilute surfactant solution. Various concentrations of an extra surfactant have been added to the aqueous phase, and the resulting dynamic interfacial tensions were measured at fixed values of the mass flow rate and the length of the wetting film. Fig. 7.3 presents both dynamic and equilibrium interfacial tensions as a function of the concentration of Teepol. The interfacial tension of the purified water-oil system is also indicated in this figure.

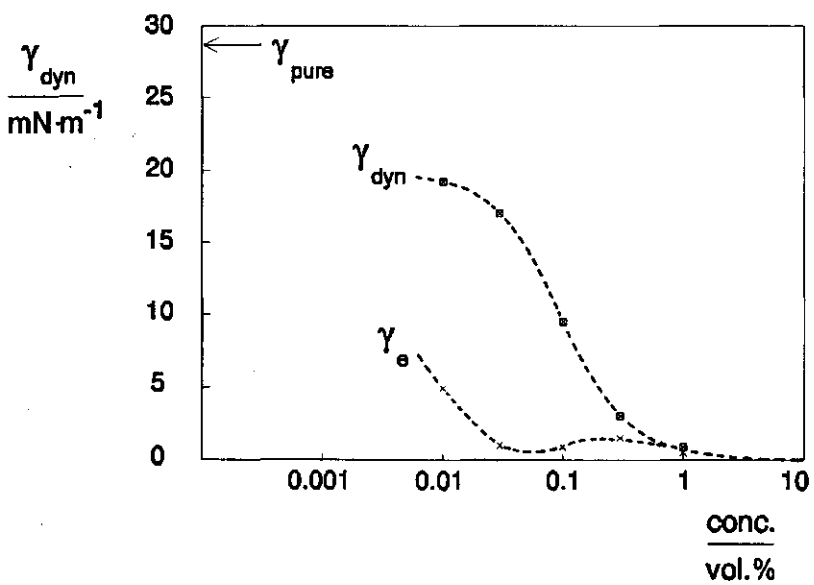

Fig. 7.3: The dynamic and equilibrium interfacial tensions as a function of the concentration of Teepol; L > 4 cm; Q = 33 cm³/s; (measurement by Arne van Kalsbeek).

Although only very few measured points are available, Fig. 7.3 may be noticed to look like Fig. 5.14 which relates the same parameters to the concentration of Teepol for the liquid-air overflowing cylinder. Also in Fig. 7.3

there is a marked shift in the positions of the equilibrium and dynamic curves on the concentration axis. And again, where γ_e reaches its low plateau at ca. 0.03 vol% Teepol, the excess interfacial tension, $\Delta\gamma$, has its maximum value. Note, by the way, how small the interfacial tension gets for high concentrations of Teepol.

The mean radial velocity of the interface was measured as a function of the concentration of Teepol as well. Table 7.1 presents the results, and also reports on the data of both the impure and the purified water-soya oil systems.

Table 7.1: *The mean radial velocity of the expanding interface for various aqueous phases pumped against soya oil; L > 4 cm; Q = 33 cm^3/s; (measurement by Arne van Kalsbeek).*

	system					
	w/o	w/o	vol% Teepol - soya oil			
	pure	impure	0.03 %	0.1 %	0.3 %	1 %
v_r [mm/s]	0.7	2.0	3.3	3.5	3.5	2.1

Comparable to the results of pure water in the liquid-air overflowing cylinder, here the minimum value of the interfacial velocity was measured for the purified water-oil system. Increasing the concentration of Teepol a maximum in the expansion rate occurs. The position of this maximum is again found where the derivative of the dynamic interfacial tension $-d\gamma_{dyn}/dc$ is the highest (cf. Fig. 7.3). If, like in Fig. 5.22, the three parameters viz. $\Delta\gamma$, the interfacial expansion rate, and the interfacial dilational viscosity are presented as a function of the concentration of Teepol, a similar graph will be obtained. The maximum in dilational interfacial viscosity will again appear at a smaller concentration than where the maxima in $\Delta\gamma$ and v_r are found. The magnitude of the maximum, however, will be greater than in the case of the liquid-air

overflowing cylinder, since the expansion rate of the interface of the water-oil overflowing cylinder is considerably smaller.
The experimental data of the water-oil overflowing cylinder with respect to various concentrations of Teepol show the same trends as the corresponding data of the liquid-air overflowing cylinder. These findings illustrate again that both systems principally operate in the same way.

7.3 Practical utility

The water-oil overflowing cylinder is a new dimension to the known overflowing cylinder technique, since the opportunity of creating an expanding water-oil interface forms an extension of the user possibilities. Studying a continuous expanding water-oil interface is for instance relevant when the preparation of emulsions is considered. During emulsification freshly created thin liquid films in between the emulsion droplets are exposed to all kinds of mechanical disturbances. Because these thin liquid films can be made unstable, especially when subjected to expansion, the study of the expanding interface by means of the water-oil overflowing cylinder can result in a better understanding of the emulsifying properties of surfactant solutions. This is illustrated by the following experiment: 10 ml soya oil was emulsified in 90 ml Teepol solution by shaking the system in a glass cylinder for ten seconds. After one minute at rest the thickness of the cream layer on top of the emulsion was measured. In Fig. 7.4 the fraction of the oil phase still present in the emulsion is compared to the equilibrium and dynamic interfacial tensions as a function of the Teepol concentration. Fig. 7.4 shows that, in the concentration region where the equilibrium interfacial tension has reached its low plateau value, the amount of emulsified oil still increases considerably. This increase correlates with the decrease in the measured dynamic interfacial tension. These data qualitatively demonstrate that the process of emulsification benefits from a low interfacial tension during

expansion, as measured by means of the water-oil overflowing cylinder technique. Besides that, these results offer an analogy with the foamability results of Teepol solutions which have been compared with surface tension data from the liquid-air overflowing cylinder in Fig. 6.5.

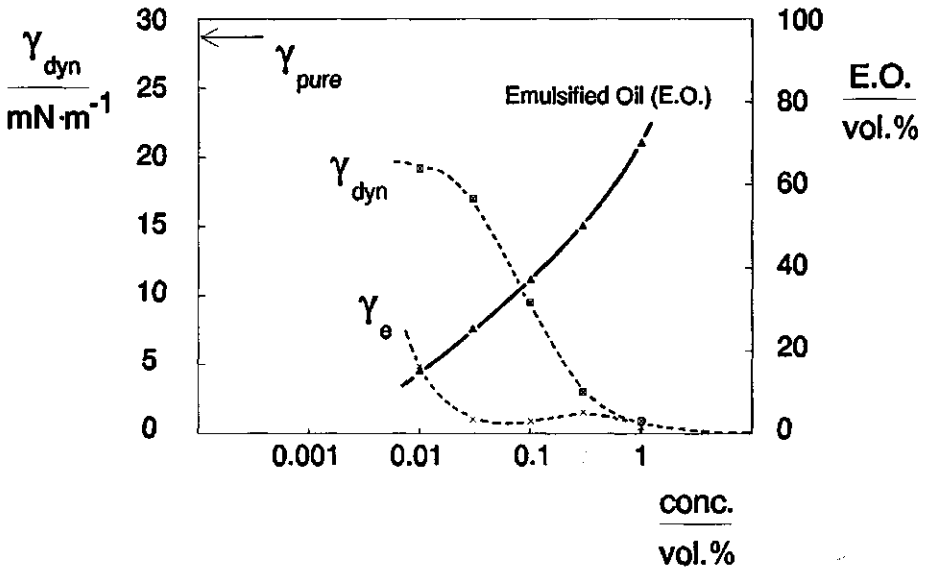

Fig. 7.4: The dynamic and equilibrium interfacial tensions and the fraction of emulsified oil (E.O.) as a function of the concentration of Teepol; for experimental conditions see Fig. 7.3; (measurement by Arne van Kalsbeek).

This was a rather rough and simple experiment illustrating the practical possibilities of the new water-oil overflowing cylinder. The experiment only serves to symbolize the potential for new applications of the overflowing cylinder technique. The results are very promising. The water-oil overflowing cylinder may become a very important tool for studying dynamic properties of water-oil interfaces.

Acknowledgments. The author wishes to thank Arne van Kalsbeek for performing the experiments and the preliminary analysis. Arne was very involved in the project and now and again came up with valuable new ideas.

References Chapter 7

[1] D.J.M. Bergink-Martens, H.J. Bos, H.K.A.I. van Kalsbeek and A. Prins, in E. Dickinson and P. Walstra (Eds.), Food Colloids and Polymers: Stability and Mechanical Properties, Royal Society of Chemistry, Cambridge, (1993), pp. 376-386.

Chapter 8

General discussion and conclusions

The present findings concerning the overflowing cylinder technique are considered to be also relevant to processes like foaming, emulsification, and the spreading of droplets and thin liquid layers. In addition to a discussion about the significance of the present findings, the physical mechanism of operation of the overflowing cylinder technique is elucidated in a diagram, and an overview of the behaviour of practical systems in the overflowing cylinder is given. The overflowing cylinder has always been experienced to be a very simple and handy tool which suits its purpose very well. In addition the present investigation supplies fundamental knowledge about the operation of the technique, and herewith the overflowing cylinder may even become more valuable to present-day users.

The significance of the present findings

The overflowing cylinder technique has always shown to be an interesting technique. On the one hand interesting for the users who experienced the overflowing cylinder to be a simple, handy and useful tool for studying dilational properties of liquid interfaces far from equilibrium. On the other hand, despite the practical simplicity, one specific question has always aroused the curiosity: why is the overflowing cylinder technique that relevant to many processing applications of surfactant solutions? The present investigation which gave the answer to the question, also brought other remarkable aspects to light. These findings hold the attention, because they are not explicitly confined to the overflowing cylinder technique, but may have more general importance beyond. Some of the conclusions which were drawn in the previous chapters, are also considered to be relevant to processes like foaming, emulsification, and the spreading of droplets and thin liquid layers. These processes have in common with the overflowing cylinder technique that the value of the surface expansion rate is mostly not directly imposed on the liquid system. Process conditions like the mixing rate, the

pressure difference or the flow rate, are directly imposed on the system, but the system autonomously determines the value of its surface parameters, the value of the relative surface expansion rate included. The following results of the present investigation may be relevant to these processes as well:

* the surface propulsion mechanism in the case of surfactant solutions is fundamentally different from the mechanism, when dealing with pure liquids. In the latter case the surface is hydrodynamically driven, whereas surfactant solutions are able to accomplish a surface tension gradient driven surface deformation according to the Marangoni-effect;
* already a very small surface tension gradient induces a considerable increase in relative surface expansion rate;
* the bulk viscosity only has minor effect on the surface behaviour;
* dealing with practical systems and protein solutions there is a marked shift in the positions of the curves of the equilibrium and the dynamic surface tensions on the concentration axis;
* during expansion far from equilibrium minor components are hardly present at the surface, and the value of the dynamic surface tension is determined by the major surfactant component(s);
* minor components do highly influence the magnitude of the surface dilational viscosity. The surface dilational viscosity is in fact rather a measure for the degree of purity of the surfactant, than a tool for describing the behaviour of a continuous expanding surface.

Further investigation is required to reveal the extent to which these aspects are of value for the applications of surfactant solutions. Studying the practical processes mentioned within the framework of the present findings may give a better insight in the physical mechanisms which dominate these processes.

An overview of the physical mechanism of operation

Table 8.1 schematically elucidates how the overflowing cylinder operates both in the case of a pure liquid and a surfactant solution.

Dealing with pure liquids the bulk flow completely determines the magnitude of the resulting relative surface expansion rate, and the surface deformation is hydrodynamically driven. The fluid-dynamical behaviour of the overflowing liquid was analyzed numerically. Good agreement was found between experimentally obtained values for the overflowing cylinder parameters and those calculated numerically.

Table 8.1: *Diagram elucidating the operation of the overflowing cylinder technique.*

pure liquid	**surfactant solution**
imposed: Q	Q, L
↓	↓ ← via free falling part wetting film
observed: dlnA/dt	$d\gamma/dr \rightleftharpoons$ dlnA/dt
$(d\gamma/dr = 0)$	↓ ← transport properties surfactant
$\gamma_{dyn} = \gamma_e$	γ_{dyn}, $\Delta\gamma$
↓	↓ ← curvature meniscus
h_{dyn}	h_{dyn}
hydrodynamically driven surface deformation	surface tension gradient driven deformation of the top surface

The behaviour of the overflowing liquid changes considerably when a surfactant is added. Due to the basic bulk flow the surface is stretched nonuniformly, and a surface tension gradient is created over the horizontal top surface. The creation is strengthened by the condition of mechanical equilibrium with the vertical film surface. Corresponding with the hypothesis given in §3.4, the weight of the free falling part of the wetting film influences the magnitude of the resulting surface tension gradient. The system bears a limit value of $d\gamma/dr$. The resulting $d\gamma/dr$ can be diminished via a decrease in weight of the free falling film part by decreasing either the flow rate or the length of the wetting film. For fixed values of the flow rate and the length of the wetting film the magnitude of the surface tension gradient depends on the transport properties of the applied surfactant(s). Due to the surface tension gradient an additional flowfield, which is superimposed on the basic flow of pure liquids, originates. The surface tension gradient accelerates a thin layer on top of the bulk flow. So dealing with surfactant solutions the deformation of the top surface is surface tension gradient driven.

The magnitude of the resulting relative surface expansion rate is directly related to the magnitude of the surface tension gradient. Via this relation the relative surface expansion rate gives rise to a dynamic surface tension which is generally higher than the equilibrium surface tension. Its absolute value is again determined by the transport properties of the applied surfactant(s). If γ_e of a model system which contains only one low molecular weight surfactant, is known as a function of the concentration, γ_{dyn} can be calculated by applying the theory of Van Voorst Vader et al (see §3.2 and §5.3).

The dynamic surface tension directly determines the height of the meniscus above the rim of the cylinder via the curvature of the meniscus. The curvature appears to be independent of both the applied surfactant and its concentration.

In the past users of the overflowing cylinder and the overflowing funnel (see §1.2 and §3.3) tried to relate $d\ln A/dt$ to the flow rate by means of h_{dyn}. Hereabout this thesis has not revealed direct unique relations, neither

between dlnA/dt and h_{dyn}, nor between dlnA/dt and the flow rate. Applying a fixed length of the wetting film, for every imposed flow rate the solution itself determines autonomously via the creation of a surface tension gradient what the resulting surface expansion rate will be.

The behaviour of practical systems

In this thesis the relations existing between the physical parameters which describe and determine the operation of the overflowing cylinder technique, have been studied for various surfactant solutions. Since in industry the overflowing cylinder is used to experiment on practical systems, which are in general far from being model systems, here in the interest of the (potential) users an overview of the behaviour of these 'dirty systems' is given in Fig. 8.1. The physical parameters presented have been studied extensively for the liquid-air overflowing cylinder. The experimental data of the water-oil overflowing cylinder, however, showed the same trends.

A 'dirty' system is a practical system containing more than just one surfactant component. In order to be able to describe the surface behaviour, as a simplification the system is assumed to consist of a major and a minor surfactant component. The minor component distinguishes itself from the major component by two characteristics. Firstly the minor component is present at a relatively low concentration, and secondly the minor component is much more surface active than the major component.

Dealing with 'dirty' systems in the overflowing cylinder there is a marked shift in the positions of the curves of the equilibrium and dynamic surface tensions on the concentration axis. The minor component lowers the equilibrium surface tension, especially at low total surfactant concentration. The dynamic surface tension is mainly determined by the transport properties of the major surfactant component, since the minor component has not got enough time to adsorp at the expanding surface.

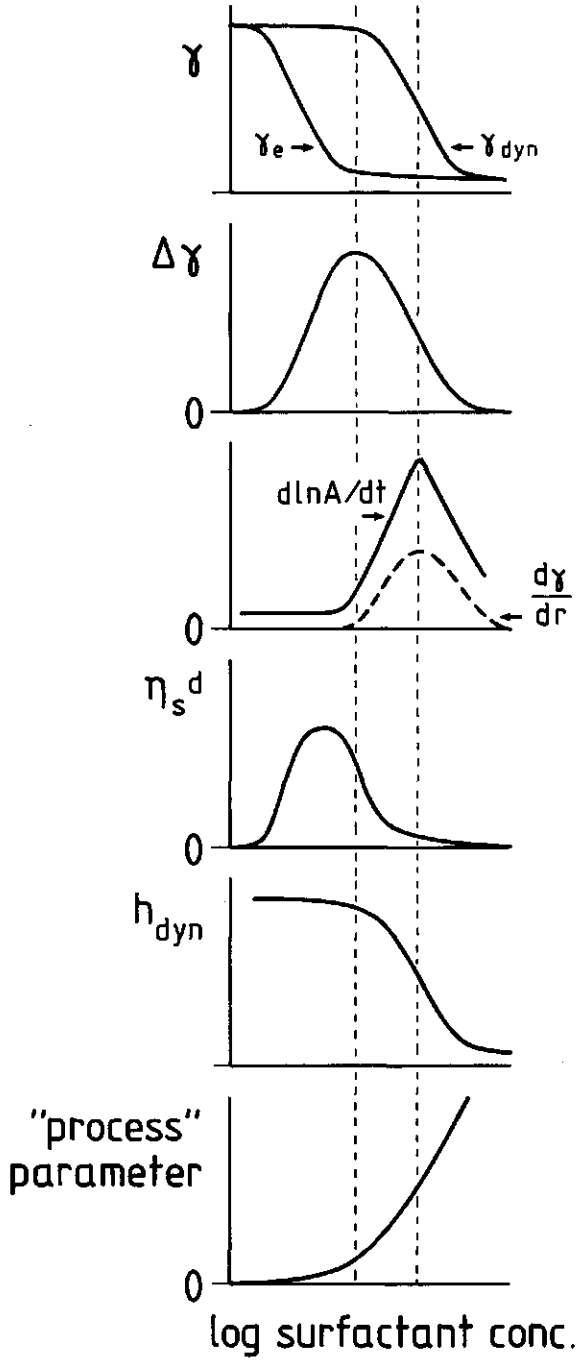

Fig. 8.1: Course of the physical parameters as a function of the surfactant concentration for practical systems.

Since the generated surface tension gradient directly accelerates the surface, the curves of dlnA/dt and $d\gamma/dr$ show the same course versus the concentration. Their maxima are found to occur where the derivative of the dynamic surface tension, $-d\gamma_{dyn}/dlogc$ is the highest.

The surface dilational viscosity is defined to be the ratio of $\Delta\gamma$ ($= \gamma_{dyn} - \gamma_e$) to dlnA/dt, and consequently the maximum in η_s^d appears where γ_{dyn} still approximates the surface tension of pure water. The minor component highly influences the magnitude of η_s^d via the lowering of the equilibrium surface tension.

Because of the fact that the height of the meniscus above the rim of the cylinder is linearly proportional to the dynamic surface tension, the course of both parameters versus the concentration is similar.

The last graph of Fig. 8.1 presents a process parameter relevant to a practical process which implies expansion of liquid interfaces far from equilibrium. Dependent on the process under investigation the process parameter is for instance the foamability, the spreading or wetting ability, or an emulsifying property. The greatest increase in magnitude of the process parameter correlates with the decrease in dynamic surface tension as measured by means of the overflowing cylinder technique. Here under dynamic conditions the system is able to generate the highest surface tension gradient.

Dealing with foams and emulsions, the stability of the created product is for the greater part determined by the stability of the freshly created thin liquid films in between respectively the air bubbles and the emulsion droplets. In turn, corresponding with the last graph of Fig. 8.1, the stability of these thin liquid films may benefit from a low surface tension as measured during expansion of the liquid surface in the overflowing cylinder.

Practical utility

The overflowing cylinder technique accomplishes a steady-state dilation of a liquid interface far from equilibrium. The resulting dilation is a pure dilation without any shear components. Moreover in the vicinity of the centre of the

circular interface the relative surface expansion rate is a constant. Its magnitude shows to be practically relevant to many applications of surfactant solutions implying expansion of liquid interfaces far from equilibrium. Also during these processes minor components have no ability to play any role of importance at the expanding interface. The overflowing cylinder has shown to be useful for investigating these processes which are, like the expanding interface of the overflowing cylinder itself, dominated by the major surfactant component(s). Studying dilational properties of surfactant solutions the overflowing cylinder is experienced to be a very handy tool which is easy to operate.

Before the present investigation had been carried out, despite the observed practical utility, there was a lack of fundamental knowledge of the operation of the overflowing cylinder technique. Now an idea has been formed of the physical mechanism of operation, and relations existing between the physical parameters have been revealed for various surfactant solutions, the overflowing cylinder technique may even become more valuable to present-day users.

List of symbols

Roman symbols

A	area	m^2
a	computational constant (Langmuir-Von Ssyszkowski)	$mol\ m^3$
$dlnA/dt$	relative surface expansion rate	s^{-1}
$\{dlnA/dt\}_0$	relative surface expansion rate of the pure liquid	s^{-1}
c	concentration	$mol\ m^{-3}$
c_b	surfactant concentration in the bulk	$mol\ m^{-3}$
c_0	surfactant concentration in the sub-surface layer	$mol\ m^{-3}$
D	diffusion coefficient	$m^2\ s^{-1}$
D_w	thickness cylinder wall	m
d	diameter of the Wilhelmy cylinder	m
d	distance between light fringes in the probe volume	m
f_{body}	body force	$N\ m^{-3}$
F_{ma}	inertial force	N
F_{vis}	viscous force	N
Fo_s	surface Fourier number	-
f_D	Doppler frequency	Hz
$f(\eta)$	stream function	-
g	gravitational constant	$m\ s^{-2}$
g^*	apparent gravitational constant of the water-oil system	$m\ s^{-2}$
H_{oil}	height of the oil layer with reference to the rim	m
h	capillary height	m
h_0	height of the meniscus of zero flow	m
h_{dyn}	height of the overflowing meniscus	m
h_e	height of the equilibrium meniscus	m
Δh_{flow}	excess height due to the liquid flow	m

L	length of the wetting film	m
L_{crit}	maximum length of the free falling film part	m
l	distance covered by diffusion	m
M	molecular weight	g mol^{-1}
n_s	amount of surfactant	mol
p_0	atmospheric pressure	N m^{-2}
ΔP	Laplace pressure difference	N m^{-2}
Q	flow rate	m^3 s^{-1}
R	gas constant	J $mol^{-1}K^{-1}$
R	radius of the overflowing cylinder	m
R_1, R_2	principal radii of curvature of the overflowing meniscus	m
R_a, R_b	principal radii of curvature of the equilibrium meniscus	m
R_p	particle radius	m
r	radial coordinate	m
T	temperature	K
T_0	room temperature	K
t	time	s
V	liquid volume	m^3
V_z	mean vertical velocity in the cylinder	m s^{-1}
V_f^0	mean velocity of the wetting film near the rim	m s^{-1}
v	velocity	m s^{-1}
v_r	radial velocity	m s^{-1}
v_s^0	surface velocity of the wetting film near the rim	m s^{-1}
v_z	vertical velocity	m s^{-1}
z	vertical coordinate	m

Greek symbols

α	angle of incidence of the laser beams	deg
Γ	surfactant adsorption	mol m^{-2}
Γ_∞	saturation adsorption	mol m^{-2}
γ	surface tension	N m^{-1}
γ_{dyn}	dynamic surface tension	N m^{-1}
γ_e	equilibrium surface tension	N m^{-1}
γ_L	surface tension of the pure solvent	N m^{-1}
$\Delta\gamma$	excess surface tension ($= \gamma_{dyn} - \gamma_e$)	N m^{-1}
δ_0	thickness of the wetting film near the rim	m
δ_Q	thickness of the accelerated fluid layer	m
η	dimensionless coordinate	-
η_s^d	surface dilational viscosity	N s m^{-1}
η_b	dynamic viscosity	N s m^{-2}
θ	angle between the two intersecting laser beams	deg
λ	wavelength of the laser light	m
ρ	fluid density	kg m^{-3}
ρ_p	density of the particle	kg m^{-3}
ν	kinematic viscosity	m^2 s^{-1}

Summary

The overflowing cylinder technique is pre-eminently useful for studying expanding liquid surfaces far from equilibrium. The technique is experienced to give information about processes like coating, finishing, foaming, and the spraying of plants. These processes also imply expansion of liquid surfaces far from equilibium.

During an experiment a liquid is pumped upwards through the vertical cylinder, and when next the liquid flows over the top rim, a pure steady-state dilation of the horizontal surface is accomplished.

The aim of the present investigation is to gain fundamental knowledge of the physical mechanism of operation of the overflowing cylinder. Herewith the overflowing cylinder may even become more valuable to present-day users.

From all the physical parameters describing and determining the operation of the overflowing cylinder technique, for a given cylinder geometry only the flow rate through the cylinder and the length of the wetting film on the outside of the cylinder can be imposed on the overflowing liquid. The liquid system determines autonomously the values of all other parameters, the surface expansion rate included.

Dealing with pure liquids the bulk flow fully determines the relative surface expansion rate of the horizontal surface, and the surface deformation is hydrodynamically driven.

The propulsion mechanism changes completely, when a surfactant is added. Then a surface tension gradient is generated which induces a considerable acceleration of the free surface. In this case the continuous expansion is a surface tension gradient driven surface deformation. Both the flow rate and the length of the wetting film influence the resulting relative surface expansion rate via the magnitude of the surface tension gradient. The relative surface expansion rate is found to be constant near the centre of the surface.

Typical values range from 1 s^{-1} for pure water to 10 s^{-1} for particular surfactant solutions. The relative surface expansion rate is measured by means of the differential laser Doppler technique which is succesfully applied to the overflowing cylinder technique.

For surfactant solutions the surface tension of the expanding surface is generally higher than the equilibrium value.
Dealing with a model surfactant solution containing only one surfactant component, the excess surface tension can be calculated by applying the theory Van Voorst Vader developed.
In industry, however, the overflowing cylinder is used to experiment on practical systems. During expansion almost only the major surfactant component(s) of these systems are present at the surface. Minor components lower the equilibrium surface tension, but have not got enough time to adsorp at the expanding surface. Minor components also highly influence the value of the surface dilational viscosity. The latter quantity is found to be in fact rather a measure for the degree of purity of the low molecular surfactant than a tool for describing the behaviour of the continuous expanding surface.

A new dimension to the known overflowing cylinder technique is explored by creating an expanding water-oil interface. The technique shows to be very promising when the preparation of emulsions is considered. Experimental results support the statement that the water-oil and liquid-air overflowing cylinders operate according to the same physical principle.

The overflowing cylinder technique provides a characteristic image of the solution under investigation. The image is considered to be also relevant to for instance foaming, emulsification, and the spreading of droplets and thin liquid layers.

Zusammenfassung

Gerade die Überlaufzylindertechnik eignet sich besonders für Untersuchungen an sich ausdehnenden Flüssigkeitsoberflächen weit vom Gleichgewichtszustand. Die Technik erteilt brauchbare Auskunft über Prozesse der Verfahrenstechnischen Praxis wie Lackierung und Imprägnierung sowie Besprengung von Pflanzen. Auch während dieser Prozesse findet ja eine Expansion von Flüssigkeitsoberflächen weit vom Gleichgewichtszustand statt. Während eines Experiments wird Flüssigkeit durch den vertikalen Zylinder hochgepumpt. Anschließend überfließt die Flüssigkeit den Zylinderrand und es ergibt sich eine reine stationäre Expansion der horizontalen Oberfläche.
Ziel dieser Forschung ist es die physische Wirkung der Überlaufzylindertechnik zu ergründen und damit einen wesentlichen Beitrag zur Kenntnis der (potentiellen) Anwender dieser Technik zu leisten.

Es gibt verschiedene physische Parameter, die die Wirkung der Überlaufzylindertechnik beschreiben und bestimmen. Für eine bestimmte Zylindergeometrie kann man aber nur die Flüssigkeitsleistung und die Länge des fallenden Films an der Außenseite des Zylinders einstellen. Die Werte der übrigen Parameter ergeben sich von selbst. Auch der der relativen Expansionsgeschwindigkeit der Oberfläche.
Bei reinen Flüssigkeiten wird die Expansionsgeschwindigkeit der Oberfläche ganz von der Bulkströmung bestimmt und liegt der Oberflächendeformation ein hydrodynamischer Antrieb zugrunde.
Die Antriebsart ändert sich total wenn der Flüssigkeit ein oberflächenaktiver Stoff hinzugefügt wird. Der demzufolge hervorgerufene Oberflächenspannungsgradient beschleunigt die freie Oberfläche erheblich. In diesem Fall ist die Rede von einer vom Oberflächenspannungsgradient angetriebenen Deformation. Sowohl die Flüssigkeitsleistung wie die Länge des fallenden Films beeinflussen die Expansionsgeschwindigkeit der Oberfläche je nach der

Größe des Oberflächenspannungsgradients. Es stellt sich heraus daß die relative Expansionsgeschwindigkeit in Mittelpuntnähe der Oberfläche konstant ist. Typische Werte variieren von 1 s^{-1} für reines Wasser bis 10 s^{-1} für bestimmte oberflächenaktive Lösungen. Zur Messung der Expansionsgeschwindigkeit wird die Differential-Laser-Doppler-Technik mit Erfolg verwendet.

Während der Expansion ist die Oberflächenspannung von oberflächenaktiver Lösungen im allgemeinen höher als im Gleichgewichtszustand.
Bei einem hochreinen oberflächenaktiven Stoff eröffnet sich die Möglichkeit die Erhöhung mit Hilfe der Transporttheorie Van Voorst Vaders zu berechnen. In der Industrie wird der Überlaufzylinder jedoch für Praxissysteme verwendet. Nur die Hauptkomponente(n) dieser Systeme können die Oberfläche während der Expansion erreichen. Sogenannte 'minor components' ermäßigen die Werte der Gleichgewichtsoberflächenspannung, aber sind nicht gut zur Adsorption an der sich ausdehnenden Oberfläche imstande. Diese 'minor components' beeinflussen auch in hohem Maße die Werte der Dilatationsviskosität. Diese Größe stellt sich vielmehr als ein Reinheitsmaß eines niedermolekularen oberflächenaktiven Stoffes heraus als wie ein Hilfsmittel bei der Beschreibung des Verhaltens der sich kontinuierlich ausdehnenden Oberfläche.

Neulich ist der bekannten Überlaufzylindertechnik eine neue Dimension hinzugefügt worden. Jetzt ist es auch möglich sich ausdehnende Wasser-Öl-Grenzflächen zu kreieren. Diese Erweiterung ist vielversprechend, besonders in bezug auf die Zubereitung von Emulsionen. Die experimentellen Ergebnisse deuten darauf hin daß der Wasser-Öl- und der Wasser-Luft-Überlaufzylinder beide nach demselben physischen Prinzip funktionieren.

Die Überlaufzylindertechnik vermittelt ein charakteristisches Bild der untersuchten Lösung. Das Bild ist möglich auch in der Praxis von Bedeutung, wie zum Beispiel bei Schaumbildung und Emulgation, sowie bei der Applikation von dünnen Flüssigkeitsschichten.

Samenvatting

Juist de overlopende cilinder techniek is uitermate geschikt voor het bestuderen van expanderende vloeistofoppervlakken ver van evenwicht. De techniek blijkt nuttige informatie te geven over processen als opschuimen, coaten, finishen en het besproeien van planten. Ook tijdens deze processen vindt expansie van vloeistofoppervlakken ver van evenwicht plaats.
Tijdens een experiment wordt vloeistof omhoog gepompt door de verticaal opgestelde cilinder. Vervolgens stroomt de vloeistof over de rand van de cilinder, waardoor er een zuivere, stationaire expansie van het horizontale oppervlak plaatsvindt.
Het doel van dit onderzoek is het doorgronden van de fysische werking van de overlopende cilinder techniek. Deze kennis kan ook voor de (potentiële) gebruikers waardevol zijn.

Verschillende fysische parameters beschrijven en bepalen de werking van de overlopende cilinder techniek. Echter, voor een gegeven cilinder geometrie kunnen slechts het vloeistofdebiet en de lengte van de vallende film aan de buitenzijde van de cilinder aan het systeem worden opgelegd. De waarden van de overige parameters, inclusief de relatieve expansiesnelheid van het oppervlak, stellen zichzelf in.
Bij zuivere vloeistoffen wordt de expansiesnelheid van het oppervlak geheel bepaald door de bulk en hebben we te maken met een hydrodynamisch aangedreven oppervlakte deformatie.
De aard van de aandrijving verandert totaal, wanneer een oppervlakte-actieve stof wordt toegevoegd. Er ontstaat dan een oppervlaktespanningsgradiënt die het vrije oppervlak aanzienlijk versnelt. In dat geval hebben we te maken met een oppervlaktespanningsgradiënt aangedreven deformatie. Zowel het vloeistofdebiet als de lengte van de vallende film beïnvloeden de expansiesnelheid van het oppervlak via de grootte van de oppervlaktespanningsgradiënt. De

relatieve expansiesnelheid blijkt constant te zijn in de nabijheid van het centrum van het oppervlak. Karakteristieke waarden lopen uiteen van 1 s^{-1} voor zuiver water tot 10 s^{-1} voor bepaalde oppervlakte-actieve oplossingen. De relatieve expansiesnelheid wordt gemeten met behulp van de differentiële laser Doppler techniek die hier met succes is toegepast.

Tijdens expansie is de oppervlaktespanning van oppervlakte-actieve oplossingen in het algemeen hoger dan in evenwicht. Voor een zuivere oppervlakte-actieve stof kan dit verschil in oppervlaktespanning berekend worden met behulp van de transport theorie van Van Voorst Vader.
In de industrie wordt de overlopende cilinder echter gebruikt ten behoeve van praktijksystemen. Alleen de hoofdcomponent(en) van deze systemen kunnen tijdens expansie het oppervlak bereiken. Zogenaamde 'minor components' verlagen de evenwichtsoppervlaktespanning, maar zijn niet goed in staat tot voldoende adsorptie aan het expanderende oppervlak. Minor components beïnvloeden ook in hoge mate de waarde van de oppervlaktedilatatie-viscositeit. Deze grootheid blijkt eerder een maat te zijn voor de zuiverheid van een laagmoleculaire oppervlakte-actieve stof dan een hulpmiddel bij het beschrijven van het gedrag van het continu expanderende oppervlak.

Recent is er een nieuwe dimensie toegevoegd aan de bestaande overlopende cilinder techniek. Het is nu ook mogelijk daarin olie-water grensvlakken te laten expanderen. Deze uitbreiding is veelbelovend, vooral ten aanzien van het bereiden van emulsies. De experimentele resultaten duiden erop dat de olie-water en de water-lucht overlopende cilinder allebei volgens hetzelfde fysische principe functioneren.

De overlopende cilinder techniek geeft een karakteristiek beeld van de onderzochte oplossing. Dit beeld kan ook in de praktijk van belang zijn bijvoorbeeld bij schuimvorming, emulgeren, het spreiden van druppels en het aanbrengen van dunne vloeistoflagen.

Curriculum Vitae

Diane Martens kwam op 6 maart 1963 in Heemskerk ter wereld. In 1981 legde zij met gunstig gevolg haar eindexamen gymnasium β af aan het Bonhoeffer-College te Castricum. Daarna begon zij in 1982 aan de toenmalige Technische Hogeschool Twente - nu Universiteit Twente (UT) - met de studie Technische Natuurkunde. Zij vervulde haar stage aan de Loughborough University of Technology in Engeland op het gebied van de holografie. Na het behalen van het diploma Stralingshygiëne, niveau 3, en een korte doctoraal-opdracht kolloïd- en grensvlakchemie aan de faculteit der Chemische Technologie van de UT, studeerde zij in juni 1988 als natuurkundig ingenieur af bij de vakgroep Reologie van prof. dr. P.F. van der Wallen Mijnlieff op een onderzoek naar de structuur van een micro-emulsie. Tijdens haar studententijd in Enschede was zij bestuurlijk actief in de natuurkundige studievereniging en in de Twentse Jong Odd Fellow club.

Van 15 oktober 1988 tot 15 januari 1993 was Diane Bergink-Martens aangesteld als assistent in opleiding bij de sectie Zuivel en Levensmiddelen-natuurkunde van de Landbouwuniversiteit te Wageningen. In deze periode verrichtte zij het onderzoek waarover dit proefschrift handelt. In het kader van het onderzoek verzorgde zij vier lezingen en drie posterpresentaties op symposia in binnen- en buitenland.
In november 1990 werd de auteur benoemd in het bestuur van de vereniging Katholieke Radio Omroep te Hilversum.

Omslagontwerp: Ernst van Cleef

Financiële bijdrage in de drukkosten: LEB-Fonds